NASA Technical Memorandum 87359

NASA Geodynamics Program: Fifth Annual Report

Geodynamics Program Office

OCTOBER 1984

NASA

NASA Technical Memorandum 87359

NASA Geodynamics Program: Fifth Annual Report

Geodynamics Program Office
NASA Office of Space Science and Applications
Washington, D.C.

National Aeronautics
and Space Administration

**Scientific and Technical
Information Branch**

1984

TABLE OF CONTENTS

I. INTRODUCTION

The purpose of these annual reports is to inform the geodynamics community of the status, progress, and plans of the NASA program.

The first annual report (NASA, 1980) contained a section of background and historical information covering the period from the beginning of the program in 1964 as the National Geodetic Satellite Program, through the end of 1979. The second report (NASA, 1981) highlighted the progress in instrumentation development and theoretical research, and the preparation for initiation of crustal motion measurements in the western United States. The third report (NASA, 1982) emphasized progress made in 1981 in achieving improved measurement precision and in establishing the foundation for the acquisition and analysis of scientific data. The last report (NASA, 1983) focused on the crustal measurements underway and included, for the first time, abstracts of papers presented at the annual NASA Geodynamics Conference.

This, the fifth annual report, summarizes program activities and achievements for the period of May 1983 to May 1984. This year the annual NASA Geodynamics Program Conference was held in Cincinnati, Ohio during May 14-17, 1984, in conjunction with the Spring Meeting of the American Geophysical Union (AGU). Abstracts of papers presented at the Conference are included in this Report (Appendix 2). Current publications associated with the NASA Geodynamics Program are listed in Appendix 3.

In 1983, the NASA Office of Space Science and Applications (OSSA) was reorganized and the Geodynamics Branch of the Earth and Planetary Exploration Division (now the Solar System Exploration Division) was integrated into the newly formed Earth Science and Applications Division.

A. HIGHLIGHTS AND ACHIEVEMENTS

Over the past year the Geodynamics Program has made major advances in the acquisition of global plate motion data and regional crustal measurements in the western United States. Significant Crustal Dynamics Project (CDP) results were reported and preparations made to intensify and expand to the "full rate" data acquisition phase which will be maintained through 1988. Studies of the Geopotential Research Mission (GRM) were continued and a new mission concept, the Magnetic Field Explorer (MFE), was introduced.

The major highlights and achievements of the past year are summarized below.

1. Changes in interplate baseline lengths determined using satellite laser ranging (SLR) and very long baseline interferometry (VLBI) were found to be in general agreement with the Minster-Jordan model.

2. The contemporary rate of movement along the Quincy - Otay/Monument Peak, CA, baseline as determined by satellite laser ranging combined with the rate of spreading in the Basin and Range (based on available geological data) has been used to infer rates of motion on off-shore faults west of the San Andreas.

3. Initial baseline measurements were obtained across the subducting area associated with the Nazca and South American Plates. These measurements are currently being repeated to determine motion rates between these two plates.

4. Analysis of length-of-day (l.o.d.) variations for 1983 have shown that atmospheric angular momentum changes associated with the 1982-83 El Nino decreased the l.o.d. by about five milliseconds in late 1983 with a return to normal value after the event.

5. The National Oceanic and Atmospheric Administration (NOAA) Polaris Network, developed cooperatively by NOAA and NASA, was placed into operational use.

6. In partial implementation of an interagency agreement for the establishment of a National Crustal Motion Network (NCMN), Mobile VLBI-3 (MV-3) and the VLBI station at Mojave, CA, were transferred to NOAA by NASA.

7. Agreements were concluded with Austria for laser data exchange and with Israel for operation of a laser system to be provided by NASA on indefinite loan. In addition, agreements with Japan for an initial Pacific Plate experiment was expanded to provide for long-term measurements and, through the European Wegener Consortium, new agreements were concluded with Turkey, Egypt and Tunisia.

8. Interagency field tests of four Global Positioning System (GPS) geodetic receivers were conducted over various baselines to determine their relative performance. (These data are now being analyzed by NOAA.)

9. Transportable GPS Satellite Emission Range Inferred Earth Surveying (SERIES) receivers were tested on a baseline from Owens Valley to Mammoth Lake, CA. Tests coincided with determination of the same baselines using mobile VLBI systems. Five successful GPS observations were made and demonstrated internal consistency in the SERIES data of 3 cm in the horizontal plane and 7 cm in the vertical.

10. Laser and VLBI systems were upgraded; advanced lasers were installed in several Moblas systems and cooled receivers were installed in fixed and mobile VLBI systems. In addition, work was begun on fabrication of Transportable Laser Ranging System (TLRS) -3, and -4.

11. Additional studies of the along-track acceleration of the Laser Geodynamics Satellite (Lageos) -1 orbit have shown that earth albedo radiation asymmetry could be a significant source of this perturbation contribution.

12. An agreement was concluded with Italy for the fabrication and launch of a second Lageos into an orbit with an inclination different from that of Lageos-1. Lageos-2 should help resolve the acceleration source question in addition to expediting and facilitating SLR measurements.

13. Conceptual studies were conducted of a Scout-launched MFE which would be similar to Magsat but have an extended lifetime for studies of the main magnetic field and its secular variation.

14. In a related program, an agreement was signed by NASA and the Italian Space Agency for the development, fabrication and use of a Tethered Satellite System (TSS). Since the TSS is a potential source of high resolution gravity and magnetic field data, provisions will be included in the first TSS flight to permit analysis of the suitability of the TSS for these measurements.

15. Reports were issued on the Geodynamics and Gravity Gradiometer Workshops held in early 1983.

II. PROGRAM OVERVIEW

A. OBJECTIVES

The objectives of the NASA Geodynamics Program are:

- To contribute to the understanding of the solid earth; in particular, the processes that result in movement and deformation of the tectonic plates; and

- To improve measurements of the earth's rotational dynamics and its gravity and magnetic fields in order to better understand the internal dynamics of the earth.

The Geodynamics Program is subdivided into three areas: Earth Dynamics, Crustal Motion, and Geopotential Research.

The objective of the Earth Dynamics Program is to develop models of polar motion and earth rotation, and to relate studies of global plate motion to the dynamics of the earth's interior. This program is expected to lead to an increased understanding of the global structure of the earth and the evolution of the crust and lithosphere. The research conducted in this program includes studies of the dynamic interaction between different regions of the earth's interior and its relationship to crustal magnetization, gravity anomalies and tectonic features. A significant portion of this program element includes activities performed under the CDP, which makes highly accurate measurements of earth rotation and polar motion.

Field measurements and modeling studies of crustal deformation in various tectonic settings are the primary objectives of the Crustal Motion Program. These activities provide measurements, analyses, and models which describe the accumulation and release of crustal strain and the crustal motion between and within the tectonic plates, particularly the North American, Pacific, Eurasian, South American, and Australian plates. Activities include development of quantitative descriptions of the geophysical and geological constraints on the motions of measuring sites, including refinements of global plate motion models and block-tectonic models of the western United States. The investigations also compare the geologically-determined motion vectors between project sites with the geodetically-determined values to test the predictions of geological models.

The Geopotential Research Program uses space and ground measurements to construct gravity and magnetic field models and to investigate data analysis techniques and software systems. Studies of the Lageos orbit and the orbits of near-earth satellites are part of the efforts directed toward advancing gravity field studies. Gravity field data derived from satellite altimetry, satellite-to-satellite tracking, and gradiometry; magnetic field data from satellite magnetometers, and ancillary data, are used in constructing the models.

B. FUNDING

Funding distribution for the Geodynamics Program for fiscal years 1983 and 1984 and planned funding for 1985 is shown in Figure II-1 by program objective, by function, and by organization.

The fiscal year 1984 funds provide for the continuation of a baseline CDP which includes measurement and analysis of regional crustal deformation in the western United States and Alaska, of North American Plate stability, and of global plate motion. Attempts at restoration of Project funding, deleted in earlier years, for studies of regional crustal deformation in the Caribbean Basin, the Mediterranean, and along the western coast of South America were not successful for FY 1985. An earlier, one time increase of $1.9M provided for this purpose in FY 1984 was insufficient (without follow-on year funding) to initiate a program of measurements in 1984. However, the funds did allow the initiation of TLRS-4 fabrication and further development of SERIES in preparation for future measurement programs in these areas.

C. PROGRAM STATUS AND PLANS

Since its inception in 1978, the Geodynamics Program has promulgated the development and use of new techniques for precise position and baseline determination and the formulation and implementation of plans for acquiring the improved gravity and magnetic field models needed for solid earth studies. In the interest of global geodynamics, the NASA program is closely coordinated with other Federal agencies and international groups and, at present, arrangements exist with 27 other countries. These arrangements provide for the acquisition and exchange of data and for coordinated observing programs. While the current precision of the laser and VLBI methods for single measurements of transcontinental and intercontinental baseline is about $\pm$3cm, the ultimate goal of $\pm$1cm appears to be attainable. Similarly, while plans for the acquisition of new gravity and magnetic field data have suffered extensive delays, it now appears that these plans will be implemented in the next few years.

In crustal studies, the past year was transitory in many respects: the development of the systems need for these studies was essentially completed; a vigorous program of global plate motion and western United States regional measurements was initiated; and plans for measurements in the Pacific were developed. In mid 1984, the measurements of regional crustal deformation in the western United States will be extended, with the cooperation of Mexico, to the Gulf of California and, with the cooperation of Canada, to more stable portions of the North American Plate. In addition, initial baseline measurements using VLBI and GPS will be made in Alaska including sites along the Aleutians. The measurements in the United States using mobile VLBI systems will be made by the National Geodetic Survey (NGS) of NOAA under contract to NASA.

Plans for measurement of crustal deformation and plate motion in the Mediterranean in cooperation with the WEGENER Consortium (which consists of representatives from The Federal Republic of Germany, the Netherlands, France, Italy, and Switzerland) are being finalized with the actual measurements to begin in 1985.

The Consortium has concluded arrangements for SLR sites in Turkey, Tunisia and Egypt and is continuing discussions with Greece (Figure II-2). NASA has concluded an agreement with Israel for the location of an SLR station near Jerusalem. This station is expected to be operational in early 1985. NASA has also installed an SLR system at Matera in southern Italy, the operation of which is supported by the Italian government. An agreement was also concluded with Austria for SLR data exchange.

Studies of regional crustal deformation along the western coast of South America in cooperation with Peru, Chile and Bolivia (using SLR) and deformation studies in the Caribbean region (using GPS) were to begin in late 1984 and late 1985, respectively. However, budget constraints continue to impact these studies. A partial solution to the funding problems, currently under discussion, provides for a shared arrangement whereby the United States and European SLR systems would conduct measurements in the Mediterranean and South America in alternate years. However, it is likely that the Caribbean studies will either be delayed several years or postponed indefinitely. A prolonged delay would indeed be unfortunate both because of the scientific importance of studying the tectonics of this complex and interesting region and because of the need for early verification of the value of GPS for scientific studies in seismically active areas of the world.

Measurements of the relative motion of the major tectonic plates using SLR and VLBI are continuing and are beginning to provide rates of motion which are generally consistent with the Minster-Jordan model. In the summer of 1984, extensive Pacific Plate motion measurements will be initiated (using VLBI) in cooperation with Japan and involving temporary sites in Alaska, Hawaii, and the Kwajalein Island in addition to sites in the Continental United States and Europe. Beginning in late 1984, it is planned that plate motion measurements from the United States sites will be primarily obtained for NASA by NOAA using the Polaris Network. Measurements of plate motion involving South America will begin in early 1985 using temporary VLBI sites in Brazil and Chile. Epoch measurements of baselines between the Nazca and South American Plates were made in 1983 using the TLRS. These measurements are being repeated now and will be continued on a yearly cycle.

The global network of fixed SLR stations is providing essentially continuous observations of baselines between plates (along with polar motion and length of day). Stations in the United States, Australia, Tahiti, Mexico, Peru, Japan, China, the Federal Republic of Germany, the Netherlands, Italy, France, Finland, Egypt, Austria and England are participating in these measurements. In 1983, NASA selected the Bendix Field Engineering Corporation (BFEC) as the contractor for management and operation of the NASA global laser tracking network and for assisting cooperating SLR stations in other countries.

In 1984, NASA expects to complete the upgrade of Moblas-3 and -6, and to complete the development and test of TLRS-3 and -4 as well as two Transportable VLBI Data Systems (TVDS-2 and -3).

For a number of years, NASA has been attempting to establish a new Lunar Laser Ranging (LLR) and SLR capability, the McDonald Laser Ranging Station (MLRS), at the McDonald Observatory in Texas, and LLR at Haleakala Observatory in Maui, Hawaii. In addition, under contract with the Australian Division of National Mapping, NASA has provided funding for upgrade of the LLR capability and the addition of SLR.

The new Australian station will be named the Natmap Laser Ranging Station (NLRS). In May 1984, the MLRS successfully ranged to the moon. The NLRS is expected to demonstrate LLR and SLR in the next few months. However, technical difficulties at the Haleakala Observatory have continued and ranging to the moon from this Observatory is not expected prior to the end of 1984.

Intercomparison tests of several models of GPS geodetic receivers were conducted in cooperation with NGS and Defense Mapping Agency (DMA) in late January - early February 1984. Tests were carried out at 10 sites, mostly in California. Long baseline measurements were obtained between the Mojave and both the OVRO, CA, and Ft. Davis, TX, VLBI observatories. The other sites were 22 to 171 km apart. The tests included the Geostar receiver, a single frequency Macrometer, and SERIES. SERIES-X also participated and acquired data for a limited number of baselines. The results of these tests are being analyzed by NOAA and a report is expected in a few months.

Tests were also carried out using SERIES and mobile VLBI receivers stationed at OVRO and Mammoth Lake, CA. Preliminary results indicate an internal consistency for SERIES of 3 cm in the horizontal and 7 cm in the vertical. A report on the SERIES project has been published (NASA 1984c). NASA plans to continue development of SERIES-type receivers and to conduct limited measurements in selected areas.

In November 1983, the Polaris station in Richmond, FL was completed and NOAA began routine acquisition of polar motion and earth rotation data using the full three station network. This marked the completion of a joint NOAA/NASA effort, initiated in 1980, to transfer fixed VLBI technology to NOAA for operational use. In March 1984, per arrangements concluded in late 1983, NASA transferred the VLBI station at Mojave, CA and the newly-developed MV-3 to NOAA: the MV-1 and MV-2 systems will be transferred in early 1985. As provided in the arrangement, NOAA will operate these systems under contract to NASA. In addition NOAA will operate these systems for its own use and as requested by other Agencies. The initial period of operation will be primarily in support of NASA investigator requirements for baseline measurements in the western United States and Alaska. The NASA sites and others included by NOAA have been defined as the sites for the NOAA NCMN.

Progress in the development of field models, particularly gravity field models, has lagged considerably due to funding constraints. However, efforts were initiated in 1983 to develop a specialized gravity field model for the Ocean Topographic Experiment (Topex) orbit determination and work continues on studies of the GRM for launch in the early 1990s. An international working group was established under the auspices of the International Union of Geodesy and Geophysics (IUGG) to continue work on the development of techniques for modeling and analysis using GRM gravity data. NASA established a Science Steering Group to develop and define the scientific rationale for a GRM mission. Its report (GRM SSG, 1983) was published in February 1983.

The last detailed global survey of the earth's magnetic field was accomplished with Magsat in 1980. Predicated on expected changes in the field due to secular variations, the Magsat field models are now obsolete and a new survey is urgently needed before the end of this decade to update international reference main field models and to explore the possibility, identified by several investigators, of sudden accelerations of the westward drift of the main field.

Requirements for earth magnetic field data were determined by a Magnetic Field Survey Working Group (1984) established by NASA. Studies by the Johns Hopkins Applied Physics Laboratory (Galupps and Mobley, 1984) have shown that the MFE, a mission similar to Magsat and launched by a Scout vehicle, could meet requirements for the initiation of a decade or more of continuous field measurements. If an MFE is approved by NASA, the mission could be launched in early 1989.

In December 1983, NASA and the Italian National Research Council signed agreements for the development and launch of Lageós-2 and the TSS. The Lageos-2 satellite and apogee kick motor will be provided by Italy and launched by NASA in 1987. The requirements for, and the mission characteristics of, Lageos-2 were established by the U.S./Italian Lageos-2 Study Group (NASA/PSN, 1983). The TSS is a potential platform for magnetic field and gravity gradiometer measurements. To determine its suitability for these measurements, the TSS will include special accelerometers and "gyros" to measure tether dynamics.

In February 1983, NASA held a workshop to discuss long-range requirements for geodynamics. Another workshop (February 28 - March 3, 1983), was held on the status and plans for gravity gradiometry development. The reports of these workshops were published in 1984 (NASA 1984a, 1984b).

An overview of the NASA Geodynamics Program which describes its inception, rationale, status and plans was published in 1983 (NASA 1984d).

III. CRUSTAL DYNAMICS PROJECT

A. MEASUREMENTS

The observational program of the CDP grew substantially in 1983. New SLR stations in Huahine (French Polynesia), Easter Island (Chile), Mazatlan (Mexico), Matera (Italy), and Herstmonceaux (England) contributed significantly to the measurement of relative motion between the North American, Pacific, Eurasian, Australian, South American and Nazca plates. As shown in Table III-1, the number of monthly baselines measured in 1983 for plate motion was up 42% over 1982, and the number of unique (initial) lines increased 125%. Plate stability measurements also increased in 1983 by a factor of two, and the number of unique intra-plate lines measured was up by a factor of three. Figure III-1 shows the tectonic plates and the location of major global CDP sites.

SLR regional deformation measurements were restricted to the western United States, and particularly California, in 1983. TLRS-1 and TLRS-2 visited Owens Valley Radio Observatory (OVRO), Yuma, Otay Mountain, Quincy, Vandenberg and Bear Lake for measurements between these sites and the western North American base stations. Table III-2 summarizes these measurements, and shows the 1983 total of 123 monthly baseline measurements, which includes colocations at Quincy and Monument Peak. Figures III-2 and III-3 show locations of CDP sites in California and North America, respectively.

VLBI plate motion measurements between North America and Europe are now routinely done by NOAA's Polaris Network, which grew to three North American stations late in the year when Richmond (Florida) joined the Westford (Massachusetts) and Ft. Davis (Texas) stations. In Europe the dedicated VLBI stations at Wettzell (W. Germany) joined Onsala (Sweden) in monthly measurements to North America. North American plate stability measurements were augmented by locating a mobile VLBI system at Platteville (Colorado) between the ends of the OVRO, CA to Westford, MA baseline (Figure III-4).

Regional deformation measurements by mobile VLBI systems (MV-2 and MV-3) and base stations in California and western North America increased from 32 baselines measured in 1982 to 132 measured in 1983. A new base station was established by permanently locating MV-1 at Vandenberg AFB, and the dedicated base stations at Mojave became operational. Reoccupation of sites in the San Francisco area, extensive southern California observations and intercomparison measurement of the SLR San Andreas Fault Experiment (SAFE) baseline were carried out simultaneously using two highly mobile VLBI systems (MV-2 and MV-3). Table III-3 lists the measurements accomplished.

B. VLBI SYSTEM DEVELOPMENT

During 1983 several VLBI stations were upgraded, some new stations were added to the network, and a new mobile system (MV-3) became operational. Arrangements were completed for the transfer of one newly operational base station (Mojave) and the MV-3 mobile system to the NGS; the actual transfer was made in early 1984. For the first time, measurements were made in the western United States with a pair of mobile stations, working together with fixed base stations. Plans were made for a major measurement campaign in Alaska, due to begin in July 1984.

Significant VLBI system milestones achieved in 1983 included:

1. A new base station at Mojave, CA, incorporating an antenna obtained from the NASA STDN complex at Goldstone, CA, became operational. Initial measurements from this station were made in June; data quality was excellent. The station was transferred to the NGS in March 1984.

2. A second highly mobile system, MV-3, became operational, and was first used in the February 1983 VLBI campaign. In the spring of 1983, NGS crew members began training in the operation and maintenance of the MV-3. This training period was completed in 1983 and an operational readiness review was conducted in February 1984. The system was transferred to the NGS in March 1984.

3. During 1983, the upgrade of the MV-1 and MV-2 mobile systems was completed. A dichroic subreflector and feed were added to MV-2, completing the dual S/X frequency capability on all mobile systems. The three electronics vans were completed, and electronics installed and tested. The MV-1 was installed as a permanent base station at Vandenberg AFB, CA.

4. VLBI campaigns in the western United States were conducted in February, June, August, and October 1983. MV-2 and MV-3 visited a large number of mobile sites; fixed stations included in some or all of these bursts included OVRO, Hat Creek Radio Astronomy Observatory, Mojave, Vandenberg (MV-1), and Fort Davis, Texas.

5. VLBI system tests between Mojave and a new station at Kashima, Japan, were successfully made in January 1984 and plans were made to adapt fixed antennas at Hawaii (Kauai) and Kwajalein Island for VLBI measurements. These will be used for the first time in July 1984, in conjunction with the Alaskan VLBI measurements.

6. Eight sites (Figure III-4) were chosen for mobile measurements in Alaska and western Canada, to be conducted in the summer of 1984. The base station will be the fixed NOAA antenna at Fairbanks, Alaska.

7. NASA assisted NGS in bringing up its new station at Richmond, FL which began measurements in November 1983. Weekly measurements are now being made from Richmond, Ft. Davis, TX and Westford, MA. European stations at Wettzell, Germany, and Onsala, Sweden participate in these measurements on a monthly basis.

8. Plans were completed for VLBI measurements in 1984 from fixed antennas at Sao Paulo, Brazil, and Santiago, Chile.

9. Development of the Mark IV Correlator Facility at Caltech continued. However, hardware implementation problems have caused delay of the first operational processing until the summer of 1984. Initial, quick-look fringe verification tests were successfully obtained in real time on two baselines from the November 1983 experiment.

C. LASER SYSTEM DEVELOPMENT

The Geodynamics Program laser network consists of several laser systems located thoroughout the world. Sites in Mazatlan, Mexico; Huahine, French Polynesia; and Matera, Italy were constructed and occupied during 1983. Under the on-going tracking precision improvement program, three additional laser tracking systems were upgraded to a ranging precision of 3 cm rms.

Significant laser system milestones during 1983 included:

1. Upgrades of the Moblas systems at Monument Peak, CA; Greenbelt, MD and Yarragadee, Australia, with passively mode-locked Nd:YAG lasers manufactured by Quantel International, were completed in 1983. The new lasers, with pulse widths of 200 picoseconds, are a significant improvements over the 7 nanosecond pulse width of the previous laser. The new lasers have proven to be reliable for both daytime and nighttime tracking. The CDP plans to complete the upgrade of the remaining Moblas systems with this new laser. Upgraded components (photomultipliers, gating circuits, amplifiers, time intervals units, and discriminators) will also be added to optimize performance of the narrower-pulse Quantel laser to give a single-shot ranging precision of the order of 1 cm rms.

2. The site at Matera, Italy was completed and an upgraded SAO laser system (formerly located at Natal, Brazil) was installed in September, 1983. The system, supplied by NASA, is operated by the Italians under cooperative agreement between NASA and CNR/PSN. The narrower two nanosecond pulse and new analog pulse processing system, have reduced nighttime systematic range errors to 3-5 cm and range noise to 5-15 cm on low satellites and 10-18 cm on Lageos. The pulse repetition rate has been increased to 30 pulses per second (pps), and considerable improvement has been made in signal-to-noise ratio by using a three Angstrom interference filter and by reducing the range gate window to 200-400 nsec.

3. The Goddard Laser Tracking Network mission contract was awarded to the Bendix Field Engineering Corporation in November 1983, concurrent with termination of SAO laser tracking activities. The Arequipa, Peru SAO laser tracking station and certain cooperative foreign laser tracking station support activities previously carried on by SAO were brought under the mission contract. The mission contractor is responsible for upgrading and preparing for shipment the remaining, available SAO laser tracking system for installation in Israel, sometime in 1985.

4. Construction of TLRS-3 and TLRS-4 began in 1983. Completion of these laser tracking systems which are similar to TLRS-2, is scheduled for the latter part of 1984. They employ modular construction, low-power lasers and single-photon detection techniques in order to meet the rapid deployment and high-precision tracking requirements of the CDP. Packaged in shipping containers that are used as part of the system during tracking, they will fit in the cargo hold of standard normal commercial passenger jet aircraft.

5. The site at Mazatlan, Mexico was completed and operational tracking was initiated with Moblas 6 in June 1983. Occupation was made possible through a cooperative agreement between NASA and the Mexican Navy. Located on the Pacific coast of Mexico just south of the Gulf of California, the station has been one of the network's better producers of laser tracking data. It was upgraded in late Spring of 1984 with a new Quantel laser.

6. The site at Huahine, French Polynesia was completed and operational tracking was initiated with Moblas 1 in July 1983. The utility of this site was found to be compromised by generally poorer sky conditions than was anticipated. Although the system is the network's oldest, it produces quality data when weather permits it to track.

7. The TLRS-1, developed and operated for NASA by the University of Texas at Austin, traveled to Yuma, AZ in April 1983; Quincy, CA in July 1983; Monument Peak, CA in September 1983 and Bear Lake, UT in November 1983, tracking the Lageos satellite and acquiring data required to support CDP objectives. The system traveled to Santiago and Cerro Tololo, Chile in early 1984.

8. The TLRS-2, constructed and fielded by GSFC in 1982, successfully completed its data acquisition campaign at Easter Island, Chile and was moved to Otay Mountain, CA in August 1983. At Otay Mountain, CA it acquired data to remeasure the relative position of this site with respect to Monument Peak, CA and Quincy, CA; key sites in the San Andreas Fault Experiment. The system returned to Easter Island, Chile, in March 1984 after a short period at Cabo San Lucas, Mexico.

D. DATA BASE

The CDP Data Information System (DIS) provides for cataloging all Project-acquired data from 1974-1983 as well as new data to be acquired during the lifetime of the Project through 1988 (NASA, 1981a). The main objective of the DIS is to provide approved Project-funded investigators with the necessary scientific data for their studies toward the advancement of the understanding of earth dynamics, tectonophysics, and earthquake mechanisms. The DIS includes a large selection of pre-processed laser and VLBI data acquired at fixed and mobile stations. In addition, analyzed data products, such as baselines, station position coordinates, polar motion data, l.o.d. data, and other related ancillary data products, are made available from the laser and VLBI observations. The information is stored in a Crustal Dynamics Data Information System (DIS) and is directly accessible via a menu-driven user language. The DIS uses a data base management system to enable the users to query, access, and cross-reference the information.

After the completion of conceptual design phase of the DIS in July 1981, the detailed design of the data base was followed by system implementation. Shared utilization of a VAX 11/780 computer at GSFC enabled a rapid implementation of the system, and the system became fully operational in September 1982.

E. CRUSTAL DYNAMICS SCIENCE WORKING GROUP MEETINGS

Working Group Meetings attended by most of the Principal Investigators were held twice in 1983, at JPL in April and at GSFC in October. At each of these meetings, CDP personnel and the investigators exchanged views about the observing stratagies, and the investigators presented their most recent scientific results.

IV. SCIENTIFIC RESULTS

The major source of the results presented in this Section was the Sixth Annual Geodynamics Conference which, this year, was held in conjunction with the Annual Spring Meeting of the American Geophysical Union. At this Meeting, Geodynamics was considered a separate "Theme" (GD). The presentations were coordinated with, and jointly sponsored by other Sections of the AGU (i.e., Geodesy (G), Geomagnetism (GP), and Tectonophysics (T)). Abstracts of Geodynamics Conference papers were prepared in the AGU format and appear in Appendix 2 as extracted from the Program.

References giving the Section designation (GD, G, GP or T) in the following text are to abstracts appearing in Appendix 2. Those expressed as the year of publication appear in the References.

A. CRUSTAL DYNAMICS

1. Plate Motion and Deformation

It is extremely interesting to note, as reported by Ryan, et al. (GD21-07) that over almost a decade, the North American continent appears to have been completely rigid. Within a three-sigma error of 0.5 cm., no change has been detected in 46 VLBI measurements of the baseline between Westford, MA and Owens Valley, CA from 1976 to the present. For the same period, 160 measurements from Westford to Ft. Davis TX have produced the same null result. However, motion over the past four years on the baseline from Westford to Onsala, Sweden appears to have been detected at the rate of 1.3 cm/yr with a three-sigma error of 1.0 cm/yr.

Recent values determined by satellite laser ranging for motion along the baseline from Quincy to Monument Peak, CA were reported by Smith, et al. (GD21-16) as 6.5 +/- 1.5 cm/yr. Using 11 years of satellite laser ranging data acquired with Lageos and BE-C, Christodoulidis, et al. (GD32-06) have determined the right lateral movement across the San Andreas fault to be 6.4 +/- 2.0 cm/yr, in good agreement with the values predicted by the Minster-Jordan model: 5.6 cm/yr. As seen in Figure IV-1, satellite ranging values can be divided into three epochs which can best be fitted by three separate lines: The BE-C line from 1972-79 (-7.2 cm/yr); the early Lageos line from 1979-81 (-5.0 cm/yr) and the late Lageos line from 1981-82 (-7.4 cm/yr). A similar rate, 6.8 cm/yr, was reconfirmed by geodetic data for Baja, CA reviewed by Ness, et al. (GD32-13).

Smith (1984) and Tapley, et al. (1984) have reported values for the relative plate motion between Yaragadee, Australia and sites on the North American plate as determined by satellite laser ranging. There is excellent agreement among the values determined by the two groups and those predicted by the Minster-Jordan model (in cm/yr):

Baseline	Smith	Tapley	M/J
Yaragadee-GSFC	-1.0	-1.4	-1.1
Yaragadee-Texas	-2.0	-1.6	-2.0
Yaragadee-California	-3.5	-3.2	-3.1

Determinations reported by Smith for movement between Yaragadee and Hawaii (-5.3 cm/yr) are in relatively good agreement with those predicted by Minster-Jordan (-6.7 cm/yr). This is also true of the values reported by Tapley, et al. for observations up to mid-1981 (-7.9 cm/yr). However, the values reported for the apparent relative motion from mid-1981 to late 1983 fall off to -2.2 cm/yr. The reason for this discrepancy awaits explanation.

Rates of relative motion among the North American, Austro-Indian, Pacific and South American plates as determined by Christodoulidis and Smith (1983) using satellite laser ranging are shown in Figure IV-2. In this figure, the relative motions determined between barycentric points on the plates are contrasted, with good agreement, to the motions estimated by Minster and Jordan on the basis of the geological record for the same points. On the other hand, Wahr (1984) has observed that due to the effect of the earth's free wobble on crustal motion (1-2 cm over a few years), variations of individual baseline lengths could be as large as 3-4 cm. (Wahr, 1984).

2. Regional Crustal Deformation

Several studies address the problems of regional strain modeling and earthquake source mechanisms.

Cohen (GD12-04) has found that the pattern of surface deformation during the development and release of strain on a strike-slip fault was found to be most sensitive to the rheology of the material lying beneath the fault. Deformation patterns from 10 - 100 km from the fault, especially as determined shortly after an earthquake, are best able to distinguish among alternative models.

Das and Sholz (1983) used spontaneous rupture models with depth gradients of stress drop and frictional strength to investigate the reasons why large earthquakes nearly always nucleate near the base of the seismogenic layer. They find that earthquakes which originate within the (shallow) region of low stress drop are inhibited from propagating.

Smalley, et al. (1984) modeled fault planes as two-dimensional arrays of asperities with statistical distributions of strengths. Stress is transferred from a failed asperity to adjacent asperities. At a critical applied stress, the solutions bifurcate leading to an earthquake, corresponding to stick to slip behavior on the fault. The result explains why the stress on a fault at rupture is less than that predicted using a standard value of the coefficient of friction. A quantitative comparisons of subduction zone earthquakes reveals that the largest earthquakes occur in zones with young lithosphere and fast convergence rates and that the maximum earthquake size is directly related to the distribution of asperities on the fault plane. Ruff and Kanamori (1983) thus infer that plate age and rate affect asperity distribution.

The recurrence interval for major earthquakes in northern California was determined by Scholz (1983) on the basis of slip vs. rupture length laws to be 82 +/- 30 years.

Measurement and understanding of the mechanisms of regional crustal deformation remains a primary objective of the Geodynamics Program. Much of this effort is focused on the tectonics of the western US, particularly California.

Geodetic data from southern California were found by Cohen (GD32-07) to suggest motion of 4.2-4.8 cm/yr with the possibility of additonal deformation north of the Garlock fault near the southern end of the Sierra, Nevada. Similar data covering the Quincy-Monument Peak region indicate a total contraction rate of 5.7 cm/yr which is consistent with the SLR observations. On the other hand, Jordan and Minster (GD32-08) and Minster and Jordan (GD32-09) also used a tectonic plate model to describe the deformation in the zone between the North American and Pacific plates. The difference between the 5.6 cm/yr motion between the two plates, as predicted by their earlier model, and the 3.4 cm/yr observed in the San Andreas fault zone is attributed to motion east and west of this zone. Motion to the east of the zone, estimated by integration of motion through the Basin and Range perceived in the geological record, is 1.01 +/- 0.07 cm/yr with extension to N63W. On this basis, deformation west of the San Andreas must involve 0.4-1.3 cm/yr of crustal shortening orthogonal to the San Andreas and 0.6-2.5 cm/yr parallel to it. Additional evidence for the complexity of the San Andreas fault zone was provided by Crippen, et al. (GD32-11) who used Landsat Thematic Mapper and Seasat imagery.

The results of two years of VLBI baseline measurements were reported by Allen, et al. (GD32-03). Four sites were occupied: Pasadena, CA (JPL), Goldstone, CA (DSS 13), Owens Valley, CA (OVRO) and Fort Davis, TX. The four baselines: Ft. Davis/JPL; DSS 13/JPL, Ft. Davis/OVRO and DSS 13/OVRO showed no movement at the one sigma level. The 335 km OVRO/JPL line shows a possible contraction at 1.3 +/- 0.6 cm/yr. To explain these results, Wallace, et al. (GD32-04) have developed a strain model of southern and central California and Lyzenga, et al. (GD32-05) have carried out numerical simulations of the strain fields in the vicinity of the San Andreas fault. The model emphasized the possibility of a subsurface fault being offset from the surface trace and fault motion being driven by deep basal drag. The anelastic model produces temporally varying strain which might explain the small motions being observed between Owens Valley, JPL and Goldstone.

The zone of strain accumulation adjacent to the San Andreas fault extends only a few tens of kilometers. To explain the narrowness of the zone, Turcotte, et al (1983) proposed a four-layer model of the lithosphere. The model consists of an upper elastic plate extending to 15 km, a soft, intracrustal aesthenosphere, a second elastic layer made up of the tough lower crustal and upper mantle rocks, and finally the aesthenosphere.

Trilateration data were used by Matsu'ura and Jackson (1983) to estimate the relative movement between the North American and Pacific plates in central California as 44 mm/yr in the N34W direction. Their model assesses stress to be rapidly accumulating on the Sargent fault which is locked to a depth of 2.5 km and on a southern segment of the Calavaras Fault, locked to the depth of 15 km.

Complex transform fault boundaries are also modeled by allowing for slip and stress heterogeneity on the fault plane which, itself, can be comprised of individual fault segments of any orientation and individual slip history. Such models are used to understand the horizontal distribution of strain which may be observed in California (Rundle, G12-03). Strain on the OVRO (Owens Valley)-JPL (Pasadena) baseline should be insensitive to variations in assumed thickness of the seismic zone (20-40 km) as well as recurrence interval (20-100 yrs) and is predicted to be -20 mm/yr.

The rate of shortening on the south side of the Transverse Ranges varies from 6 to 14 mm/yr, increasing eastward with the "Great Bend" of the San Andreas fault gradually straightening by a 3 degree/Ma clockwise rotation (Bird and Rosenstock, 1983). Ivins and Lyzenga (GD12-01) have found that the Ranges obstruct the channeling of stress between the North American and Pacific plates in this region and act as a zone of stress concentration (Ivins and Lyzenga, GD12-01). The excess elastically-stored energy may be ten times the stored internal energy.

Based on seismic velocity structure, a model of small-scale convection in southern California predicts upwelling under the Salton Trough and downwelling beneath the Transverse Ranges. This agrees with deformation found on the Moho. An implication of the model is that the "Big Bend" of the San Andreas fault is due to mantle dynamics and not horizontal plate forces (Humphreys and Hager, GD32-12). Models of deformation following the 1940 Imperial Valley earthquake assuming viscoelastic relaxation yield similar vertical magnitudes (ca. 5 cm) and wavelengths (ca. 50 km) to those observed by geodetic measurements after the event (Sauber, et al., GD12-05). At Pinon Flats in southern California, geodetic measurements indicate tilt and strain variations on the order of 3×10^{-7}/yr with fluctuations of the same order of magnitude over periods of months (Wyatt and Agnew, 1983).

Models of regions other than California were also investigated:

- An aseismic deformation may have occurred within the Shumagin seismic gap in the Aleutians between 1978 and 1980. This would increase the stress on the shallow, locked portion of the plate boundary bringing it closer to rupture in a great earthquake (Beavan, et al., 1983);

- The rate of uplift over the mid-crustal magma body of the Rio Grande Rift, as determined by geodetic leveling, has been found to be less (1.8 mm/yr) in the three decades since 1951 than it was for the four decades before that year (3.4 mm/yr) (Larsen, et al., GD22-05);

- Geodetic leveling surveys from 1960 to 1979 in the Ashley River fault zone in South Carolina indicate localized uplift of 2-3 mm/yr on the southwest side of the fault (Poley and Talwani, GD12-10);

- The tectonics of the "Easter Platelet", just west of Easter Island, deviate from an ideal propagating rift. Because of the rapid propagation rate, a significant time is required for the dying ridge to stop and the growing one to assume all the spreading with the result of a "platelet" between the two ridges Engeln and Stein (1983a,b);

- Movement along the southern Caribbean strike-slip plate boundary zone was estimated as 1.6 cm/yr by study of the deformation of six-million year old mud diapirs (Burke, et al., GD12-11);

- Field, seismic and satellite remote sensing data of the North and East Anatolian Faults indicate considerable deformation in the plate between these two fault zones (Hempton, GD12-06);

- The 1700-km long Altyn Tagh fault is seen, using satellite remote sensing data, as a complex structure with parallel faults and rotated blocks. The fault is predominantly strike-slip east of 80°E and thrust to the west of this longitude (Preisig and Gillespie, GD12-08);

- Off-ridge earthquakes near the Southeast Indian Ridge are characterized by normal faulting mechanisms. This may be due to the on-going collision between India and Asia and has implications for the study of apparent velocities between plates separated by long baselines crossing oceanic regions (Bergman, et al., 1983).

3. Global Tectonics

Nakanishi and Anderson (1983), using data on long-period Love and Rayleigh seismic waves have mapped mantle heterogeneity between 100 - 600 km. However, some regions are anistropic as well, with seismic wave propagation being a function of the direction of propagation. Using available phase and group velocity data, inverted for ocean structure as a function of age, and taking into account anelastic dispersion, sphericity and anisotropy, Anderson and Regan (1983) have created models of the mantle having a high-velocity layer which thickens with age at the top, and an anistropic low-velocity zone with age-dependent anisotropy beneath. They find that the seismic lithosphere reaches a maximum thickness of 50 km: comparable in thickness to the elastic or flexural lithosphere. This raises the possibility that both are controlled by effects other than temperature, stress or time such as mineralogy, crystal orientation or partial melting. This is attributed (Tanimoto and Anderson, 1984) to the alignment of anistropic olivine crystals along flow directions in the mantle. The flow appears to be disturbed at hotspots. There is also a strong correlation between the geoid and surface wave velocity at degree and order 4 and 5 with slow regions associated with geoid highs and high heat flow. This is consistent with upwelling convective flow or with isostatically compensated regions of low density.

Richards and Hager (1983) have modeled the mantle's dynamic response to an arbitrary distribution of density contrasts using self-gravitating flow models and a variety of viscosity variations and flow configurations. They have found that boundary deformation due to such loading reaches equilibrium on the same timescale as glacial rebound; much less than that required for significant change in the convective flow pattern. Thus, for uniform mantle viscosity, the geoid signature due to boundary deformation is much larger than that due to internal loads resulting in negative anomalies for positive density contrasts. They also find that geoid anomalies are primarily the result of density contrasts in the interior of convecting layers. Viscosity stratification leads to more complicated spectral signatures.

The Hager/O'Connell global flow model was used by O'Connell and Hager (1983) to estimate stresses contributing to the plate driving forces. On transform faults and collisional boundaries, these were determined to be 70 bars distributed over a lithosphere which is 100 km thick. The RMS residual torque is 25% of the force required to drive the plates and thus the model can account satisfactorily for present-day global plate motions.

The correlation between Benioff zones beneath island arcs and seismic coupling at the slab-mantle interface strongly suggests that the global return convective flow extends below 700 km. (Hager, et al., 1983). Vasiliou, et al. (1984) found that a barrier to mantle flow at 670 km is required in order to match the seismicity and stress required by numerical models of subducting slabs. This barrier might be a viscosity increase or a chemical discontinuity. The model predicts downward compression in the slabs at depths below 300 - 400 km.

Using data on earthquake focal mechanism, Weins and Stein (1983) found that oceanic lithosphere older than 35 Ma is almost entirely in a compressional state. Their data support the idea of oceanic plates largely decoupled from the mantle by a thin, low-viscosity asthenosphere. In oceanic lithosphere younger than 35 Ma, thrust and strike-slip faulting predominate except in the Indian Ocean where many extensional events occur. Vasiliou (1983) has found that deep earthquakes in subducting slabs tend to have their compression axes aligned with the dip of the slab. For intermediate earthquakes (from 70 to 300 km), there is some evidence for down-dip tension, but the alignment is not obvious.

The indication of cyclical sedimentation sequences at passive Atlantic margins in the range of 20,000-300,000 yr correspond to possible changes in global gravity anomalies on the order of 10 mgal. The latter change is hypothesized to be due to instabilites in upper mantle convection and observed vertical plate motions (Officer and Drake, GD22-08).

Low rates of plate motion were found to be correlated with the emplacement of kimberlites in old continental crust by England and Houseman (1983) who suggest that this might be related to small scale convection in the mantle. In further studies, (Houseman and England, 1983) they found that deformation of continental lithosphere by buoyant plumes could produce substantial stretching of the lithosphere and the formation of sedimentary basins and suggested that this might be the origin of some intracontinental extensional features. Centrifuge experiments carried out by Nataf and Hager (1983) have demonstrated that such plumes could well play the most important role in small scale convection within the earth.

Chase and Spraul (GD22-11) determined that, on geological timescales, well dated and defined hotspots in the northern Pacific move northerly at 1-2 cm/year while those in the southern Pacific move southerly at the rate of 1.5-7 cm/yr. It thus appears that the apparent fixity of hotspots is misleading and that differences between paleomagnetic reconstructions and fixed hotspot reconstructions are not necessarily indicative of true polar wander. The apparent lack of true polar wander corresponds, according to Davis and Solomon (1983) to the cancellation of trench-pull and ridge-push torques. True polar wander may have occurred in earlier geologcal times when these forces did not cancel each other.

The preference of hotspot locations for geoid highs (especially over the African, Eurasian and Antarctic plates) was noted by Stefanick and Jurdy (1983). The velocities of plates in the early Tertiary with respect to hotspots was found by Jurdy and Gordon (1983) to resemble those at the present.

B. EARTH DYNAMICS

Recently, there has been a great deal of scientific interest in the problem of the transfer of angular momentum among the atmosphere, the oceans, and the solid earth. It is possible to compute the amount of angular momentum contained in the atmosphere as a function of time from the data collected by meteorological centers for use in weather forecasting. Using the axial component of the atmospheric angular momentum (AAM) computed from the zonal wind data obtained by the U.S. National Metoerological Center (NMC), Rosen and Salstein (1983) previously showed that, on time scales of a year or less during the period 1976-1981, changes in the l.o.d. were closely correlated with changes in the AAM (See Figure IV-3).

Salstein and Rosen (G41-05) are attempting to obtain all three components of the AAM from the NMC data for 1976 to the present. In order to judge the accuracy of AAM values, they compared values of the axial components derived from NMC data and data from the European Center for Medium-Ranged Forecasting (EC). There is good agreement between EC and NMC values of AAM in high northern latitudes but for equatorial latitudes and the southern hemisphere, the AAM values derived from NMC data are larger than those derived from EC data. They also reported that axial AAM values during January and February, 1984 appear to be anomalously low corresponding to very strong easterly trade winds during this period.

Rosen, et al. (1984) have shown that during late January 1983, when the unusually strong El Nino/Southern Oscillation (ENSO) event was at its peak, record values of the axial component of the AAM were obtained which were well correlated with an observed peak in the l.o.d. In order to test the statistical significance of this relationship, Eubanks, et al. (G41-06) constructed an estimate of the "normal" yearly behavior of these time series by averaging all of the data for the same time of year during the period 1976-1982.5. They found that the anomaly seen in the axial AAM and l.o.d. values were 3.9 and 3.8 standard deviations, respectively, greater than "normal".

Potash and Clark (G41-08) point out that weekly averages of l.o.d. measurements obtained by the POLARIS network using VLBI are accurate to better than than 25 microseconds. Comparison between these and weekly axial AAM data for the period from 1980 to the present yielded a correlation coefficient of 0.87; after periodic terms of 6, 12 and 24 months were removed, the correlation coefficient was 0.77. Pronounced excurions of both l.o.d. and axial AAM values were noted during the 1982-1983 El Nino event.

The Southern Oscillation Index is used to quantify fluctuations in the atmospheric circulation cell above the equatorial Pacific. (It is defined as the seasonally adjusted surface pressure difference between Tahiti and Darwin normalized by the standard deviation of each station's monthly pressure values.)

The 1982-1983 ENSO event caused this index to achieve its lowest value ever recorded. Chao (G41-07) compared BIH l.o.d. values from which both short (i.e., <1 yr) and long (i.e., 10 yrs) period terms had been removed with SOI values for the period 1957-1983 and found a correlation coefficient of -0.55 (See Figure IV-4). In a similar study using data from 1970 to the present, Eubanks, et al. (G41-06) found a coefficient of -0.52. The latter authors also evaluated an earlier suggestion that axial AAM was transferred to the earth due to torques resulting from pressure differences on opposite sides of mountain ranges. However, they found the correlation coefficient between the SOI and solid earth torques to be only 0.27 suggesting a more complicated mechanism for momentum transfer.

Gross and Chao (G41-10) tested whether the 1982-1983 ENSO event had any influence on the Chandler Wobble by comparing the SOI data to data on the y-component of the Chandler wobble's excitation function derived from Lageos polar motion data. A slow drop and rise in the y-component values match the behavior of the SOI values and a minimum in the SOI in January, 1983 was matched by a valley in the y-component of the excitation function. These results provide some empirical evidence that the Southern Oscillation affected the Chandler wobble.

Wahr (G42-01), however, states that the combined effects of the atmosphere and oceans account for no more than 20 - 25 per cent of the total excitation of the Chandler wobble during the period 1900-1973; that the limited effect is due to transfer of angular momentum from the atmosphere to the earth by mountain torques.

LLR, SLR and VLBI are now providing more accurate data on earth rotation rate and polar motion than ever before possible. Eanes, et al. (G42-06), using Lageos data, reported an internal precision (3-day averages) of 2 milliarc seconds for polar motion and 0.15 millisec. for earth rotation. Gaussian filtering was used by King, et al. (G42-02) who found differences between SLR and VLBI pole position values of 2.3 milliarc seconds for x and y components. Hernquist, et al. (G42-03) and Spieth, et al. (G42-04) described the use of the Kalman filter smoothing to analyze VLBI data sets.

C. GEOPOTENTIAL FIELDS

1. Gravity Field Modeling

Continued and expanded analyses of Lageos laser tracking data have enabled refinement of the value of GM (the product of the gravitational constant and the earth's mass). Kolenkiewicz, et al. (GD41-03) report this new value as $398600.434 \pm 0.005 Km^3 sec^{-2}$. Lageos data have also been used to estimate some rheological properties of the mantle at decadal time scales; i.e., intermediate between those determined by seismology and geology (>minutes; <100's of years). Sabadini and Yuen (GD41-01) showed that data on the secular variation of the gravitational harmonic, J_2 are consistent with viscosities in the range 1021 - 1022 P and with modest values of the modulus defect parameter. The tidal Love number for the 18.6 year tide has been determined to be 0.36. The long-term viscosity of 1022 P can contribute 25% of the tidal Love number at 18.6 years.

On the other hand, the strong correlation between the geoid and the depth of crustal structures in the marine regions of Fennoscandia indicates, according to Anderson (G32-07), that the isostatic geoid anomaly has been over-estimated. The re-evaluated anomaly is consistent with an upper mantle viscosity closer to 1021 P rather than the 4X1022 previously assumed.

2. Analysis of Geoid Data

Data acquired by the Seasat altimeter on the shape of the geoid continue to form the basis for significant investigations. Turcotte (G32-01) pointed out that, considering the age of the lithosphere near fracture zones, the slope of the geoid indicates a crustal thickness of 75-100 km.; that there was no evidence of the asthenosphere near hot spot swells, just the thinning of the oceanic lithosphere; that Iceland appears to have deep structure but Hawaii does not. However, it was pointed out (Watts, G32-02) that the gravity field was a better tool for the study of the Hawaiian anomaly and that the geoid/age relationship places a lower limit of 50 km. on the thickness of the oceanic lithosphere. McAdoo, et al. (G32-04) studied flexures at the outer rise and concluded that the effective elastic thickness (less than the lithospheric thickness) is 60 km. They also determined that oceanic lithosphere continues to thicken at ages at least up to 150 Myr.

In a related study of source mechanisms of earthquakes near mid-ocean ridges (in lithosphere <30 Ma old), Bergman and Solomon (1984) have found that seismic deformation occurs in young (<15 Ma) lithosphere. Horizontal compressive stress (ridge-push) does not seem to be the dominant source of the earthquakes but thermoelastic stress resulting from cooling of the lithosphere seems to play an important role.

Two distinct thermal regimes in the south and northeast Pacific Ocean lithosphere were noted by Cazanave and Lefebvre (G32-05): one for crust less than 25 Ma, the other greater than 30 Ma. The associated crustal thicknesses are about 65 and 90 km, respectively.

The Seasat altimeter data were used in developing or analyzing several tectonic models although, as pointed out by Richards and Hagar (G32-03), the interpretation of geoid anomalies is complicated by the effects of deformation of the earth's surface and internal boundaries caused by convection. However, their model based on seismic data and linear viscous response functions correlates to 70% with the geoid measured at degree and order 2-9. They conclude that boundary deformation is highly dependent of viscosity structure and that the thermal structure of the lower and upper mantle is continuous.

Two new fracture zones which record the movement of Africa and India away from Antarctica have been discovered and roll-like features on the Indo-Australian plate may reflect small-scale convection beneath that plate (Weissel and Haxby, G32-12).

3. Magnetic Field Modeling

The problem of determining the value of the magnetization of the crustal source-layer from Magsat data was discussed by Harrison and Hayling (GP32-01) and Hayling and Harrison (GP32-02). Quite surprisingly, they have found that continental and oceanic crusts have nearly equal magnetization and that the natural remanent magnetization of the oceanic crust is about 1.4 A/m.

On the other hand, Arkani-Hamed and Strangway (GP32-03) have found that young ocean basins have low susceptibility while cratons and rifts have higher values. In order to eliminate effects from external magnetic fields they first separated data acquired in dawn and dusk Magsat overpasses. Correlation of the two data sets in terms of their spherical harmonic variations indicated significant correlation between degree and order 18-44. Data from both sets in this harmonic interval were then averaged to form a global crustal scalar magnetic anomaly map.

Magsat data were used in studying specific tectonic features:

- The Ontong-Java submarine plateau can be modeled by a simple thickened magnetic crust with magnetization corresponding to the surrounding oceanic crustal layer (Frey, GP32-10);

- The Shatsky rise of the north Pacific ocean is magnetized by induction of rocks with susceptibility = 0.006 emu/cc. The model was produced using bathymetric and seismic refraction data suggesting that the Moho is the lower boundary of the magnetized layer in this area (Raymond and LaBrecque, GP32-06);

- The Lord Howe Rise between Australia and New Zealand shows a positive Magsat anomaly and thus cannot simply be submerged ordinary continental crust Frey (1984) assumed an induced origin for the satellite-elevation anomaly, used known crustal structure and constructed a model of the Rise having a lower layer of unusually high susceptibility which might have been caused by alteration related to subsidence of the plateau.

- The north Atlantic seems to be a source of remanent magnetization; its slow spreading ridge does not produce a magnetic signature (Raymond and LaBrecque, GP32-06);

- The Middle-America trench can be modeled by a down-going slab with a magnetization contrast of 5 A/m (Vasicek, et al., GP32-11);

- Magnetic contrast at continent/ocean boundaries are discernable in reduced-to-pole Magsat data when these boundaries are at high angles to the local magnetic longitude and to the satellite orbital track (Schnetzler, et al., GP32-12);

- A new magnetic anomaly map of South America (Ridgeway, et al., GP32-09) based on Magsat data indicates that alacogens are correlated with negative features and ridges with positive anomalies;

- The large "Kentucky" anomaly in the southeast United States seen in Magsat is, according to aeromagnetic data, composed of three smaller anomalies. Ruder and Alexander (GP32-13) found that the granitic crust, which contributes little to the total crustal magnetic field, is thinned in this region (according to seismic evidence) and the effect was stripped from the total anomaly. This enabled them to assess the magnetic susceptibility of the three lower crustal magnetic bodies.

The positive magnetic anomaly in the south-central United States was found to result from the superposition of the effects of two primary elements: granite intrusions, rhyolite flows and metamorphic basement rocks of the Texas panhandle and a northern segment corresponding to the Wichita igneous complex (Starich, et al., GP32-08);

The enhanced data set expected from the proposed GRM mission was investigated by Strangway and Arkani-Hamed (GP32-04) and Taylor, et al. (GP32-05) using existing large-scale magnetic maps. The former determined Magsat noise levels to be +/-2nT but that this could be reduced to +/-1nT in the future mission. Taylor, et. al., determined that the GRM mission should be able to resolve two distinct magnetized bodies by a factor of 10 better than Magsat.

V. ADVANCED STUDIES AND MISSIONS

The activities this year are in two main subdivisions: geopotential (gravity and magnetic) fields and improved crustal motion measurements. Except for the addition of the Lageos-2 mission, the activities parallel the efforts of last year.

A. GRAVITY AND MAGNETIC FIELD MEASUREMENTS

Studies supporting the initiation of the GRM continued. This included the completion of a major guidance and control system simulation, discussions with the Italian scientific community aimed at the formulation of a joint U.S./Italian GRM and the formation of the GRM SSG. The SSG issued a report which updated the scientific goals and objectives of the GRM (GRMSSG, 1983). A GRM Science Conference is being planned for the Fall of 1984.

Work continued on the development of a cryogenic gravity gradiometer following the successful test of the single axis unit which was discussed in the previous Annual Report (NASA, 1983). The design of the three-axis unit has been completed and construction has begun. This unit will be equipped with a six-component cryogenic accelerometer which will be located in the central cavity, The U.S. Air Force and the U.S. Army have begun to share in the cost of the program. The final measurement goal for the gradiometer is a sensitivity of better than 10^{-3} E/Hz$^{1/2}$ and for the accelerometer, asensitivity of better than 10^{-9} g/Hz$^{1/2}$.

The Announcement of Opportunity for the United States investigations for the joint U.S./Italian TSS was issued this past year. The system will provide an opportunity for obtaining high resolution gravity and magnetic field data.

B. CRUSTAL MOTION AND EARTH DYNAMICS

The previous Annual Report described three techniques which utilized the GPS. These are the Geodetic Navstar (GEOSTAR) supported by DMA, NGS and the USGS; the SERIES sponsored by NASA; and the Miniature Interferometeric Terminal for Earth Surveying (MITES) supported by NASA, the U.S. Geological Survey (USGS) and the USAF.
A fourth and new system called the Macrometer has been developed commercially having benefited from support through MITES. In February, 1984, the GEOSTAR, SERIES, and Macrometer systems were operated in a test in which 10 separate baselines in the western US ranging from about 20 km to about 1500 km were occupied over a two week period. The results of this intercomparison experiment are to be reported by NOAA/NGS in the latter part of 1984.

In February, 1983, the NASA Administrator and the President of the National Research Council of Italy signed an agreement whereby a second Lageos satellite will be launched by the Space Shuttle. The satellite will use an interim stage built by Italy to place it into an orbit with an altitude similar to that of Lageos-1. The only difference between these satellites is that Lageos-2 will be in a prograde 52 degree orbit compared with the retrograde 110 degree orbit of Lageos-1. The availability of Lageos-2 should strengthen the geodetic results of satellite laser ranging and permit more accurate baselines, pole positions, earth rotation, gravity and time-dependent gravity parameters to be obtained. Due to the increased number of observing possibilities, the enhanced results should be possible with less total effort on the part of tracking stations.

REFERENCES

Anderson, D. L. and J. Regan, Uppermantle anisotrophy and the oceanic lithosphere, Geop. Res. Letters, 10, 841-844, 1983.

Beavan, J., E. Hauksson, S. R. McNutt, R. Bilham and K. H. Jacob, Tilt and seismicity changes in the Shumagin seismic gap, to be published in Science, 1983.

Bergman, E. A., J. L. Nabelek and S. C. Solomon, An extensive region of off-ridge normal-faulting earthquakes in the southern Indian Ocean, MIT preprint, Submitted to JGR, June, 1983.

Bergman, E. A., and Solomon, S. C., Source mechanisms of earthquakes near mid-ocean ridges from body waveform inversion; Implications for the early evolution of oceanic lithosphere, submitted to JGR, 1984.

Bird, P., and R. W. Rosenstock, Kinematics of present crust and mantle flow in southern California, Bull. Geol. Soc. Amer., in press, 1983.

Christodoulidis, D. C., and D. E. Smith, The role of satellite laser ranging through the 1990's, NASA Technical Memorandum 95104, Goddard Space Flight Center, Greenbelt, MD 20771, Sept., 1984.

Das, S., and C.H. Scholtz, Why large earthquakes do not nucleate at shallow depths, Nature 305, 621-623, 1983.

Davis, D. M., and S. C. Solomon, True polar wander and plate driving forces (Abs.), EOS 64, 843, 1983.

Engaln, J. F., and S. Stein, Constraints (?) on Easter platelet tectonics (Abs.), EOS 64, 310, 1983a.

Engeln, J. F., and S. Stein, Tectonics of the Easter plate, sub. to Earth and Planetary Science Letters, July 1983b.

England, P., and G. Houseman, On the geodynamic setting of kimberlite genesis, Earth Plan. Sci. Lett. 67, 109-122, 1984.

Frey, H., Magsat and POGO magnetic anomalies over the Lord Howe Rise: Evidence against a simple continental crustal structure, Preprint, Goddard Space Flight Center, Greenbelt, MD, 20771, 1984.

Galupppi, R. G., and F. F. Mobley, Conceptual Design for the Magnetic Field Explorer MFEx Satellite, Space Dept., Applied Physics Laboratory, Johns Hopkins Univ., Laurel, MD 20707, May, 1984.

Geopotential Research Mission Science Steering Group, Geopotential Research Mission - Scientific Rationale - Geodynamics Branch, Code EEG, NASA, Washington, DC 20546, Feb., 1983.

Hager, B. H., R. J., O'Connell and A. Raefsky, Subduction, back-arc spreading and global mantle flow, tectonophysics 99, 165-189, 1983.

Jurdy, D. M., and R. G. Gordon, Global plate motions relative to the hotspots 64 to 56 m.y. B.P., submitted to JGR, 1983.

Matsu'ura, M., and D. D. Jackson, Inverse dislocation model for Hollister trilateration data, UCLA preprint, 1983.

Magnetic Field Survey Working Group, A Satellite Mission to Measure the Geomagnetic Field and its Secular Change, Geodynamics Branch, Code EEG, NASA Washington, DC 20546, Jan., 1984

NASA, Geodynamics Program: Annual Report for 1979. NASA TM 81978, National Aeronautics and Space Administration, Washington, DC, 1980.

NASA, Geodynamics Program: Annual Report for 1980. NASA TM 84010, National Aeronautics and Space Administration, Washington, DC, 1981.

NASA, Geodynamics Program: Annual Report for 1981. NASA TM 85126, National Aeronautics and Space Administration, Washington, DC, 1982.

NASA, Geodynamics Program: Annual Report for 1982. NASA TM 85842, National Aeronautics and Space Administration, Washington, DC, 1983.

NASA, Spaceborne Gravity Gradiometers, NASA Conference Publication 2305, Scientific and Technical Information Branch, NASA Washington, DC 20546, 1984a.

NASA, Report of the Geodynamics Workshop, NASA Conference Publication 2325, Scientific and Technical Information Branch, NASA, Washington, DC 20546, 1984b.

NASA, Satellite Emission Range Inferred Earth Surveying (SERIES) Project: Final Report on Research and Development Phases 1979 to 1983. JPL Publication 84-16, 1984c.

NASA, The NASA Geodynamics Program: An Overview. NASA TP 2147, National Aeronautics and Space Administration, Washington, DC, 1984d.

NASA/PSN, Report of the NASA/PSN Lageos-II Study Group. Geodynamics Program, NASA Headquarters, Washington, DC, January, 1983.

Nataf, H.-C., B. H. Hager and R. F. Scott, Hot spots in a very viscous fluid: Convection experiments in a centrifuge, Cal. Inst. Tech. preprint, to be submitted to Annals Geop., July, 1983.

O'Connell, R. J., and B. H. Hager, Estimates of driving forces and stresses for lithospheric plates (Abs.), EOS 45, 673, 1983.

Richards, M. A., and B. H. Hager, Geoid anomalies in the dynamic earth, Cal. Inst. Tech. preprint, sub. to JGR, Sept. 1983.

Ruff, L., and H. Kanamori, Seismic coupling and uncoupling at subduction zones, Tectonophysics 99, 99-117, 1983.

Scholz, C. H., Earthquake prediction and siesmic hazard, sub. to Earthquake Prediciton Research, May, 1983.

Smalley, R. F., Jr., D. L. Turcotte and S.A. Solla, A renormalization group model for the stick-slip behavior of faults, sub. to JGR, 1984.

Smith, D. E., Report to Crustal Dynamics Project Principal Investigators Meeting, Boulder, CO, March 1984.

Stefanick, M., and D. M. Jurdy, the distribution of hotspots, sub. to JGR, 1983.

Tanimoto, T., and D. L. Anderson, Mapping convection in the mantle, Geop. Res. Let. 11, 287-290, 1984.

Tapley, B. D., B. E. Schutz, R. J. Eanes and G. W. Rosborough, Determination of baselines using satellite laser ranging, Report to Crustal Dynamics Principal Investigators Meeting, Boulder, CO, March, 1984.

Turcotte, D. L., J. Y. Liu and F. H. Kulhawy, The role of intracrustal asthenosphere on the behavior of major strike-slip faults, Cornell U. preprint, sub. to JGR, 1983.

Vassiliou, M.S., The state of stress in subducting slabs as revealed by earthquakes analysed by moment tensor inversion, Cal. Inst. Tech. preprint, sub. to Earth and Planetary Sciences Letters, Sept., 1983.

Vassiliou, M. S., B. H. Hager and A. Raefsky, The distribution of earthquakes with depth and stress in subducting slabs, J. Geodynamics 1, 11-28, 1984.

Wahr, J. M., Deformation induced by polar motion, in preparation, 1984.

Weins, D. A., and S. Stein, Implications of oceanic intraplate seismicity for plate stresses, driving forces and rheology, sub. to Tectonophysics, 1983.

Wyatt, F., and D. C. Agnew, High-precision continuous deformation measurements in southern California (Abs.), presented at IUGG, Hamburg, August 1983.

TABLE III-1

SLR PLATE MOTION, PLATE STABILITY BASELINES

			1982		1983	
PLATE MOTION BASELINES:						
NORTH AMERICA	-	PACIFIC	76	(8)	119	(15)
		NAZCA	--	--	16	(5)
		AUSTRALIA	41	(4)	26	(5)
		EURASIA	63	(11)	107	(30)
		SOUTH AMERICA	29	(4)	50	(5)
PACIFIC	-	NAZCA	--	--	8	(3)
		AUSTRALIA	22	(2)	14	(3)
		EURASIA	63	(11)	62	(18)
		SOUTH AMERICA	15	(2)	28	(3)
NAZCA	-	AUSTRALIA	--	--	2	(1)
		EURASIA	--	--	4	(6)
		SOUTH AMERICA	--	--	4	(1)
AUSTRALIA	-	EURASIA	18	(3)	17	(6)
		SOUTH AMERICA	8	(1)	6	(1)
EURASIA	-	SOUTH AMERICA	7	(2)	24	(6)
			342	(48)	487	(108)
PLATE STABILITY BASELINES:						
		NORTH AMERICA	51	(6)	84	(10)
		PACIFIC	11	(1)	20	(3)
		NAZCA	--	--	--	--
		AUSTRALIA	--	--	--	--
		EURASIA	6	(1)	27	(15)
		SOUTH AMERICA	--	--	--	--
			68	(8)	131	(28)

( ) = Possible unique lines

TABLE III-2

SLR REGIONAL DEFORMATION MEASUREMENTS IN 1983

THOUSANDS OF POINTS

	TLRS-1		TLRS-2		SUPPORTING BASE STATIONS					
	SITE	PTS	SITE	PTS	QUINCY, CA	PLATTEVILLE, CO	FT DAVIS, TX	MAZATLAN, MX	MONUMENT PK, CA	BASELINES TOTAL (1)
JAN	OVRO	14.0			23.1	2.2	3.2		15.3	10
FEB	VANBRG	0.3			3.8	1.2	5.5		5.9	6(b)
MAR	YUMA	0.8			6.6	5.2	30.0		8.9	6(b)
APR	YUMA	5.3			19.3	1.9	7.3	4.7	15.2	15
MAY	YUMA	2.3			24.5	1.6	1.8	9.9	3.7	15
JUN	YUMA	6.8			1.1	0.5	0.9	9.5	9.4	6
JUL	QUINCY	0.5			62.4	0.7	0.3	3.1		1(b)
AUG	QUINCY	7.1			76.6	0.1	4.2	16.2		3(b)
SEP	MON PK	25.8	OTAY	----	126.5	2.8	8.2	12.6	T	10(b)
OCT	MON PK	53.8	OTAY	40.0	48.7	8.3	2.0	23.9	86.8	15
NOV	BEAR L	2.9	OTAY	8.0	2.2	3.6	4.7	16.6	21.4	21
DEC	BEAR L	5.4	OTAY	6.6	7.0	0.4	1.9	7.1	11.9	15
										123 (1983)
										79 (1982)

(b) = all baselines between base stations

(1) Requires 1000 points per station for month to be a valid baseline between stations; e.g. during July the only valid baseline was between the two base stations at Quincy, CA and Mazatlan, MX. TLRS-1 at Quincy, CA with only 500 points was not valid.

TABLE III-3

VLBI REGIONAL DEFORMATION, PLATE STABILITY MEASUREMENTS IN 1983

	MOBILE SITES		PURPOSE*	SUPPORTING BASE STATIONS							
DATE	MV 2	MV 3		OVRO, CA	MOJAVE, CA	HAT CREEK, CA	FT DAVIS, TX	WESTFORD, MA	PASADENA, CA	VANDENBERG, CA	LINES
FEB	PEAR BLOSSOM, CA	VANDENBERG AFB, CA	R	*					*		6
	PINYON FLATS, CA	VANDENBERG AFB, CA	R	*			*		*		10
JUN	---	PLATTEVILLE, CO	S	*		*	*	*			10
	(1) ELY, NV	PLATTEVILLE, CO	S	*		*					3
	(1) VERNAL, UT	PLATTEVILLE, CO	S			*	*				6
	QUINCY, CA	MONUMENT PEAK, CA	RI	*	*	*	*				15
	MAMMOTH LAKES, CA	JPL, PASADENA, CA	R	*	*	*					10
AUG	JPL, PASADENA, CA	PEAR BLOSSOM, CA	R	*	*					*	10
			S	*	*		*				3
	THE PRESIDIO, CA	FORT ORD, CA	R	*	*					*	10
	THE PRESIDIO, CA	POINT REYES, CA	R	*	*					*	10
	DEADMAN LAKE, CA	SANTA PAULA, CA	R	*	*					*	10
OCT	JPL, PASADENA, CA	PEAR BLOSSOM, CA	R		*					*	6
	JPL, PASADENA, CA	PINYON FLATS, CA	R	*	*					*	10
NOV	YUMA PROVING GROUNDS, AZ	PINYON FLATS, CA	R		*					*	6
	YUMA PROVING GROUNDS, AZ	MONUMENT PEAK, CA	RI	*	*		*				10
	BLACK BUTTE, CA	MONUMENT PEAK, CA	RI		*		*			*	10
	BLACK BUTTE, CA	(1) OCOTILLO, CA	R		*					*	3
	PALOS VERDES, CA	(1) OCOTILLO, CA	R	*	*					*	6

TOTAL BASELINES (1983) 154

REGIONAL (1983) 132

REGIONAL (1982) 32

(1) SYSTEM FAILURE AT THESE STATIONS

* R - REGIONAL DEFORMATION
  S - PLATE STABILITY
  I - INTERCOMPARISON

FIGURE CAPTIONS

II-1. Geodynamics Funding Distribution. Funding in FY 83, FY 84 and projected for FY 85 by objective, function and organization.

II-2. Mediterranean Sites. Existing and proposed laser ranging sites for use in studying the tectonics of the Mediterranean region in cooperation with the Wegener Consortium.

III-1. Global Crustal Dynamics Project Sites. Outlines the major tectonic plates and shows global locations of Crustal Dynamics Project (CDP) observation sites for both fixed and transportable VLBI and laser ranging stations.

III-2. California Crustal Dynamics Project Sites. Shows California locations of all CDP observation sites for both fixed and transportable VLBI and SLR stations.

III-3. North American Crustal Dynamics Project Sites. Shows North American locations of all CDP observation sites for both fixed and transportable VLBI and SLR stations.

III-4. Alaska Regional Deformation and North America Stability VLBI Sites. Shows Alaska and western Canada mobile VLBI sites operating with the Fairbanks, Alaska VLBI base station for regional deformation measurements; also shows the fixed VLBI stations in North America used for plate stability measurements along with the added mobile VLBI site at Platteville, Colorado. (See Table III-3)

IV-1. San Andreas Fault Experiment. Results of 10 years of measurements of motion on the San Andreas Fault using laser ranging to the BE-C (upper line) and Lageos (lower lines). (from Smith, 1984).

IV-2. Inter-Plate Deformations Observed by SLR. Relative motions as computed using laser ranging data for barycentric points on the respective plates and compared with values estimated using the Minster-Jordan model for the same points. (from Christodoulidis and Smith, 1984).

IV-3. Variation of atmospheric angular momentum and excess length of day. Excess length of day (l.o.d.) compared with axial component of the atmospheric angular momentum (M) for the period 1981.5-1983.5. (from Salstein and Rosen, 1984).

IV-4. Variation of Southern Oscillation Index and excess length of day. Excess length of day (l.o.d.) compared with values for the Southern Oscillation Index (see text) for the period 1957-1983. Arrows indicate occurrence of El Nino events: length of arrow proportional to severity. (from Chao, 1984).

GEODYNAMICS FUNDING DISTRIBUTION

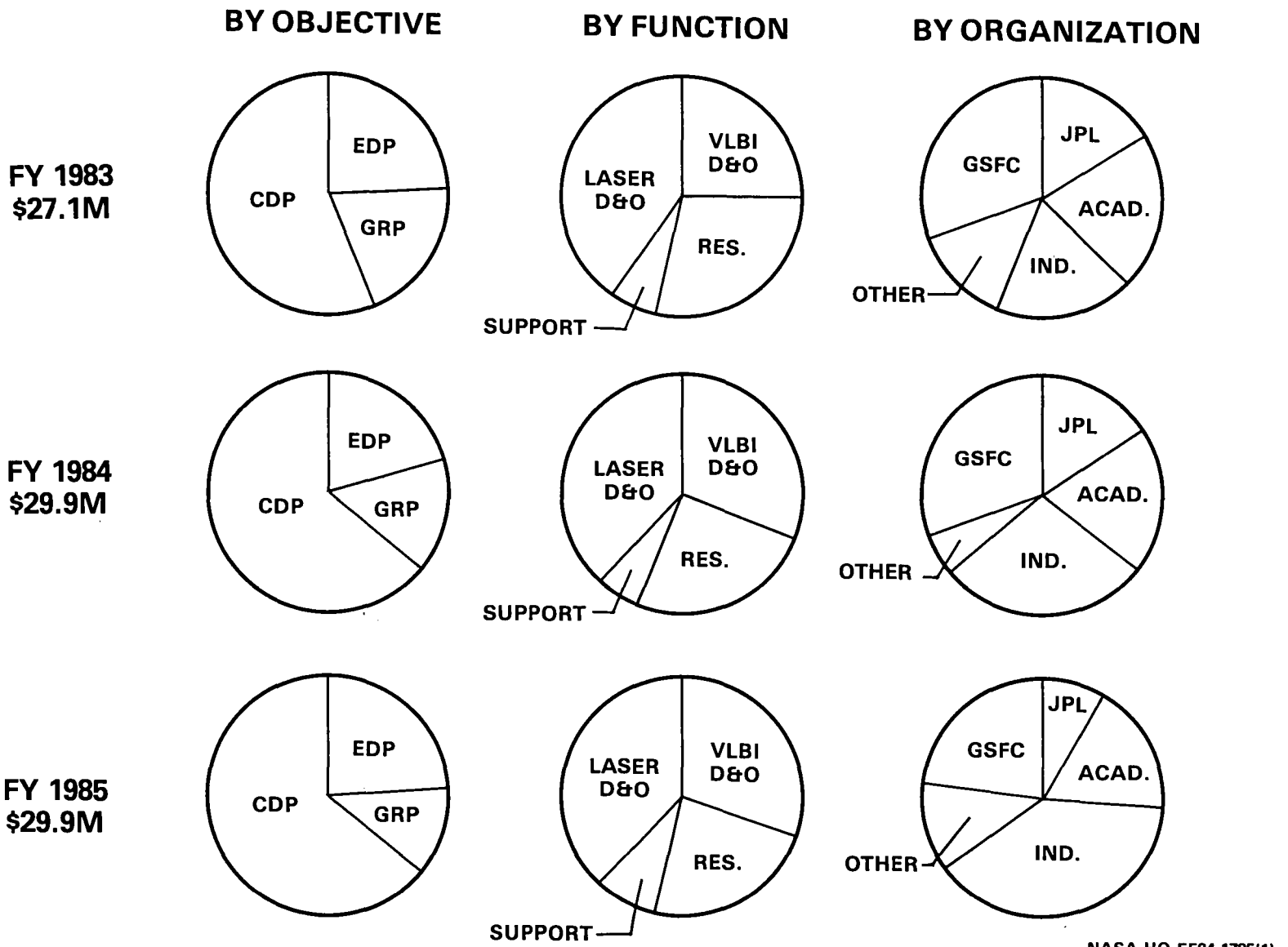

FIGURE II-1

MEDITERREAN SITES

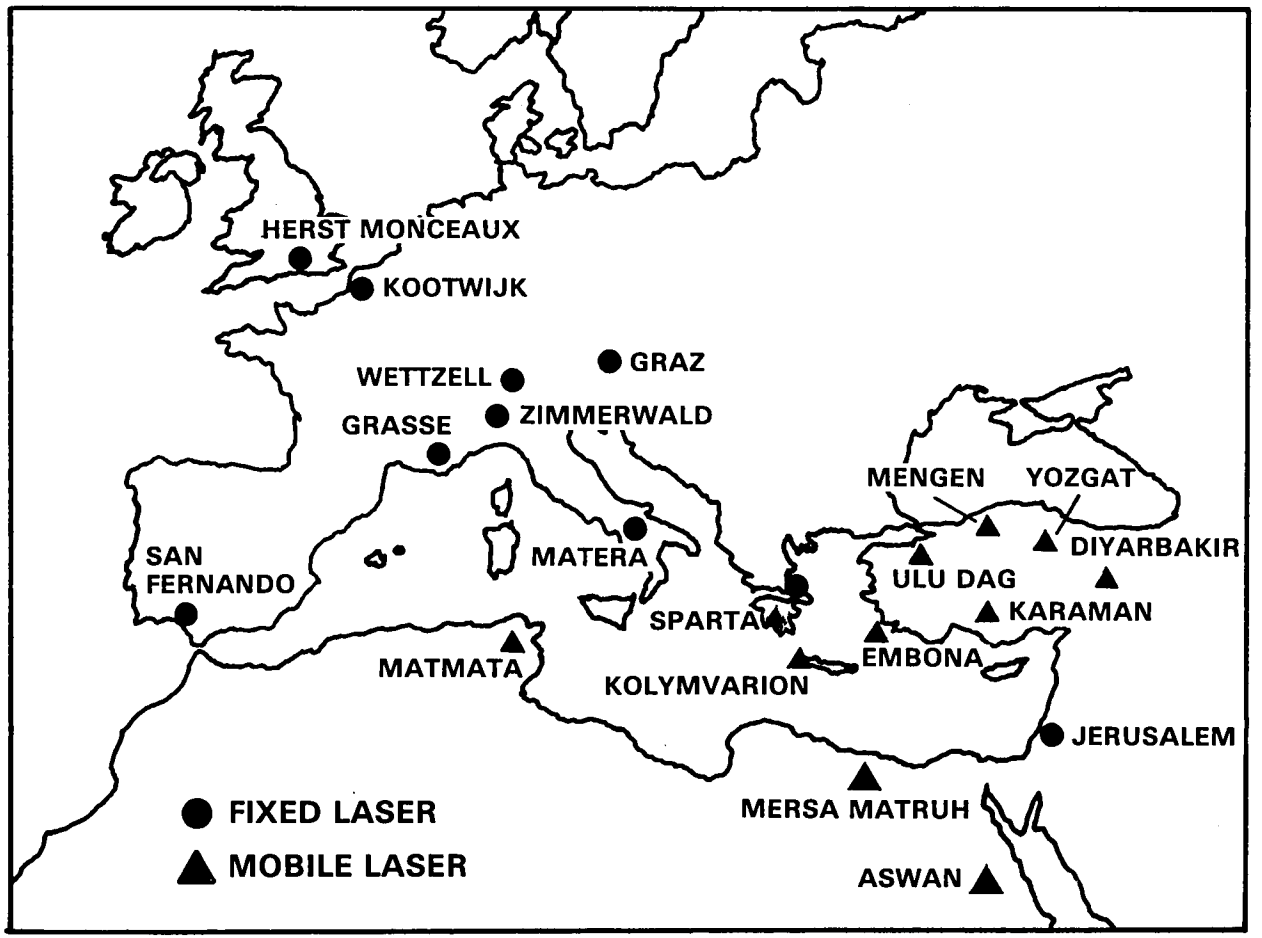

FIGURE II-2

NASA HQ EE84-1776(1)
7-6-84

GLOBAL CRUSTAL DYNAMICS PROJECT SITES

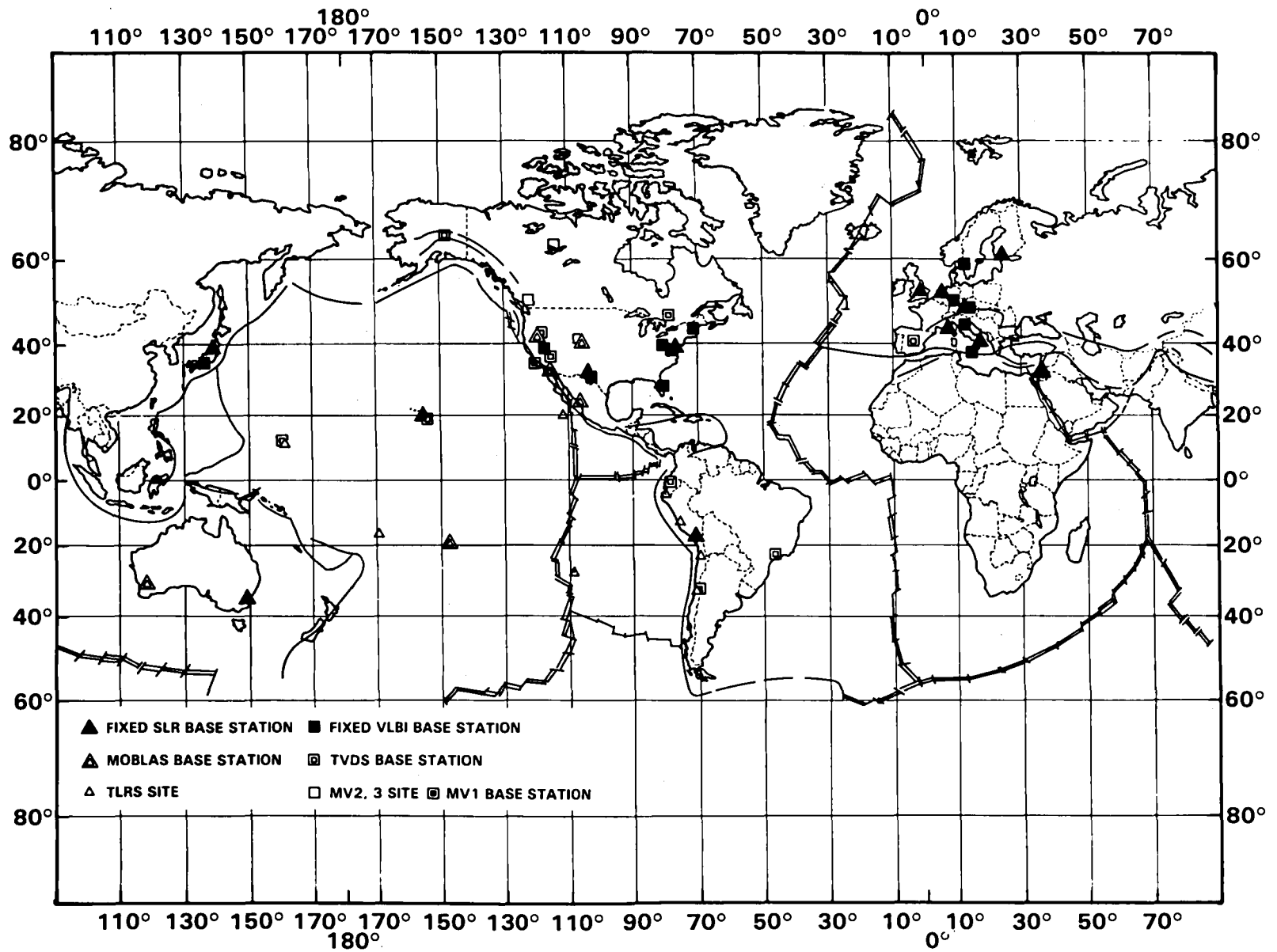

FIGURE III-1

CALIFORNIA CRUSTAL DYNAMICS PROJECT SITES

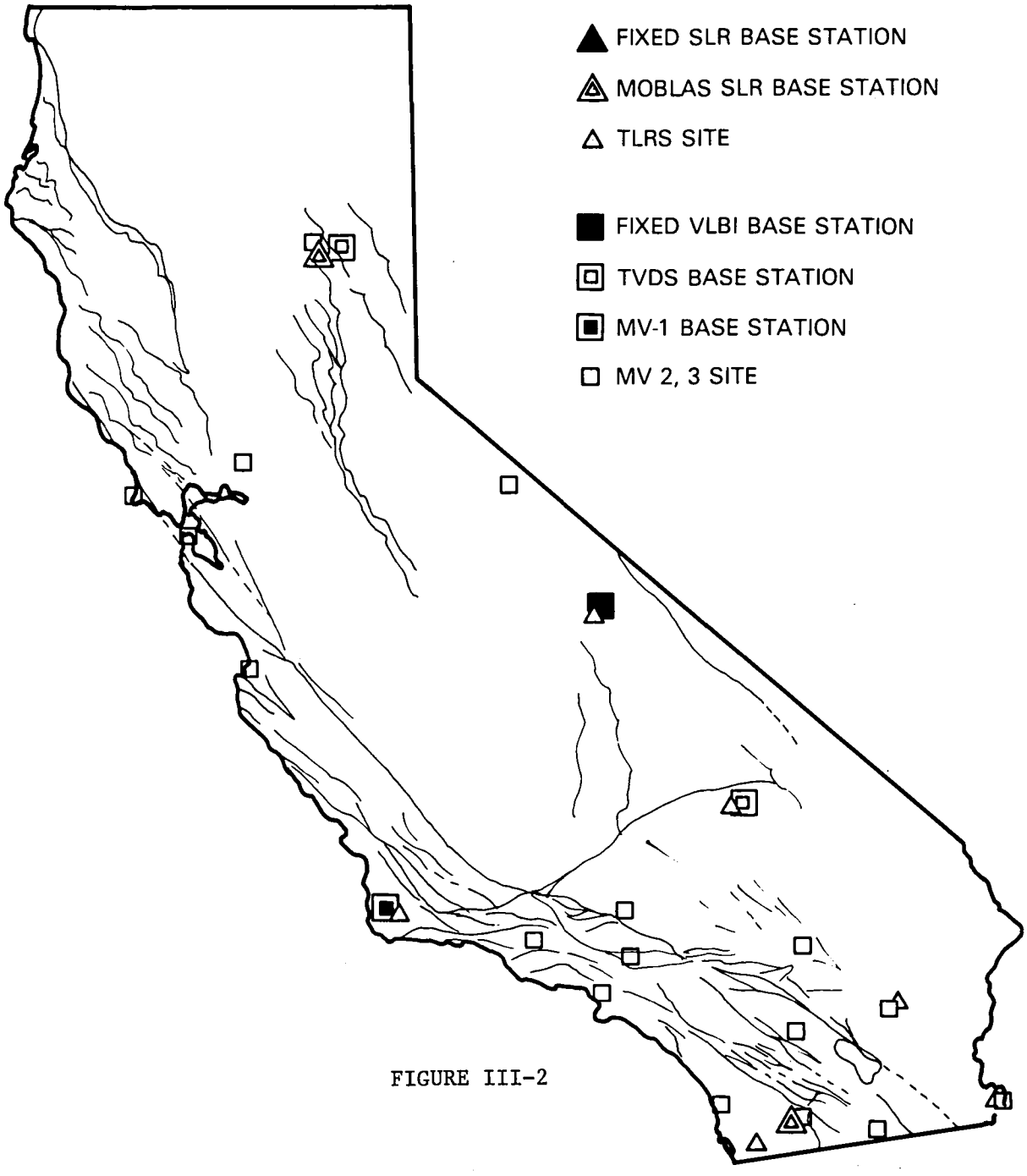

FIGURE III-2

NORTH AMERICAN CRUSTAL DYNAMICS PROJECTS SITES

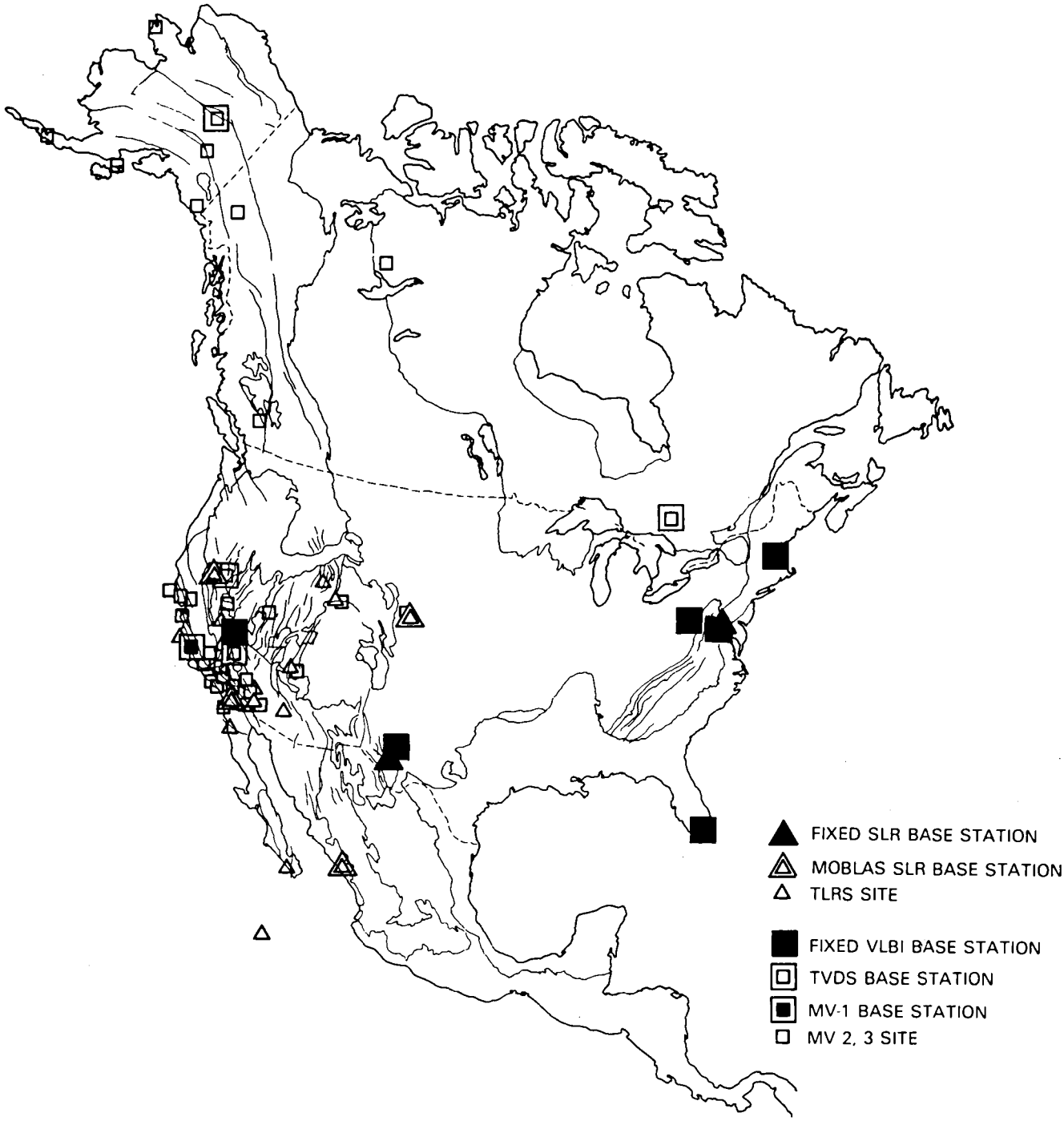

FIGURE III-3

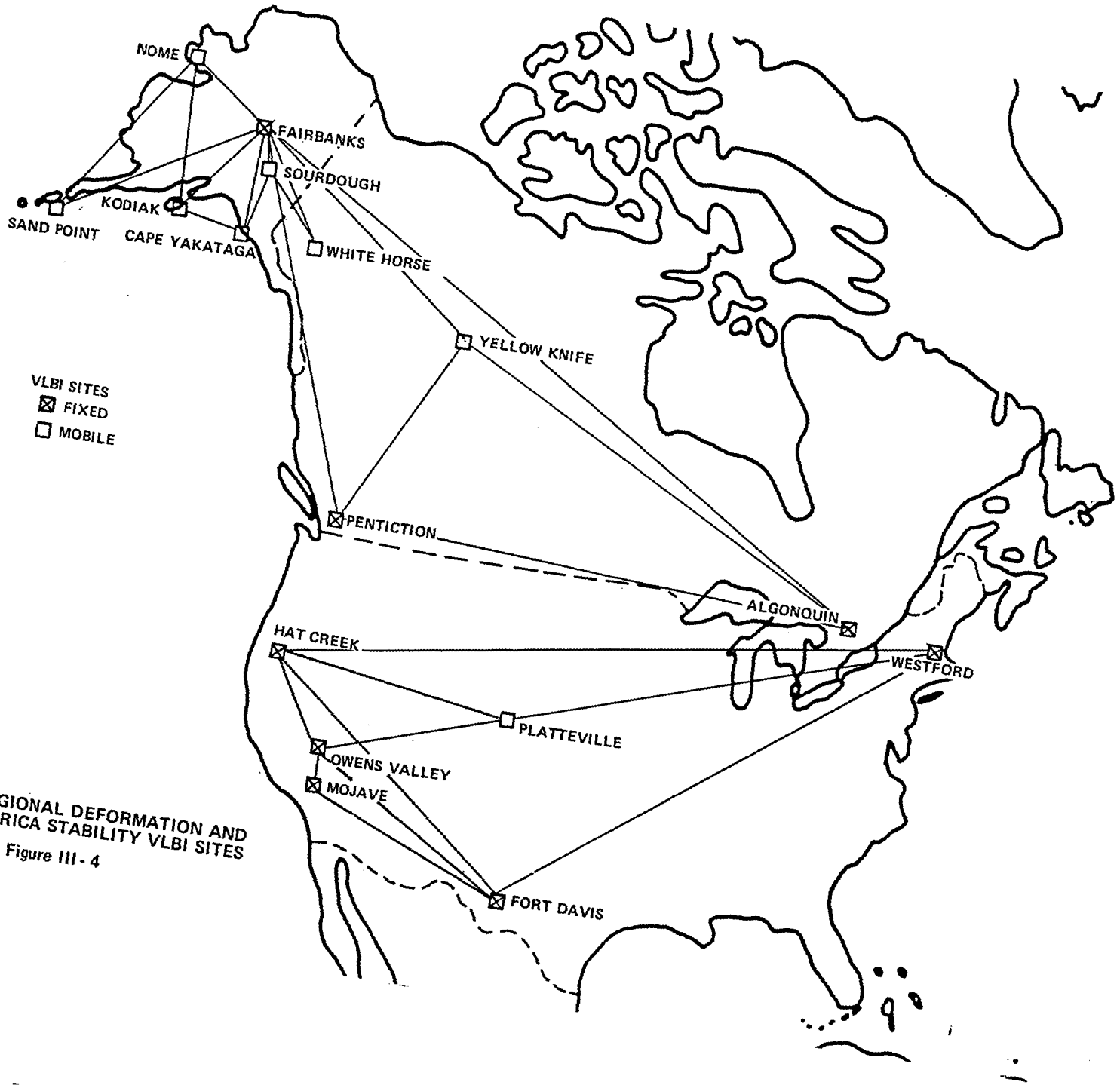

ALASKA REGIONAL DEFORMATION AND NORTH AMERICA STABILITY VLBI SITES

Figure III - 4

SAN ANDREAS FAULT EXPERIMENT

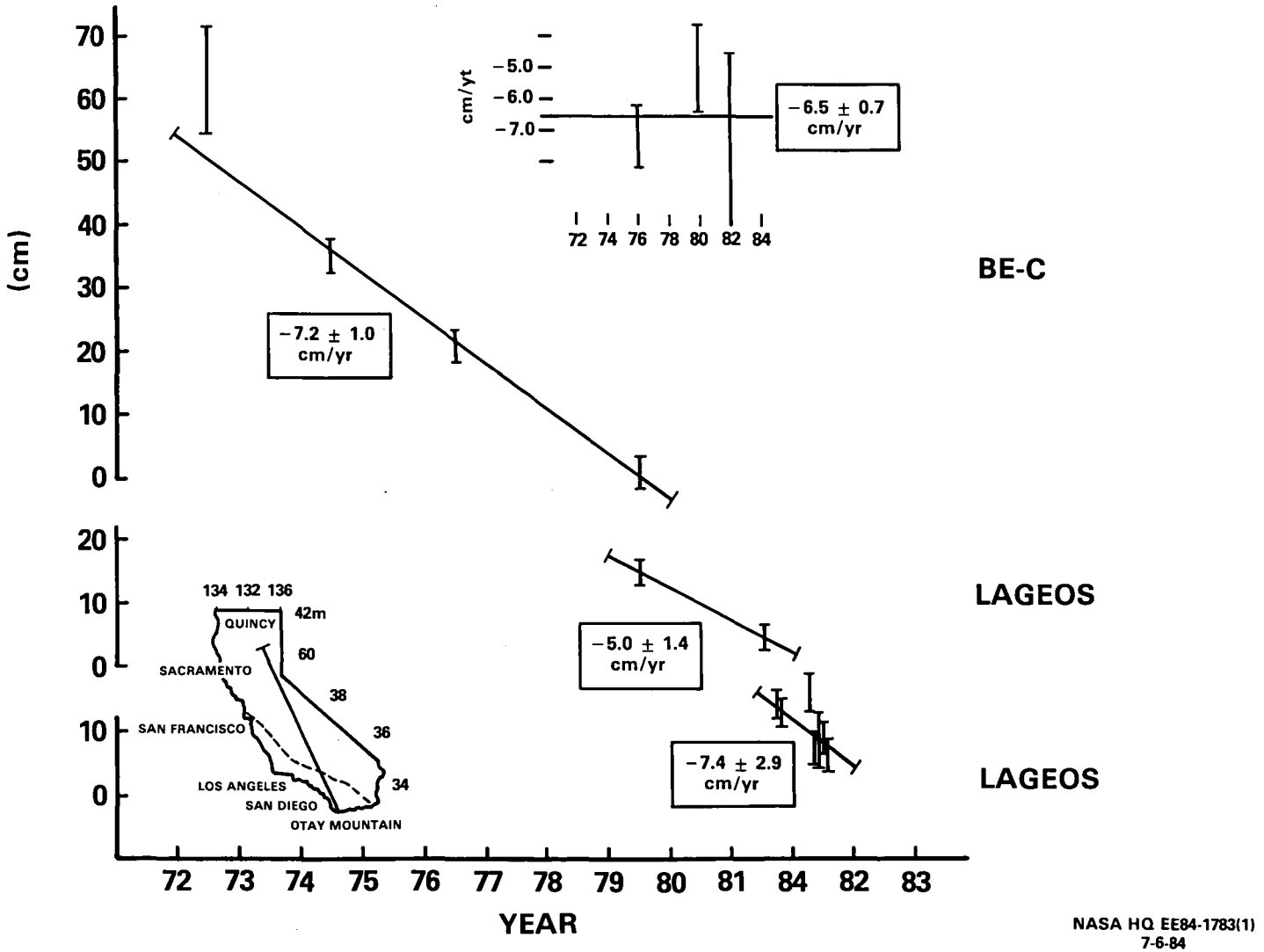

NASA HQ EE84-1783(1)
7-6-84

FIGURE IV-1

INTER-PLATE DEFORMATIONS OBSERVED BY SLR

AVERAGED ELLIPSOIDAL CHORD RATES VS. RATES GIVEN BY MINSTER & JORDAN (cm/yr.)

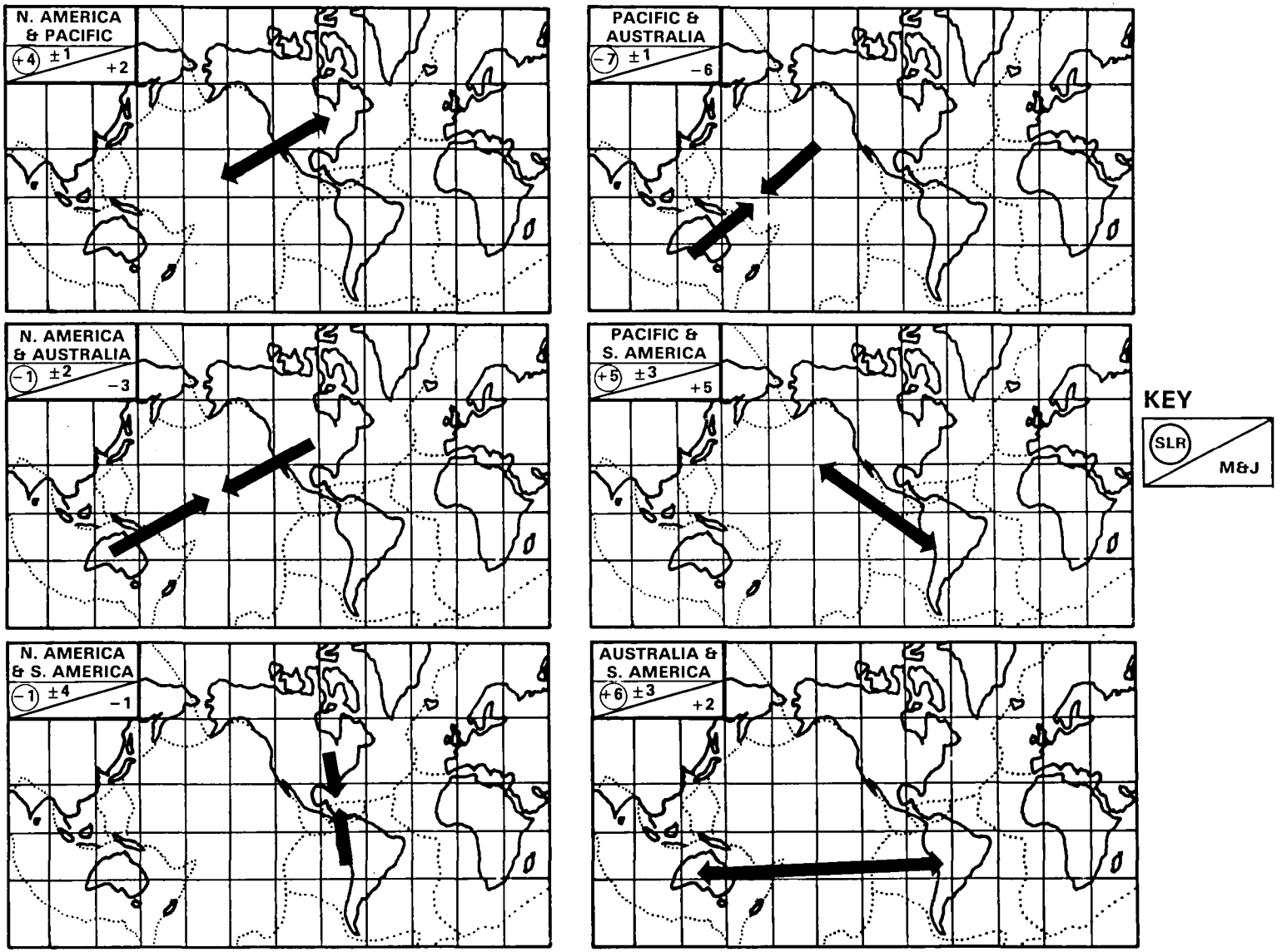

FIGURE IV-2

NASA HQ EE84-1781(1)
7-6-84

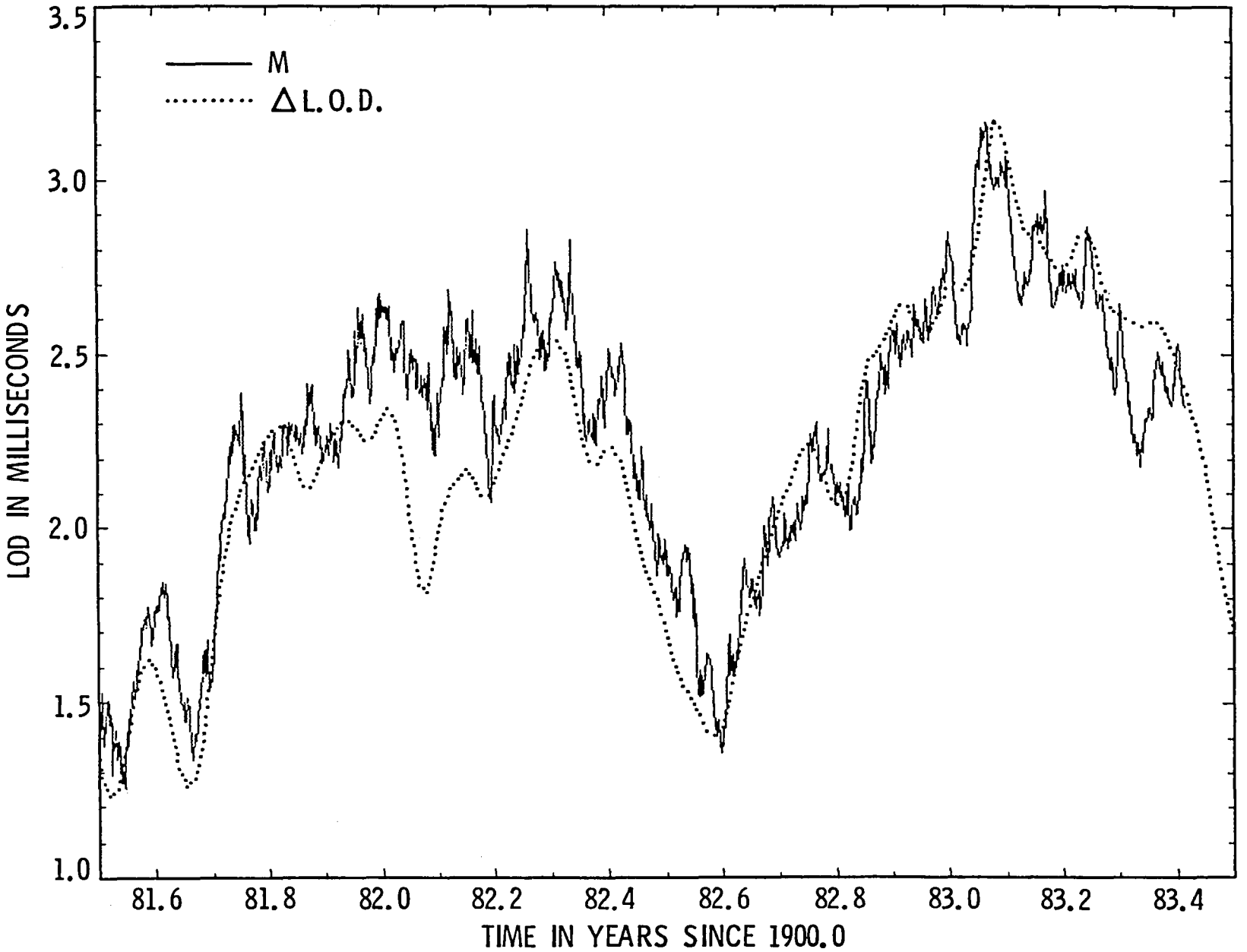
M
ΔL.O.D.
LOD IN MILLISECONDS
3.5
3.0
2.5
2.0
1.5
1.0
81.6
81.8
82.0
82.2
82.4
82.6
82.8
83.0
83.2
83.4
TIME IN YEARS SINCE 1900.0

FIGURE IV-3

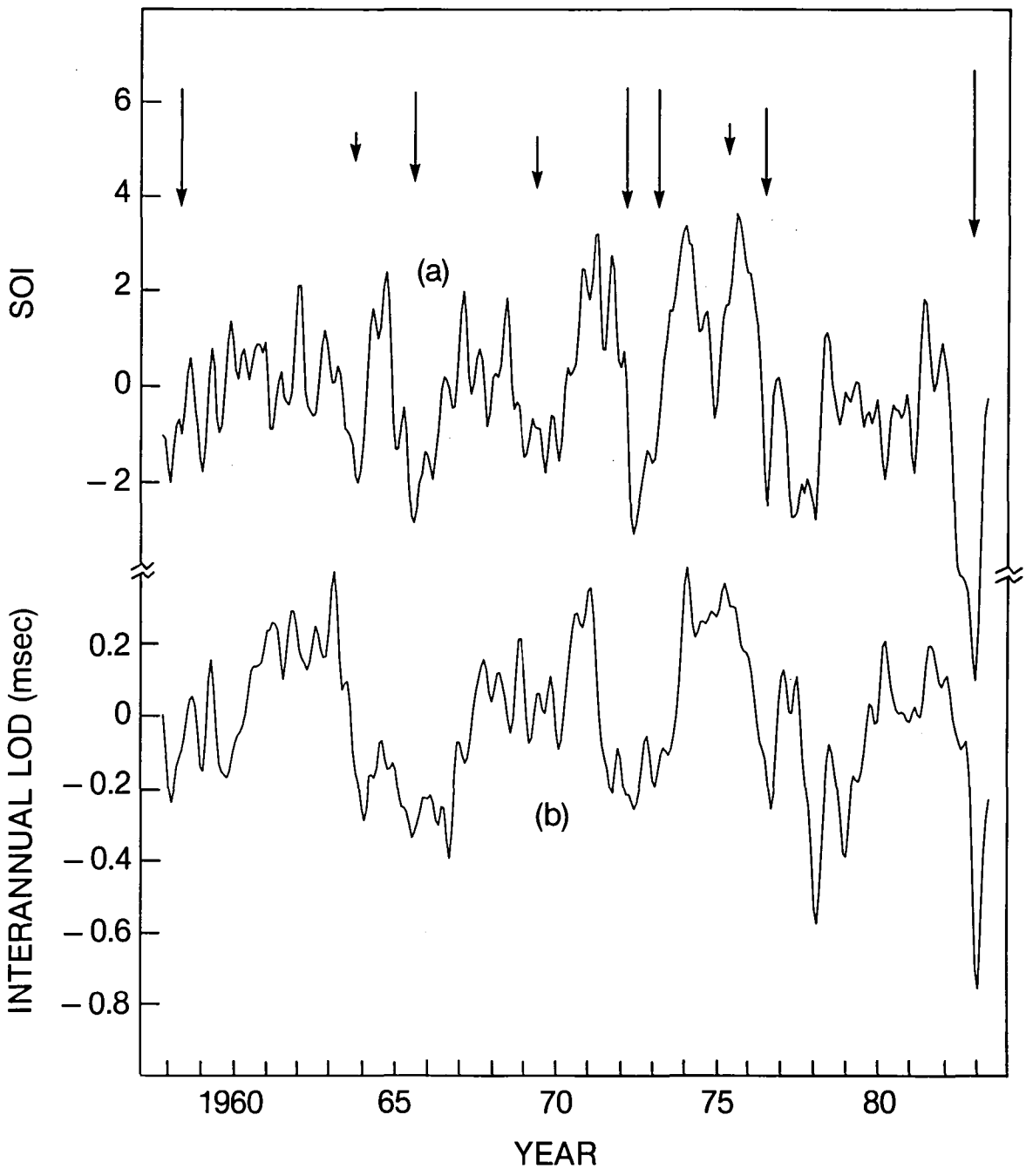
SOI
6
4
2
0
−2
(a)
INTERANNUAL LOD (msec)
0.2
0
−0.2
−0.4
−0.6
−0.8
(b)
1960
65
70
75
80
YEAR

FIGURE IV-4

APPENDIX 1

GLOSSARY OF ACRONYMS AND ABBREVIATIONS

A	Amperes
AAM	Axial Angular Momentum
AGU	American Geophysical Union
BE-C	Beacon Explorer-C
BIH	Bureau International de l'Heure
CDP	Crustal Dynamics Project
CNR	Consiglio Nazionale delle Recerche (Italy)
DIS	Data Information System
DMA	Defense Mapping Agency
EC	European Centre for Medium-Ranged Forecasting
ENSO	El Nino/Southern Oscillation
GEOSTAR	Geodetic Navstar Receiver
GPS	Global Positioning System
GRM	Geopotential Research Mission
GRMSSG	GRM Science Steering Group
IRIS	International Radio Interferometric Surveying
IUGG	International Union of Geodesy and Geophysics
JPL	Jet Propulsion Laboratory
Lageos	Laser Geodynamics Satellite
LLR	Lunar Laser Ranging
l.o.d.	length of day
Ma	Million Year
Magsat	Magnetic Field Satellite
MFE	Magnetic Field Explorer
MITES	Miniature Interferometric Terminals for Earth Surveying
MLRS	McDonald Laser Ranging Station
Moblas	Mobile Laser System
MV	Mobile VLBI
NASA	National Aeronautics and Space Administration
Natmap	Division of National Mapping (Australia)
NCMN	National Crustal Motion Network
NGS	National Geodetic Survey
NLRS	Natmap Laser Ranging Station
NMC	National Meteorological Center
NOAA	National Oceanic and Atmospheric Administration
nT	Nanotesla
OVRO	Owens Valley Radio Observatory
P	Poise
pps	pulses per second
Polaris	Polar Motion Analysis by Radio Interferometric Systems
PSN	National Space Plan (Italy)
SAFE	San Andreas Fault Experiment
SAO	Smithsonian Astrophysical Observatory
SERIES	Satellite Emission Range Inferred Earth Surveying
SLR	Satellite Laser Ranging
SOI	Southern Oscillation Index
TLRS	Transportable Laser Ranging System
Topex	Ocean Topography Experiment
TSS	Tethered Satellite System
TVDS	Transportable VLBI Data System
VLBI	Very Long Baseline Interferometry
WEGENER	Working Group of European Geo-scientists for the Establishment of Networks for European Research

SIXTH ANNUAL CONFERENCE ON THE NASA GEODYNAMICS PROGRAM

MAY 14 - 17, 1984
Cincinnati Convention Center
Cincinnati, Ohio

Abstracts

Gravity Measurement and Analysis I

Room 24 Mon PM

Presider, S.M. Klosko, EG&G/ WASC, Inc.

G12-01

The National Geodetic Survey Gravity Network

R. E. MOOSE (National Geodetic Survey, Charting and Geodetic Services, National Ocean Service, National Oceanic and Atmospheric Administration, Rockville, Maryland 20852, U.S.A.)

In 1966 the United States National Gravity Base Network was established through the cooperative efforts of government and academic organizations involved in the nationwide observation of gravity. This network was reobserved between 1975 and 1979 using field procedures designed to give high quality gravity differences, and is now referred to as The National Geodetic Survey Gravity Network. The network is tied to the U.S. Absolute Gravity Reference System by seven stations at which absolute gravity has been observed. The adjustment of these observations was completed in 1983 and the gravity station values are now available as reference points for regional gravity surveys. The intention is to keep this network up to date and improve the accuracy of the station values by additional high quality relative ties and by making observations with a new portable absolute gravity meter.

G12-02

The Observation of Vertical Gravity Gradients: Operational Considerations and Survey Results

Warren T. Dewhurst (National Geodetic Survey, Charting and Geodetic Services, NOS/NOAA, Rockville, Md. 20852)

The National Geodetic Survey (NGS) has recently begun the observation of vertical gravity gradients. The observations are performed using LaCoste & Romberg relative gravity meters and survey tripods, both fixed and variable in height.

Using this technique, a gradient survey was conducted in the Pamlico Sound area of North Carolina. Results indicate that measurements can be taken, over a distance of 2 meters in height, with a precision of approximately 3 microgals/meter.

The results of this survey, in addition to the operational limitations of using relative gravity meters to measure vertical gradients will be discussed.

Suggested system improvements such as taller platforms and electronically fedback meters will also be presented.

G12-03

Comparison of Geoid Undulation Differences in Central Ohio

T. ENGELIS (Dept. of Geodetic Science and Surveying, The Ohio State University, Columbus, OH 43210)
C.C. TSCHERNING (Danish Geodetic Institute, Copenhagen)
R.H. RAPP (Dept. of Geodetic Science and Surveying, The Ohio State University, Columbus, OH 43210)

Ellipsoidal height differences have been determined for 13 station pairs in the central Ohio region using GPS measurements. This information was used to compute geoid undulation differences based on known orthometric heights. These differences were compared to gravimetrically computed undulations (using a Stokes integration procedure and least square collocation having an internal r.m.s. agreement of ±1.5 cm in undulation differences). The two sets of undulation differences have an r.m.s. discrepancy of ±8 cm while the average station separation is of the order of 20 km. Although the accuracy level of the gravimetric quantities is clearly a function of distance between station pairs, no such correlation was found in the discrepancies of undulation differences, indicating that the agreement is below the accuracy level. This good agreement suggests that gravimetric data can be used to compute accurate geoid undulation differences that can be used to convert ellipsoidal height differences obtained from GPS to orthometric height differences. Such computations require a dense set of gravity anomalies and an optimum selection of a reference field.

G12-04

Secular Gravity Variation in the BTTZ Region of China

J. T. KUO, W. E. BROWN (Lamont-Doherty Geological Observatory and Aldridge Laboratory of Applied Geophysics, Columbia University, New York, NY 10027)
GU GUNG XU, LIU KE REN, HUA CHANG CAI (Institute of Geophysics, State Seismological Bureau, Beijing)

A cooperative research project between the Institute of Geophysics, State Seismological Bureau of the People's Republic of China and Columbia University has been monitoring gravity since early '81 in the Beijing-Tianjin-Tangshan-Zhangjiakou (BTTZ) region of China. The principal objective of the project is to investigate secular changes in local gravity relative to regional seismic phenomena. Eight semi-permanent stations, each equipped with a Geodynamics TRG-1 tidal recording gravimeter and digital data acquisition system, provide temporally continuous data to a precision of 0.1 microgals around the BTTZ region. Mobile gravity surveys, using three Lacoste and Romberg model G gravity meters, provide broad spatial coverage every four months to a precision of 10 to 15 microgals.

Results of seven mobile gravity surveys (July '81 to Oct. '83) indicate virtually no significant changes within the experimental error. Over most of the region, the total temporal range of variations is within plus or minus 20 microgals. However, around Tian Jin, gravity consistently increases to about 70 microgals over 26 months, evidently due to regional subsidence in response to groundwater withdrawal.

Results from the semi-permanent stations show relatively minor secular variations. Three of the TRG-1 meters perform exceedingly well, with long term instrumental drifts on the order of fractions of a microgal per day. Removal of this drift yields a gravity signal whose temporal variation is generally within 10 microgals.

In conclusion, our results, thus far, show no significant gravity changes which can be directly attributed to tectonic processes in the BTTZ region.

G12-05

The Effect of GPS Receiver Measurement Error on Gravity Anomaly Survey Accuracy

Alan G. Evans
Naval Surface Weapons Center
Dahlgren, VA 22448

Sponsor: Robert Hill

Recent advances in Global Positioning System (GPS) receiver capability have motivated this investigation to examine the potential for using GPS as a vertical reference in gravity anomaly surveys. For the study, all values are assumed to be known perfectly except the receiver measurement noise. The gravity anomaly statistical model used and the accuracy analysis assumptions are presented. For a receiver phase measurement error of 8 centimeters or less, the gravity anomaly estimation error was found to be less than 1 milligal for survey vehicle velocities of 100 m/s or less. The effect of other error sources, such as clock error and satellite orbit error, are discussed but are not analytically determined.

G12-06

Geoid Height Differences from GPS Surveys at the Subdecimeter-Level

L. D. HOTHEM (National Geodetic Survey, Charting and Geodetic Services, National Ocean Service, National Oceanic and Atmospheric Administration, Rockville, Maryland 20852, U.S.A.)

Since early 1983, the National Geodetic Survey has been conducting geodetic surveys with satellites of the Global Positioning System (GPS). Included in the specifications for the surveys is a standard requirement that connections be made to bench marks with elevations determined from spirit level ties to the National Geodetic Vertical Datum of 1929 (NGVD 29). Distances between bench marks occupied simultaneously ranged from less than 1 km to generally less than 100 km. Geoidal height differences were computed by differencing the GPS-derived ellipsoid (geometric) height differences from the leveled (orthometric) differences. These GPS-derived geoidal height differences (ΔN) were analyzed by comparison with ΔN values derived from astrogravimetric methods for estimating geoidal heights. The comparisons yielded differences with an rms of better than 5 cm. For those lines with repeated ΔN measurements, the rms values were 2-5 cm.

G12-07

Tests for Optimal Estimation of High Degree and Order Gravity Fields

D.P. HAJELA (Dept. of Geodetic Science and Surveying, The Ohio State University, Columbus, Ohio 43210)

The potential coefficients describing the earth's gravity field may be computed very efficiently by quadrature formulas from a global set of 1°x 1° mean gravity anomalies. The use of mean anomalies requires judicious use of desmoothing factors $1/4\pi\beta_n^2$, $1/4\pi\beta_n$, $1/4\pi$; where β_n are Pellinen's smoothing factors. The December 1981 potential coefficients field developed by R.H. Rapp at the Ohio State University used the three desmoothing factors respectively for degrees less than 60, 60 to 180, and greater than 180. This potential coefficients field has generally been employed only to degree 180 because of concern over the sharp discontinuity in the spectrum of potential degree variance at degree 180.

A more rigorous procedure is to replace the desmoothing factors in the quadrature formulas by optimal quadrature weights, which are obtained by least squares collocation based on the covariance function of the gravity anomalies. O.L. Colombo designed an algorithm, described in OSU Report No. 310 in March 1981, for the efficient computation of the optimal quadrature weights. Colombo tested this algorithm with 5°x 5° mean anomalies.

We have extended these optimal estimation procedures to various global sets of 1°x 1° anomalies with different standard deviations. With realistic standard deviations of anomalies, the percentage improvement by degree over December 1981 potential coefficients is of the order of 7%, 21% and 47% respectively at degrees 60, 120 and 180. The coefficient percentage error, which had reached 100% at degree 120 in December 1981 field, is now of the order of 44%, 67% and 88% respectively at degrees 120, 180 and 250.

G12-08

Filters for Data Noise, Problem Stabilization, and Data Combination in Physical Geodesy

J.Y. CRUZ (Dept. of Geodetic Science and Surveying, The Ohio State University, Columbus, OH 43210)

Frequency domain collocation in the continuous case provides for the derivation of a general filter for an optimal handling of data noise, incorrectly posed problems, and combination of data from different sources. Parameters for the construction of a specific filter from the general filter are: a priori noise of data, positive coefficients defining the base function being used for the gravity field representation, and radius of the Bjerhammar sphere. The constructed filter can be applied to the data in a pre-filtering, before the usual integral formula of physical geodesy is applied, or, the filter can be included in the definition of the integral kernel amounting to the use of a modified kernel in the integral formula. Graphs will be presented to illustrate the behavior of specific filters being implicitly or explicitly used in well-known computational procedures in physical geodesy. Such procedures include the various truncation methods and the spectral method for combining terrestrial and satellite data, and the inversion of data into one or more layers of interpolation coefficients in the various base function representations of the gravity field.

G12-09

The Contribution of Vertical Gravity Gradients and Geoid Height Differences to Geoid Modeling

C. C. GOAD
M. M. CHIN (both at National Geodetic Survey, Charting and Geodetic Services, National Ocean Service, National Oceanic and Atmospheric Administration, Rockville, Maryland 20852, U.S.A.)

The contribution to geoid modeling with recently obtained vertical gravity gradients using relative gravity meters and geoid height differences from a combination of leveling and Global Positioning System (GPS) relative surveys will be presented. An improvement in gravity predictions from 3 mgal to 2 mgal is found when gravity gradients are used. Geoid height differences contain the same information as deflection of the vertical observations. However, the cost of obtaining geoid height observations is much less than the traditional astronomic determinations of vertical deflections. The accuracy will be the equivalent of 0".2 or better.

G12-10

The Method of Clenshaw Sums of the Legendre Series in the Geopotential Evaluation Theories of Deprit and Tscherning, Rapp and Goad

Peter J. Melvin (Boeing Computer Services, Box 3707, Seattle, Wa. 98124) (Sponsor: R. H. Rapp)

Deprit, 1979, and Tscherning, Rapp, and Goad, 1983 have used the method of Clenshaw sums to evaluate the Legendre series for the Fourier coefficients in the spherical harmonic expansion of the geopotential. Deprit uses unnormalized functions which have an overflow problem for higher order expansions to evaluate the potential and the rectangular components of its gradient and Hessian. Tscherning, Rapp, and Goad use normalized functions to find spherical components, but use expressions that have apparent singularities at the poles. In this study, Clenshaw sums are applied to normalized functions to evaluate the geopotential and the spherical components of its gradient and Hessian from expressions that are well behaved at the poles. A 16K home computer has been used with the GEM10B coefficients to produce maps of the geoid anomalous gravity vector and gradient on the ellipsoid in five projections.

Below is a Mercator map of the radial, north-south component of the gravity gradient at 1.8 degree resolution.

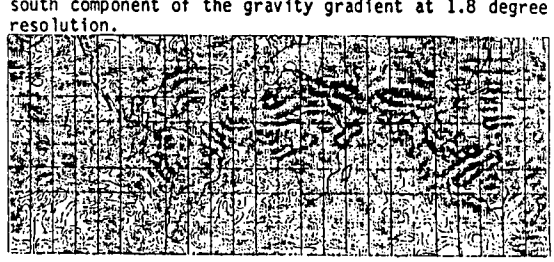

G12-11

Concerning a New Integral Equation for Gravity Anomalies Based on the Biharmonic Potential

ROLLAND L. HARDY (CNOC Research Chair in MC & G, Naval Postgraduate School, Code 68Xz, Monterey, CA 93943)

An existence theorem concerning gravitational potential inside a material body has been converted into an explicit definite integral equation of a Fredholm type for disturbing potential T inside or outside the body. The fundamental unknown is an internal density anomaly function.

The kernel of the integral equation is a distance function and the solution for the density anomaly is represented everywhere by the biharmonic disturbing potential in three dimensions:

$$\delta_A(r,\theta,\lambda) = -\frac{\nabla^2(\nabla^2 T)}{8\pi}$$

A new integral equation for gravity anomalies based on the biharmonic potential has also been derived. Numerical solutions of this integral based on gravity anomalies at the boundary may provide estimates of density at selected internal points, augmenting the already known capability of predicting gravity anomalies at points where they have not been measured.

G12-12

A Comparative Study of Spherical and Flat-Earth Geopotential Modeling at Satellite Elevations

M.H. PARROTT, W.J. HINZE, L.W. BRAILE (Dept. of Geosciences, Purdue University, West Lafayette, IN 47907)
R.R.B. VON FRESE (Dept. of Geology and Mineralogy, Ohio State University, Columbus, OH 43210)

Flat-earth modeling is a desirable alternative to the complex spherical-earth modeling process, but do errors invalidate the use of flat-earth assumptions at satellite elevations? These methods were compared using 2½-D flat-earth and spherical modeling to compute gravity and scalar magnetic anomalies along profiles perpendicular to the strike of variably dimensioned rectangular prisms at altitudes of 150, 300, and 450 km. Comparison was achieved with percent error computations (spherical-flat/spherical) at critical anomaly points. At the peak gravity anomaly value, errors are less than ±5% for all prisms. At ½ and 1/10 of the peak, errors are generally less than 10% and 40% respectively, increasing to these values with longer and wider prisms at higher altitudes. For magnetics, the errors at critical anomaly points are less than -10% for all prisms, attaining these magnitudes with longer and wider prisms at higher altitudes. In general, in both gravity and magnetic modeling, errors increase greatly for prisms wider than 500 km, although gravity modeling is more sensitive than magnetic modeling to spherical-earth effects. Preliminary modeling of both satellite gravity and magnetic anomalies using flat-earth assumptions is justified considering the errors caused by uncertainties in isolating anomalies.

Interdisciplinary Research in Geodesy and Tectonophysics

Room 1 & 15 Wed PM

Presider, R.V. Sailor, The Analytic Sciences Corp.

G32-01

The Geoid and Tectonics

D. L. TURCOTTE (Dept. Geol. Sci., Cornell University, Ithaca, NY 14853)

The simple Bouguer relation between a gravity observation and the local integrated mass anomaly allows important tectonic problems to be studied directly. The role of lithospheric flexure in the compensation of mass anomalies can explain many gravity observations. This can be done on local features such as ocean trenches, ocean islands, and sedimentary basins or by a spectral analysis on a regional basis. This approach has also been useful on a global basis for the moon and Mars. A similar simple relationship exists between the geoid and the local, first-moment of the mass anomaly if the condition of isostasy is satisfied. This relation has allowed a variety of geoid anomalies to be explained in terms of the density structure of the lithosphere. The geoid anomaly associated with ocean ridges and fracture zones provides important data on the thermal isostasy of the oceanic lithosphere. Geoid anomalies at passive margins and the geoid difference between the continents and the ocean basins provides constraints on the thickness of the continental lithosphere. Geoid anomalies associated with Hawaiian Swell, Bermuda Swell, and Cape Verde Rise can be explained by Pratt compensation with a 100 km depth of compensation; the Walvis Ridge and Agulhas Plateau with a 30 km depth of compensation.

G32-02

Gravity, Geoid and the Oceanic Lithosphere

A.B. Watts (Lamont-Doherty Geological Observatory of Columbia University, Palisades, New York 10964)

During the past decade there have been rapid advances in the aquisition, reduction and interpretation of marine gravity and geoid data. Gravity data have continued to be acquired at sea by government, university and industry groups using mainly destabilized balance beam gravimeters (e.g. Graf-Askania) and forced feedback accelerometers (e.g. Bodenseewerk, Bell). In regions of favourable sea conditions and accurate navigation these instruments produce accuracies of 1 to 2 mgal. Geoid data have been derived from measurements of sea-surface heights during NASA's GEOS-3 and SEASAT satellite radar altimeter missions. These data produce accuracies of 50 to 10 cm depending on sea-state. In the absence of noise, gravity and geoid data provide equivalent information about a body causing a gravitational field anomaly. In the oceans, surface ship gravity data have a better signal/ noise ratio at short-wavelengths while geoid data have a better ratio at long-wavelengths. Gravity data have provided constraints on the extent of static compensation of seamounts/oceanic islands, aseismic ridges, continental margins and the variation of the long-term mechanical properties of oceanic lithosphere with age. Geoid data, on the other hand, have provided constraints on the extent of static compensation at mid-oceanic ridge crests, fracture zones, continental margins and the thermal properties of oceanic lithosphere. Both gravity and geoid data have provided constraints on the dynamic compensation of mid-plate swells. However, because of its spatial extent geoid rather than gravity data have provided the most important constraints on mantle convection.

G32-03

Long-Wavelength Geoid Anomalies and Mantle Convection

MARK A. RICHARDS
BRADFORD H. HAGER (Both at Seismological Laboratory, California Institute of Technology, Pasadena, CA 91125)

Long-wavelength geoid anomalies are caused primarily by density contrasts associated with mantle convection. Interpretation is complicated by the gravitational effects of deformation of the Earth's surface and internal boundaries by convection. These boundary deformations have an effect on the geoid comparable in magnitude and opposite in sign to that of the driving density contrasts. Thus the total geoid response is a small difference between large numbers; it is sensitive in both sign and magnitude to the viscosity structure and thickness of convecting layers in the mantle. Combining our calculations for linear viscous response functions and recent seismological observations allows us to explain at least 70% of the ℓ = 2-9 geoid power. Seismically inferred subducted slabs dominate the geoid for harmonic degrees 4-9 and modelling suggests a viscosity contrast of >30 between the upper and lower mantle with slabs extending into the lower mantle. A remarkable correlation between

residual geoid degrees 2 and 3 and the recently determined lower mantle velocity heterogeneity models of Clayton and Comer (1983) and Dziewonski (1984) is successfully explained by mantle-wide flow with a viscosity contrast of approximately 10 between the upper and lower mantle. The lower mantle degree 2 and 3 anomalies are also highly correlated with the spatial distribution of hotspots. Upper mantle seismic velocities show some correlation with the geoid and hotspots, but mid-oceanic ridges do not correlate with either the geoid or the velocity models at significant depth. Mantle-wide convection with approximately an order of magnitude viscosity contrast between the upper and lower mantle, a lower mantle source for hotspot thermal anomalies, and largely passive mid-oceanic ridges with subducting slabs weakly coupled to the longest-wavelength convective circulation are consistent with the above observations.

G32-04

SEASAT Observations of Flexure: Evidence for a Strong Lithosphere

D. C. MC ADOO (*National Geodetic Survey, Charting and Geodetic Services, National Ocean Service, NOAA, Rockville, Md. 20852)
C. F. MARTIN (EG&G Washington Analytical Services Center, Inc., Riverdale, Md.)
S. POULOSE (RMS, Inc., Greenbelt, Md.)

In the past dozen years, bathymetric observations of Outer Rises have been laboriously and extensively compared with models of lithospheric flexure. These comparisons suggest that the lithosphere thickens with age out to 100 Myr as predicted by established thermal models. Further, these comparisons indicate (McNutt and Menard, 1982) that mechanical lithosphere does not continue to thicken with age past 100 Myr or, equivalently, that mechanical lithosphere does not extend much beyond depths of 40 km under the oceans.

We have tested these same elastic models of lithospheric flexure directly on SEASAT altimeter profiles over Outer Rises adjacent to nine major subduction zones. These nine include the Aleutian, Mariana (south and north), Izu-Bonin, Puerto Rico, Peru-Chile, South Sandwich, Philippine and Kuril trenches. These comparisons with SEASAT profiles indicate that the lithosphere does continue to thicken with age out to 150 Myr - the approximate age lithosphere being subducted at the northern Mariana trench. Furthermore, we can demonstrate that the lithosphere possesses an apparent flexural strength approximately equal to that predicted from rock mechanics experiments by Goetze and Evans (1979) -- after each region is adjusted for its particular age dependence.

*Work is performed at Geodynamics Branch, NASA Goddard, Greenbelt, Md.

G32-05

Thermal Cooling of the Oceanic Lithosphere . Observational Evidence for two Distinct Regimes

A. CAZENAVE,
M. LEFEBVRE (both at : GRGS-CNES, 18 Av. E. Belin, 31400 Toulouse, France)

Thermal contraction of the oceanic lithosphere causes the geoid height to decrease as age increases and gives rise to a geoid offset at fracture zones. Seasat geoid data at fracture zones in the whole Pacific ocean are used to redetermine parameters of the lithospheric cooling models. We find that the data follow closely the behavior predicted by the 'plate' thermal model and reveal two distinct regimes of cooling; one for seafloor ages in the range 0-25 Ma, the other beyond 30 Ma : this does not appear correlated with particular fracture zones but rather is representative of the whole studied area, i.e. whole south Pacific and northeast Pacific ocean. These two trends are interpreted in term of two different (asymptotic) thermal thicknesses. The smaller thermal thickness ($\sim$ 65 km) found for ages $\leq$ 25 Ma - compared to $\sim$ 90 km in the age range 30 - 60 Ma - calls for some kind of thermal perturbation in the vicinity of the ridge crest. Furthermore, the depth - age relationship obtained from the geoid derived thermal parameters departs significantly beyond 30 Ma from the widely used Parsons and Sclater's depth - age curve, and predicts a lesser subsidence. This may be of crucial importance for the evaluation of depth anomalies, thus for testing models of the mechanisms responsible of these anomalies.

G32-06

A Bathymetry and Altimetry Profile Across the Southwest Indian Ridge Crest at 31°S Latitude

A.B. WATTS (Lamont-Doherty Geological Observatory, Palisades, New York 10964.
J.R. COCHRAN (Lamont-Doherty Geological Observatory, Palisades, New York 10964.
P. PATRIAT (Institut Physique du Globe, 4 Place Jussieu, Paris, France

During March 1983 the M/V Marion Dufresne obtained a bathymetry profile along more than 1500 km of a SEASAT radar altimeter sub-track across the southwest Indian ocean ridge crest. We have used this data to estimate the thermal and elastic thickness of the oceanic lithosphere in the vicinity of the ridge and to evaluate the performance of the SEASAT altimeter. The thermal thickness appears to be in the range 72 to 109 km while the elastic thickness is approximately 5 km. The geoid height associated with the bathymetry and its compensation has been computed and compared to the observed geoid. A statistical analysis shows that there is a strong correlation between computed and observed geoid for wavelengths greater than 40-50 km while for shorter wavelengths there is a poor correlation. The poor resolution at short-wavelengths is attributed to instrument and oceanographic noise in the altimeter data. We examine the implications of these results for a) bathymetric prediction and b) tectonic studies in the world's oceans.

G32-07

Large Scale Isostatic Behavior of the Lithosphere and the Geoid Anomaly of Fennoscandia

A. J. ANDERSON (Dept. of Geodesy, University of Uppsala, Hällby, S-75590 Uppsala, Sweden)

Correlations as high as 0.92 were found between the geoid and crustal depth structure for marine regions in Scandinavia. Results agree with theoretical models indicating large scale isostatic behavior of the lithosphere. Crustal depth structure was also found to correlate with the land uplift and with the resultant change in the geoid in Scandinavia.

These results suggest that previous attempts to correlate the geoid in Fennoscandia with the causes of land uplift have overestimated the isostatic geoid anomaly. Current crustal models reduce the residual isostatic geoid anomaly considerably. Application of these results to the geoid anomaly in Fennoscandia could be interpreted as agreeing with those placing the mantle viscosity in the upper mantle closer to 10^{21} Pa s rather than 4 x 10^{22} Pa s which has earlier been assumed.

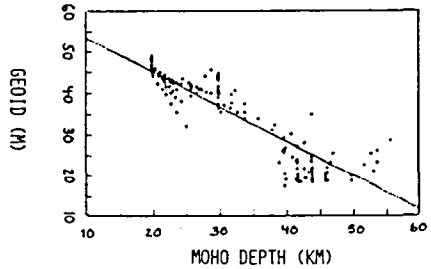

The figure shows the relation between geoid and crustal depth found for marine areas in Scandinavia.

G32-08

Use of SEASAT Geoid Anomalies to Interpret Complicated Tectonic Regions: The Macquarie Ridge Complex

LARRY RUFF (Dept. of Geological Sciences, University of Michigan, Ann Arbor, MI 48109)

ANNY CAZENAVE (Groupe de Recherches de Géodésie Spatiale, 18 Ave. Edouard Belin, Toulouse, 31055, FRANCE)

The major tectonic plates have been identified, and in most regions there is little ambiguity regarding plate boundary type. However, there are a few oceanic regions that present conflicting evidence as to the style of tectonics. A notable example is the Macquarie Ridge complex, which serves as the India-Pacific plate boundary between New Zealand and the Pacific-Antarctica spreading center. The location of the India-Pacific rotation pole is close to the Macquarie Ridge complex, hence we can expect some change in the relative motion along the complex. The predicted relative motions change from a combination of strike-slip and convergence in the north, to pure strike-slip in the southern part of the complex. The Macquarie Ridge complex has a high level of seismicity, and the focal mechanisms of the large earthquakes since 1963 are crudely consistent with the predicted motions. However, the southernmost part of the complex consists of the Hjort trench, an arcuate, deep (~6 km) trough. As troughs do occur along major fracture zones, such as the Eltanin and Romanche, perhaps the Hjort trench is simply a fracture zone, rather than a convergence zone.

We use SEASAT geoid profiles in a tectonic comparative sense. The Hjort trench geoid anomalies are characterized by a sharp geoid low, reaching 10 m in the northern Hjort trench, but lacking the obvious broad geoid high associated with well-developed subduction zones. We have examined the geoid profiles across the Romanche fracture zone, and find that the maximum amplitude of the narrow geoid low over a trough is 3 m. On the other hand, an immature subduction zone such as the South Solomon trench shows a narrow geoid low with 7 m amplitude, and a subdued broad geoid high. Thus, the geoid anomalies over the northernmost Hjort trench have an immature subduction zone affinity, implying that the tectonics in the Hjort trench region may not be predicted by the large-scale motions of the India and Pacific plates.

G32-09

Current and Future Geophysical Application of Satellite Altimeter Measurements

W. F. Haxby (Lamont-Doherty Geological Observatory of Columbia University, Palisades, New York 10964)
(Sponsor: A. B. Watts)

Marine geophysics has benefited greatly from information supplied by the Geos-3 and Seasat satellite missions. Both satellites carried radar altimeters capable of making precise measurements of the shape of the sea surface, a surface which conforms closely to the marine geoid. The more advanced Seasat altimeter achieved a precision of .05-.10 m, and recovered information on the gravitational perturbations associated with features as small as 20 km. Although its premature demise prevented Seasat from obtaining the coverage necessary to fully exploit its sensitivity, maps of the marine gravity field generated from Seasat data display a wealth of newly discovered geological features and gravity field characteristics which expand our knowledge of sea floor physiography and offer tantalizing evidence of dynamic processes occuring within and beneath the lithosphere. Investigations concerned with plate kinematics, small-scale thermal convection, and lithospheric deformation particularly stand to benefit from this information. In the near future, geophysical studies will benefit from: more sophisticated analysis of the altimeter data directed at enhancing the information present in the data; reprocessing Seasat measurements over sea ice to obtain more accurate estimates of geoid undulations in high latitudes, particularly in the southern hemisphere; and the development of techniques for combining altimeter data with conventional geophysical data. In the longer term, satellite missions such as Geosat and Topex will result in more extensive coverage and higher precision.

G32-10

DIGITAL IMAGE ENHANCEMENT OF GRAVITY AND BATHYMETRY DATA

P.C. Fisher
J.T. Parr
R.V. Sailor (The Analytic Sciences Corp. One Jacob Way, Reading, MA 01867)

Improvements in both computer technology and in the density and coverage of geophysical data have made it practical to display various maps as high resolution images. Dramatic examples of this have been developed by various investigators and include, for example, images of continental elevations and gravity data. In addition, various displays of geoid height, gravity anomaly, and vertical deflections have been made from SEASAT and GEOS-3 altimeter data. All of these image products have increased the visual impact of such data and made it easier to interpret relationships among tectonic features.

This paper illustrates several standard and "state-of-the-art" image enhancement techniques applied to geophyiscal data images. The techniques are demonstrated on images of ocean bathymetry (SYNBAPS, 5 min resolution) and the gravity field (Rapp, 1981 degree-180 harmonic coefficients). Results show the advantages and disadvantages of techniques such as: histogram equalization, pseudo illumination, feature extraction algorithms, supervised classification, local-area adaptive techniques, and image overlays.

G32-11

Lithospheric Structure in the SEASAT Geoid of the Central Pacific

B. D. MARSH (Earth and Planetary Sci., Johns Hopkins University, Baltimore, MD 21218)
J. HINOJOSA (Earth and Planetary Sci., Johns Hopkins University, Baltimore, MD 21218)
J. G. MARSH (Geodynamics, Goddard Space Flight Center, Greenbelt, MD 20771)

Although it is commonplace to remove the effects of regional lithospheric thermal subsidence from bathymetry to expose anomalies in depth, the effects of regional lithospheric structure on the geoid is less appreciated. These effects came principally from relative changes in plate age across fracture zones in relatively young (<~80 Ma) sea floor. These regional anomalies often amount to ~2 m and must be removed from the geoid before sublithospheric density variations can be revealed with the geoid. Along these lines, we have refined our previous models of the geoid due to lithospheric structure in the central Pacific and have removed these sources from a new high degree and order (n,m>12,12) SEASAT geoid, which has been corrected for orbit crossover errors. Much of the E-W geoid structure, having a wavelength of about 2000 km, over the youngest sea floor can be removed in this fashion, but there are still some large residual anomalies (NE of Hawaii) over apparently smooth seafloor plus those due to thermal swells (e.g. Hawaii). Thus we have also obtained the transfer function between geoid and sea floor topography and compared this with that of Airy-type isostatic compensation with wavenumber dependence. An additional synthetic geoid has been computed from the topography and the transfer function in hopes of further eliminating lithospheric sources. The resulting map still shows some significant anomalies which may be due to mantle convection. Nevertheless, because topographic features are mainly coherent with the geoid, to first order an isostatically compensated lithosphere cut by major E-W fracture zones accounts for most of the power in the high degree and order SEASAT geoid in the Central Pacific.

G32-12

A Tectonic Tour of the Indian Ocean via the Seasat Satellite

JEFFREY K. WEISSEL and WILLIAM F. HAXBY (both at: Lamont-Doherty Geological Observatory of Columbia University, Palisades, N.Y. 10964)

Radar altimeter data obtained by the Seasat satellite continue to play a major role in solving outstanding problems in marine and solid-earth geophysics, and will undoubtedly help define many more. The importance of Seasat data stems from their uniform distribution over the oceans worldwide, and the ±0.05 m accuracy with which sea surface height variations

were measured. In addition, the reduction of the altimeter data set to geographically-gridded gravity anomalies and the use of digital imaging techniques for the display of such gravity data, provide an ideal means for rapidly assessing the information obtained by Seasat, and for comparing Seasat data with other types of geophysical data. Many features of tectonic interest are clearly delineated by Seasat data -- this is particularly important in remote regions (such as the Indian Ocean) that have been poorly surveyed by ship. We will highlight newly-identified tectonic features in the Indian Ocean to demonstrate the valuable contribution of Seasat data to a) plate kinematics models, and b) studies of thermomechanical deformation of oceanic lithosphere. Seasat data contribute to the knowledge of past plate motions through the improved accuracy with which lithospheric age discontinuities, such as fracture zones, ridge crest jumps and abandoned spreading centers, are mapped. In the southern Indian Ocean, two new fracture zones which respectively record the movement of Africa and India away from Antarctica in Late Mesozoic time, have been discovered. Seasat data over the Indo-Australian plate provide clear evidence for deformation of the lithosphere under ~NS compression, and for roll-like gravity features aligned in the direction of absolute plate motion, which may reflect small-scale convection beneath the plate.

G32-13

An Inversion Algorithm for the Determination of Geophysical Parameters

J. M. BROZENA, L. C. KOVACS, P. LANZANO (all at the Naval Research Laboratory, Code 5110, Washington, D.C. 20375)

We have devised an algorithm that will allow us to ascertain the density profile of various lower layers consistent with the gravity anomalies measured at the upper surface. We have assumed a fixed geometry and have reached a linear system that relates the unknown layer densities to the given gravity measurements and the expected errors that will be present in the execution of the computations. The coefficients matrix is supposed to be known since it represents the self-attraction of the lower layers.

Such system, however, presents an infinity of solutions, many of which lack geophysical significance. In order to bracket our solutions, we apply a minimum principle, whereby we impose to minimize a suitable functional of densities and errors. We have chosen a quadratic expression which leads to the most compact configuration compatible with the given measurements.

It is a matter of choosing certain weighting matrices. Should these matrices be fixed once for all, we then get the densities in terms of the gravity anomalies by a onestep procedure essentially akin to least squares. It is, however, more appropriate to change the weighting matrices at each step of the computation, whereby we generate a recurrent procedure and obtain the k-th approximation of the density profile in terms of the (k-1)-st choice of the weighting matrices.

This algorithm has been computerized and will be tested against profiles of known topography and density layering.

G32-14

ALONG-TRACK DEFLECTIONS OF THE VERTICAL: GEBCO OVERLAYS

D. T. SANDWELL (National Geodetic Survey, Charting and Geodetic Services, National Ocean Service, NOAA, Rockville, Md. 20852)

To provide easy access to the vast number of Seasat altimeter observations, the National Geodetic Survey has produced overlays for the GEBCO map series (General Bathymetric Chart of the Oceans, Hydrographic Chart Distribution Office, Ottawa, Ontario, Canada, K1G 3N6). Each of the 32 sheets displays along-track deflection of the vertical for either ascending or descending altimeter passes. In poorly charted southern ocean areas the complete coverage by the Seasat altimeter reveals many previously undetected features of the seafloor. An example of descending profiles across the Udintsev Fracture Zone is shown below.

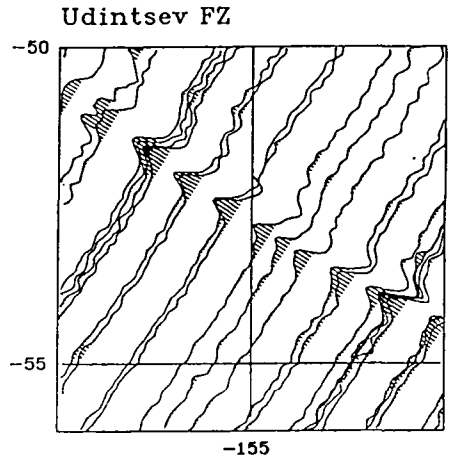

Excitations of the Earth's Rotation I

Room 21 Thurs AM

Presider, J.O. Dickey, JPL/ CALTECH

G41-01

Activities and Goals of the International Union of Geodesy and Geophysics/International Association of Geodesy (IUGG/IAG) Special Study Group 5.98, Atmospheric Excitation of the Earth's Rotation

J.O. Dickey
Jet Propulsion Laboratory,
California Institute of Technology
Pasadena, California 91109

The transfer of angular momentum between the oceans, atmosphere, and solid Earth is rapidly emerging as a problem of great scientific importance. Recent studies demonstrate that the angular momentum transfer between the atmosphere and the solid Earth makes a major contribution to short-term variations in the length of the day. The main objectives of the SSG 5.98 are to provide a forum for scientific discussions and interactions on these topics, to encourage further studies and to advocate improvements in the measurement techniques. The current goals of the study group are outlined below:

- o We will encourage cooperative multidisciplinary studies of the angular momentum transfer between the solid Earth, the oceans and the atmosphere.
- o We will strive for improved communication and data flow between the atmospheric and geodetic communities. An establishment of data base and the associated documentation will be pursued; greater interaction on models and applications of results will be stressed.
- o Considering that the Main Campaign of Project MERIT (Measurement of Earth Rotation of Intercomparison of Techniques - September 1, 1983 to October 31, 1984) will produce the highest resolution and most accurate measurements of earth rotation ever achieved, we have requested and will interact with meteorological data centers, so that every effort is made to collect the most complete possible set of global meteorological data and reduce these data in a consistent manner to obtain the highest quality atmospheric angular momentum excitation functions throughout this period.

G41-02

Excitation of Short-Term Length-of-Day Changes and Polar Motion

R. Hide
Geophysical Fluid Dynamics Laboratory
Meteorological Office
Bracknell
Berkshire RG12 2SZ, United Kingdom

Several years ago, for the purposes of meteorological and geophysical research, we established a firm theoretical basis for the use of routine determinations of fluctuations in all three components of the angular momentum of the Earth's atmosphere in the assessment of the extent to which atmospheric excitation can account for short-term fluctuations in the length of day and polar motion. We applied our methods to available data (including the meteorological data sets from the First GARP Global Experiment, FGGE) and concluded that seasonal and shorter timescale changes in the length of the day could, at least over the interval studied, be fully accounted for without invoking non-atmospheric excitation, such as angular momentum exchange between the Earth's liquid metallic core and solid mantle. (Core-mantle interactions are, however, the most probable main cause of large irregular length-of-day changes on timescales upwards of a few years.) We also concluded that atmospheric excitation could account for the observed polar motion, without finding it necessary to invoke the Earth's core or effects due to movements in the solid Earth associated with earthquakes of magnitude not exceeding 7.9 (that of the strongest experienced during the period covered by the study). Our most recent work confirms these conclusions and also extends the investigation of the 7-week fluctuation in the axial component of atmospheric angular momentum revealed by these studies. It is gratifying that in this important area of geophysical research, which is greatly benefitting from new geodetic techniques, collaborative studies are now being vigorously promoted by a new International Association for Geodesy working group chaired by Dr. Jean Dickey of the Jet Propulsion Laboratory.

G41-03

Causes of the decade variations in the Earth's rotation

M. G. ROCHESTER (Dept. of Earth Sciences, Memorial University of Newfoundland, St. John's, Nfld. A1B 3X7)

Between the short-term ($\lesssim$ 5 yr) fluctuations in the axial rotation of the solid Earth (now well explained by exchange of angular momentum with the atmospheric zonal wind system) and the long-term changes (attributable largely to tidal friction and deglaciation) lie the decade variations in the length of day, whose existence seems to require coupling of the mantle to motions in the liquid core. On this time scale the appropriate core-mantle coupling mechanisms are electromagnetic and topographic. This paper reviews the comparative effectiveness of the two mechanisms in exciting and damping changes in the axial spin rate of the solid Earth. At least another decade or two of high quality data on UT1 and global atmospheric angular momentum will be needed before we can hope for significant improvements in our understanding of core-mantle coupling.

G41-04

Excitation of Decade Fluctuations in the Earth's Rotation

A. K. Babcock
D. D. McCarthy (U. S. Naval Observatory, Washington, D. C. 20390)

One of the services of the U. S. Naval Observatory is the weekly publication of predictions of UT1. In the continuing effort to improve the accuracy of these predictions, a study is underway of variations in the Earth's rotation. This report focuses on the very low frequency variations.

Records of the Earth's rate of rotation, or length of day (l.o.d.), covering at least a few decades characteristically show large, abrupt changes in rate occurring at roughly ten-year intervals. Because of this apparent pattern, these accelerations have been called "decade fluctuations" and are one of the most serious impediments to predicting UT1 with improved accuracy.

We have developed a model which produces a series of l.o.d. variations which are statistically similar to the past 160 years of observed variations, including apparent decade fluctuations. This model produces these simulated data by integration of high frequency accelerations. It suggests that the "decade" fluctuations may result purely from higher frequency accelerations, such as those due to global winds, and that these decade fluctuations may ultimately be unpredictable.

G41-05

Time Series Studies of Meteorological Forcing Functions for Earth Rotation and Polar Motion

DAVID A SALSTEIN
RICHARD D. ROSEN (both at Atmospheric and Environmental Research, Inc., 840 Memorial Drive, Cambridge, MA 02139)

The axial component of the atmosphere's angular momentum, M, has been evaluated on a twice-daily basis for the years 1976-1983. This series has been shown to agree well with changes in the length of day (lod) on annual and shorter time scales. In particular, the maximum value of M in the record, which occurred in early 1983, was mirrored in lod observations and has been associated with a Pacific oceanic warming event (El Niño).

A three-year comparison of two M series, as derived from the National Meteorological Center (NMC) and the European Centre for Medium Range Weather Forecasts (ECMWF), does reveal some discrepancies. To find their geographical sources, we examined the contribution to both M series made by each of 22 latitudinal belts.

In addition, values of the equatorial components of atmospheric angular momentum, related to forcing functions of polar motion, are being produced both on an operational basis (since 31 August 1983) as well as from earlier archived wind and mass fields, and will be studied.

G41-06

The Southern Oscillation and Changes in the Length of Day

T. M. Eubanks
J. O. Dickey
J. A. Steppe(all at Jet Propulsion Laboratory, California Institute of Technology, Pasadena, California 91109

Changes in the Length of Day (LOD) at seasonal and higher frequencies are mostly driven by exchanges of angular momentum with the atmosphere. The atmosphere cannot be responsible for the large changes in the LOD seen over periods of decades and centuries, and the role of the atmosphere in the interannual LOD changes has been controversial. The Southern Oscillation involves a large scale interannual redistribution of atmospheric mass above the equatorial Pacific, and is also associated with wide-spread changes in the atmospheric and oceanic circulation, and with the El Nino phenomenon. There were unusually large changes in the LOD and the Atmospheric Angular Momentum (AAM) during January and February, 1983. These changes coincided with the peak of the 1982-83 El Nino, which involved unusual changes in the atmospheric pressure over the eastern and western tropical Pacific. The seasonally adjusted difference of the sea level pressure at Tahiti and Darwin, Australia, which is a common Southern Oscillation Index (SOI), reached a record low in January, 1983. The apparent connection between the SOI and the LOD in early 1983 suggests that there may have been similar LOD changes during previous El Ninos and, also, that the interannual changes in the LOD may be related to the Southern Oscillation. We will describe the relationship between the measured LOD and the Tahiti-Darwin SOI data for the period between 1970 and the present. Although there is no significant SOI-LOD coherence at periods less than annual, there is an apparent negative correlation between the interannual fluctuations in the SOI and the LOD. The nature and significance of this correlation will be explored.

G41-07

Interannual Length-of-Day Variation and Southern Oscillation/El Nino

B. Fong Chao (Geodynamics Branch, Laboratory for Earth Sciences, Goddard Space Flight Center, Greenbelt, MD 20771).

The atmospheric and oceanic mass transport associated with the southern oscillation (SO)/El Nino will inevitably induce an interannual variation in the length of day (LOD). We conduct an empirical correlation study by comparing the two relevant time series for the

period 1957-1983: the SO index (SOI) and the inter-annual LOD variation. The latter is obtained by removing the least-squares estimates for the long-period (secular and decade) and the short-period (seasonal and tidal) variations from a BIH LOD series. The two series has a very encouraging qualitative correlation, in particular with respect to El Nino events; and the linear correlation coefficient is found to be 0.55. It is believed that much, if not most, interannual LOD variation is caused by the SO, and the true correlation is considerably higher than its apparent value considering the fact that the SOI is merely an indicator derived from two local atmospheric measurements while the LOD is a global quantity. Further detailed investigation requires a workable SO model.

G41-08

Length of Day via Radio Interferometry: Correlation with Atmospheric Angular Momentum

R. Potash
(Interferometrics Inc., Vienna VA 22180)
T. A. Clark
(NASA Goddard Space Flight Center, Greenbelt MD 20771)

VLBI measurements made as part of NASA's Crustal Dynamics Project (CDP) determine vector baseline orientation, and thus UT1, with a typical accuracy of $\leq$ 100 microseconds of time. Observations at weekly intervals on the NGS POLARIS network yield length of day (LOD) measurements accurate to $\leq$ 25 microseconds. After tidal effects and long term ($\geq$ 6 months) fluctuations are removed, the data is compared with measurements of atmospheric angular momentum obtained from the CDP archives. Much of the short term ($\leq$ 3 month) fluctuations in rotation rate appear to be due to exchange of angular momentum between the atmosphere and the solid earth. VLBI LOD data from late 1980 thru the present has been analyzed. The most striking feature observed in the VLBI data is the El Nino event in early 1983.

G41-09

Atmospheric Momentum and Crustal Motion Relationships: Implications of Observed Short Term Discrepancies

H. A. TAYLOR, JR.
H. G. MAYR (both at: NASA/Goddard Space Flight Center, Greenbelt, Maryland 20771)
L. KRAMER (Institute for Physical Science and Technology, University of Maryland, College Park, Maryland 20742)

Occasional discrepancies interspersed with close correlations between globally integrated atmospheric momentum and crustal rotation present a challenge to the understanding of both the measurements and the physical processes relating them. Although similar annual and quasi-monthly modulations clearly evident in both data sets support the view of balanced momentum exchange, differences of as much as twenty percent of the annual variation in momentum sometimes occur between the two parameters. Accounting for high altitude momentum contributions above 100 mb, as well as identifiable moment of inertia variations does not resolve these discrepancies. Analysis indicates that uncertainties in the astrometric results are an important part of the inconsistency. Comparison of regional signatures of rotation change with atmospheric momentum indicates regionally dependent differences. This in turn poses questions relative to the accuracy of the determination of the crustal motion and to the potential importance of as yet undetermined sources of momentum change.

G41-10

The Observed Excitation of the LAGEOS Derived Chandler Wobble

R. S. Gross
B. Fong Chao (both at Geodynamics Branch, Laboratory for Earth Sciences, Goddard Space Flight Center, Greenbelt, MD 20771).

We have deconvolved the University of Texas LAGEOS Chandler wobble to recover its excitation function. This observed excitation function agrees with that previously obtained from the BIH data and covers the period from 1/21/77 to 1/20/84. We will discuss two interesting features of the observed excitation function for the LAGEOS chandler wobble in conjunction with two significant geophysical events.

First, the excitation axis is observed to change by 0".04 in the direction of -54° E longitude from 8/13/77 to 9/2/77. Dahlen's application of elastic dislocation theory to point tangential dislocations in a SNREI earth model predicts a shift of the excitation axis of 0".0003 towards 93°E longitude due the great Sumba earthquake which occurred on 8/19/77. Not only is this predicted shift two orders of magnitude smaller than that observed but it is in nearly the opposite direction. At present we have therefore concluded that the observed shift is due to some unknown disctontinuity in processing the laser ranging data. Nevertheless the coincidence between the time of the earthquake and that of the observed change remains remarkable.

Second, the extraordinarily intensive 1982-1983 Southern Oscillation/El Nino episode which caused a dramatic drop in the earth's rotational speed seems to have had a less prominent effect on the Chandler wobble. In fact, the X-component excitation during this period is rather quiescent. However, the correlation between the Y-component (Ψ_y) and the Southern Oscillation Index (SOI) is encouraging in the sense that Ψ_y closely follows SOI and the overall change in Ψ_y during 1982-83 has a "correct" magnitude.

G41-11

Interaction of Mantle Rheology and Plate Boundary Earthquakes in Excitation of Chandler Wobble

M. A. Slade
G. A. Lyzenga
A. Raefsky (all at Jet Propulsion Laboratory, California Institute of Technology, Pasadena, CA 91109)

Postseismic motions following great earthquakes at plate boundaries are studied for a variety of asthenospheric rheologies and low effective viscosity zones. These studies model the whole earth response to such excitation using three-dimensional finite element techniques with an explicit time-dependent algorithm. The large size of such models requires the use of an element-by-element (EBE) approximate factorization of the stiffness matrix (Hughes et al., 1983). The density and elastic structure of the earth is taken from the PEM-C radially symmetric model of Dziewonski et al. (1975). Previous whole-earth studies have only considered linear Maxwellian rheology using a Laplace transform method (Dragoni et al., 1983). In addition to such a rheology, we have studied a non-Newtonian power law rheology for n=3. Such a constitutive equation appears to describe laboratory measurements of mantle material (Kirby, 1983), and also is inferred from some observations at subduction zones (Melosh 1976). The applicability to the mantle in general, however, is still a matter of debate (e.g., Peltier, 1983). Our results enable the prediction of the effect of a large plate boundary earthquake on the motion of the pole. Given sufficient accuracy on the observations of the polar motion (e.g., via VLBI), and assuming that the atmospheric part of the excitation can be calculated quite accurately (see Rosen, 1983), such polar motion observations could be sensitive to the rheology of the asthenosphere in the vicinity of the plate boundary. Some limits on upper mantle rheologies for various thicknesses of the asthenosphere can also be derived. Results will be presented for a 90 degree dipping strike-slip and dip-slip faults.

Excitations of the Earth's Rotation II

Room 21 Thurs PM

Presider, R. D. Rosen, Environmental Research, Inc.

G42-01

Some Geophysical Problems Related to the Earth's Rotation

JOHN M. WAHR (Department of Physics and Cooperative Institute for Research in Environmental Sciences, University of Colorado, Box 449, Boulder, CO 80309)

Two general topics are discussed. First, we consider the effects of the atmosphere and oceans on the seasonal variations in the length-of-day. We use a combination of monthly atmospheric data and meteorological and oceanographic models. We consider the effects of winds, atmospheric pressure, wind and pressure induced upwelling in the oceans, and ocean currents (although we are not presently able to include the effects of the Antarctic circum-polar current). Our atmospheric estimates differ from earlier estimates by about 10%. The effects of atmospheric pressure are about 10% of the effects of winds. The effects of oceanic upwelling and ocean currents (with the exception of the circum-polar current) are negligible.

Second, we estimate the effects of wobble-induced deformation on crustal motion and surface gravity measurements. We include the effects of the oceanic pole tide. We find that peak-to-peak radial motion of an individual station is typically 1-2 cm over a few years, depending on the amplitude of polar motion and on the latitude of the station. Horizontal displacements are at least a factor of five smaller. The perturbation in a baseline depends on the relative locations of the two endpoints, but in extreme cases (eg. Greenbelt - Yaragadee) baseline lengths can be affected by up to 3-4 cm. Peak-to-peak variations in surface gravity can be on the order of 10 microgals over a few years.

G12-02

Accuracies of Recent Observations of the Earth's Rotation

R. W. KING (Department of Earth, Atmospheric, and Planetary Sciences, Massachusetts Institute of Technology, Cambridge, MA 02139)
B. A. KOLACZEK (Space Research Center, Polish Academy of Sciences, 01-237 Warsaw, Poland)
I. I. SHAPIRO (Harvard Smithsonian Center for Astrophysics, 60 Garden Street, Cambridge, MA 02138)

Lunar laser ranging (LLR), satellite laser ranging (SLR), and very-long-baseline interferometry (VLBI) are recognized as the techniques presently producing the most accurate measures of variations in the earth's rotation. We evaluate these three techniques in light of improvements effected in recent months: the resumption of lunar ranging at the McDonald Observatory, improved SLR data analyses now being performed at the University of Texas Center for Space Research (CSR), and the addition of a third NGS POLARIS station at Richmond, Florida. For Universal Time (UT1) and each component of the pole, we discuss the optimal weighting and smoothing of the results of each technique, used alone and in combination. We also evaluate the past and present contribution of classical astrometric (CA) and satellite Doppler (SD) observations. Finally, we describe the characteristics and utility for geophysical studies of combined series for UT1 and pole position for the period 1970-1983.

G12-03

A Kalman Filter and Smoother for the Earth Rotation

D. C. Hernquist
T. M. Eubanks
J. A. Steppe (all at Jet Propulsion Laboratory
California Institute of Technology
4800 Oak Grove Drive, Pasadena, CA 91109)

High frequency fluctuations in UT1 complicate the use and analysis of very precise UT1 data. These high frequency fluctuations are driven by exchanges of angular momentum between the solid earth and the atmosphere. Meteorologically derived Atmospheric Angular Momentum (AAM) data indicate that the UT1 power spectrum is proportional to the frequency**-4 at periods < 100 days. A stochastic process which has such a power law at all frequencies is an Integrated Random Walk (IRW), or doubly integrated white noise. Physically, the IRW model assumes that the torques on the solid earth can be described as a white noise, and that, in the absence of these torques, the rate of rotation of the solid earth would be constant. A Kalman filter based on this model has been developed at JPL to allow the Deep Space Network to estimate UT1 whenever necessary for spacecraft navigation while making full use of the high accuracy UT1 measurements. It can be applied either to raw UT1 or UT2 data from which the predictable UT1 fluctuations of tidal origin has been subtracted. Since the UT1 power spectrum has strong peaks at annual and semi-annual periods, if there are large data gaps it is best to apply the filter to UT2. However, with modern measurement accuracies and typical measurement densities, the seasonal variations in the UT1 are well above the noise, and, for most purposes, it is not necessary to include these explicitly in the UT1 model. We will describe the implementation of this filter and its performance under a variety of ideal measurement strategies. We will also discuss a possible improvement, the augmentation of the filter to also accept AAM data.

G12-04

Intercomparison of Independent Measurements of Earth Orientation and Rotation

M. A. Spieth
T. M. Eubanks
J. A. Steppe (all at Jet Propulsion Laboratory
California Institute of Technology
4800 Oak Grove Drive
Pasadena, CA 91109)

The JPL Time and Earth Motion Precision Observations (TEMPO) program observes station clock behavior and earth orientation to support interplanetary navigation by the Deep Space Network. The POLARIS project of the National Geodetic Survey (NGS) also provides accurate estimates of earth orientation. Both TEMPO and POLARIS obtain these measurements by Very Long Baseline Interferometry (VLBI). We shall present an analysis of the accuracy of these methods by intercomparing the available data. None of these data are simultaneous; therefore, a proper intercomparison requires accounting for the scatter introduced by the rapid, unpredictable UT1 variations driven by exchanges of angular momentum with the atmosphere. We have derived a statistical model of the uncertainty introduced by these variations based on meteorological estimates of the atmospheric angular momentum and used this model to construct a Kalman smoother for UT1. The root mean square of the difference between raw TEMPO data and smoothed POLARIS UT1 estimates is 0.57 msec for the post-1982 data. The observed scatter is consistent with the difference formal errors, which are the root sum square of the measurement formal errors and the smoothed data error estimate. These formal errors do not depend upon the actual scatter of the UT1 data. There is no evidence of an intrinsic lower limit on the accuracy of UT1 estimates from VLBI, and we think that it is unlikely that any unmodeled random error in these data has a standard deviation as large as 0.4 msec.

G12-05

IRIS Earth Orientation Results

W. E. CARTER
D. S. ROBERTSON (Both at National Geodetic Survey, Charting and Geodetic Services, National Ocean Service, NOAA, Rockville, Md. 20852)

The International Radio Interferometric Surveying (IRIS) activities to support the MERIT Main Campaign comprise 24 hour geodetic VLBI observing sessions at 5 day intervals designed to monitor UT1 and polar motion. Three observatories in the United States (the POLARIS Observatories located in Westford, Massachusetts, Ft. Davis, Texas, and Richmond, Florida) and the Wettzell Observatory, Federal Republic of Germany, routinely participate. During the period of the MERIT high intensity campaign, April through June 1984, daily determinations of UT1 using only the Westford-Wettzell interferometer are being made. After processing through either the Haystack or Max Planck correlator, the delays, delay rates, and auxiliary data are distributed to several organizations for analysis. The National Geodetic

Survey regularly processes the IRIS data to obtain UT1 and polar motion time series. The formal uncertainties vary depending on the number of observatories and the geometry of the network from session to session, but typically are about 0.1 to 0.3 milliseconds for UT1 and 5 to 10 cm for polar motion.

G42-06

EARTH ROTATION FROM LAGEOS: THE 1984 CSR SYSTEM

R. J. Eanes (Center for Space Research, The University of Texas at Austin, Austin, TX 78712)
B. E. Schutz
B. D. Tapley

Earth rotation parameters from Lageos have been routinely computed and reported by the Center for Space Research (CSR) at The University of Texas at Austin since the Short MERIT Campaign in 1980. Since 1981, these solutions have been a major contributor to the BIH polar motion system and have been analyzed by several investigators. In early 1984, substantially improved analysis techniques and models were adoted by CSR for use in the routine ERP solutions as well as in studies of station coordinate and baseline evolution. These changes have resulted in major improvements in the accuracy of the Lageos results and have significantly increased the flexibility in the choice of the averaging interval used for the ERP solutions. This paper discusses these new techniques and ERP series and compares them with previous techniques and other available ERP series. More specifically, new Lageos results computed using 5-day, 3-day and 1-day averaging inervals are intercompared and are used to study the spectrum of variations in UT1 and polar motion at periods below 50 days. The long-term stability of the Lageos ERP series and its relationship to global plate tectonic models, the predictability of the earth and ocean's response to long period tides, and to nontidal quasi-periodic changes in the geopotential are also discussed.

G42-07

Doppler Polar Motion Measurements During Project MERIT

E.G. COLQUITT, W.L. STEIN, R.J. ANDERLE
Naval Surface Weapons Center
Dahlgren, VA 22448

The Naval Surface Weapons Center has been involved in the post-processing of the NAVSAT Doppler polar motion measurements produced by the Defense Mapping Agency. The results of removing polar motion biases between satellites will be presented with emphasis on Project MERIT. A comparison will be made of these improved Doppler polar motion measurements with polar motion results from other techniques.

G42-08

The Self-Consistent Dynamic Pole Tide

S.R. DICKMAN (Dept. of Geological Sciences, State University of New York, Binghamton, N.Y. 13901)

It has been known since Newcomb (1892) that the pole tide, the oceanic response to the Chandler wobble, acts--through its mass redistribution (products of inertia)--to lengthen the Chandler wobble period. The extent of lengthening, traditionally calculated by assuming a static response, is $\sim$ 1 month.

Such estimates, however, fail to treat the pole tide self-consistently. The tide's effect on wobble period, computed according to conservation of angular momentum (Liouville equation), is a function of the tide height; the latter is found rigorously according to conservation of linear momentum (e.g. Laplace tidal eqns) and depends on the wobble period. The two must be determined jointly or the lengthening estimate will be incorrect.

At the Fall 1983 Meeting I reported on a first investigation of the self-consistent pole tide. The oceans were taken as global, and linearized bottom friction of different strengths was considered. In all cases the resulting tide lengthened the wobble period by only $\sim$ half the static amount.

But a non-static tide must be supported by non-zero currents, and relative angular momentum associated with the currents will also affect the wobble period. Self-consistent theory incorporating such effects has now been developed. Results to date indicate that the angular momentum contribution to wobble period lengthening is surprisingly large: more than three times that of the tide's products of inertia.

Although oceanic non-globality can be expected to modify these results, it appears that the self-consistent and dynamic nature of the pole tide is crucial to the tide's effect on wobble.

G42-09

The Decelerations of the Earth and Moon

ERNST W. SCHWIDERSKI (Naval Surface Weapons Center, Dahlgren, Virginia 22448)

The paper develops new formulas for the decelerations of the earth's rotation and the moon's revolution from the law of conservation of energy alone. Starting from a generally accepted earth model with real and constant tidal Love numbers and from the spherical harmonic expansion of an arbitrary ocean tide model, it is found that the ocean tides accelerate the moon. This stunning ocean-tide independent contradiction is attributed to significant shortcomings of the postulated earth tide model. For the sake of demonstration, it is shown that an earth tide phase lag of about 0.5° together with the NSWC ocean tide model (1983) can bring the computed deceleration of the moon in complete agreement with the presently prevailing empirical satellite estimate. It will be argued on physical grounds that such a moderate phase lag does not violate the seismically supported low estimate of heat dissipation in the earth which translates into an earth tide phase lag of a few thousandths of one degree. The new formulas will be compared with earlier equations, the derivation of which will be reviewed.

Geodynamics Program/Crustal Dynamics Project Overviews; Station Update

Room 27 Mon AM

Presider, R.J. Coates, GSFC

GD11-01

The NASA Geodynamics Program

T. L. FISCHETTI (Geodynamics Branch, Office of Space Science and Applications, NASA)

NASA is cooperating, with 25 countries and four other federal agencies in the study of global tectonics and earth rotation dynamics. These studies use data acquired with laser ranging (both satellite and lunar) and microwave interferometer systems. These systems are now achieving precision of a few centimeters for baseline measurements of regional, continental and intercontinental scales. Plans have been developed to evaluate the use of the Global Positioning System and other methods for rapid and economical measurements at similar scales. Plans have also been developed for the generation of improved gravity and magnetic field models of the earth and for dedicated gravity and magnetic field space missions: the Geopotential Research Mission and the Magnetic Field Explorer.

This paper will review the status of the NASA Geodynamics Program and present plans for global geodynamic studies extending into the 1990s.

GD11-02

The NASA Geodynamics Program - An Overview of Scientific Progress

L. S. WALTER (Geodynamics Branch, NASA Headquarters, Washington, DC 20546)

The objective of the Geodynamics Program is to use space technology to improve our understanding of the solid Earth. Currently, the greater part of the resources of this Program are devoted to the Crustal Dynamics Project which is engaged in developing techniques for precise position determinations and in using the resultant data for studies of plate motion and regional deformation. Now, at about the mid-point of the Project's lifetime, many epoch measurements have been made and measurements of significance to tectonic studies are beginning to emerge. The data have also been used to contrain fundamental values of the viscosity of the Earth and to study the effects of the atmosphere on its rate of rotation.

Past developments of the Program (or its progenitor, the Earth and Ocean Physics Applications Program) are still yielding valuable scientific results. Precise altimetric measurements of the oceanic geoid by Seasat have yielded spectacular images of the detailed structure of the ocean floor. Structural and tectonic models are being derived through interpretation of Magsat data.

The development of the scientific rationale for the future Program is also of some importance. This is based primarily on studies of the Geopotential Research Mission and the Magnetic Field Explorer (Magsat-B) as well as the Geodynamics Workshop all of which will be discussed.

GD11-03

The NASA Crustal Dynamics Project

R. J. COATES (NASA Goddard Space Flight Center, Greenbelt, MD 20771)

The NASA Crustal Dynamics Project was started in 1979 to initiate studies of regional deformation related to earthquakes, relative plate tectonic motions, internal plate stability, and polar motion utilizing measurements with satellite laser ranging (SLR) and very-long-baseline interferometry (VLBI) systems, developed by NASA for high accuracy geodesy. This is a cooperative project with participation of several U.S. Government agencies and many foreign agencies and institutions. Measurements of global plate motion, plate stability, and polar motion are being conducted with an 18 station laser network and a 7 station VLBI network. Regional deformation in western N. America is being measured by occupying many sites with two transportable laser ranging systems and three mobile VLBI systems working in conjunction with the laser and VLBI network stations. Recent improvements of the measurement systems have resulted in measurement precisions of about 1 cm and baseline determinations with uncertainties as small as a few cm.

GD11-04

Crustal Dynamics Project Observing Program: 1983 Results and Plans for 1984

H. FREY (Geophysics Branch, Goddard Space Flight Center, Greenbelt, MD 20771)

NASA's Crustal Dynamics Project observations for plate motion, plate stability and regional deformation studies grew substantially in 1983, and significant additional growth is planned in all areas for 1984. The global laser network grew through addition of new sites on Easter Island, on Huahine (near Tahiti) in the Pacific, in Mazatlan, Mexico and in Matera, Italy. The Easter Island site was occupied by TLRS-2 for six months; the other sites are occupied continuously. New VLBI stations became operational at Mojave, CA; Richmond, FL; Kashima, Japan and Wettzell, Germany. The Mojave station is a dedicated VLBI base station which also supports the California regional deformation measurements, as does a base station at Vandenberg Air Force Base provided by locating the 9m MV-1 system there. Mobile VLBI systems occupied 14 sites in both northern and southern California in 1983. Mobile SLR systems reoccupied Otay Mt., a site at Yuma, AZ and the VLBI base station at OVRO. For 1984, in addition to reoccupation of sites visited in 1983, major new measurement programs are scheduled in Baja California and South America for SLR, and in the Basin and Range and Alaska for VLBI. Plate motion measurements between Alaska and the rest of North America with the Pacific and Eurasian plates will be done by VLBI. Easter Island will be reoccupied by TLRS, and a new lunar and satellite SLR system will double the number of Australian sites in the global network.

GD11-05

CDP VLBI Measurement Plans for the Summer of 1984

I. A. Clark
(NASA Goddard Space Flight Center, Greenbelt MD 20771)

During the summer of 1984 the NASA Crustal Dynamics Project (CDP) VLBI groups will conduct a number of experiments to measure both interplate motions and intraplate stability as the first phase of a five year program. These first epoch measurements will involve stations on the North American, Pacific, and European plates. North American stations include stations in Alaska, California, Massachusetts, Texas and Canada. The activity in Alaska and Canada will involve the use of both fixed "observatories" and two NASA-developed mobile VLBI systems. Fixed stations on the Pacific plate will be in Hawaii, Kwajalein, and and California. Planned European stations are in Sweden and West Germany; a station in Japan near the convergence of the North American, Pacific and Eurasian plates will also participate. The difficulties associated with implementing several new VLBI sites and in coordinating such a large international network of stations for an intense observing campaign will be discussed.

GD11-06

GPS Geodesy in the South Pacific: New Zealand and Australia

C. L. Thornton
B. C. Beckman (both at Jet Propulsion Laboratory, California Institute of Technology, Pasadena, CA 91109)

Assuming simultaneous centimeter GPS range and estimates of the ultimate accuracies of the system components, expected accuracies are generated for a set of test baselines in the South Pacific. A variety of fiducial network configurations yield acceptable results, with optimum results obtained from the three-station network of Canberra, Japan, and Hawaii.

Questions to be addressed include: 1) the effect of removing all clock errors by the use of doubly differenced range, 2) the sensitivity of baseline accuracy to satellite a priori position error, 3) the minimum data arc length required to obtain centimeter baselines.

GD11-07

GPS Geodesy in the Caribbean: Sensitivity to Choice of Epoch

J. M. Davidson
B. C. Beckman
C. L. Thornton (all at Jet Propulsion Laboratory, California Institute of Technology, Pasadena, CA 91109)

We have performed a covariance analysis to investigate the sensitivity of baseline accuracy to the choice of epoch for GPS geodetic experiments in the Caribbean. This investigation was performed for both the current GPS constellation of five satellites and the constellation of eighteen satellites as it will be be configured in 1988. The hypothetical GPS network used consisted of fiducial stations located at Mojave, California; Westford, Massachusetts; and Quito, Equador and mobile stations located at San Juan, Puerto Rico and Santo Domingo, Dominican Republic. Four hour arcs were used, with single-differenced range as the data type. Satellite orbit parameters were estimated. The error budget for both cases included contributions from data noise (0.1 cm), wet troposphere (7.5 mm at zenith), and fiducial station location error (1 cm). Our covariance

analysis shows that for the 1988 constellation the accuracy of estimated baseline components can vary by up to 70% depending on the choice of epoch. Further, we find that, to the extent the assumed error budget is equally valid for both cases, there is virtually no degradation of accuracy for baselines in the Caribbean for the current GPS constellation, compared to that predicted using the 1988 constellation, provided the epoch of observation is properly chosen.

GD11-08

National Geodetic Survey Mobile VLBI Operations

G. L. MADER (National Geodetic Survey, Charting and Geodetic Services, National Ocean Service, NOAA, Rockville, Md. 20852)

The National Geodetic Survey, in accordance with an interagency agreement between the National Oceanic and Atmospheric Administration (NOAA) and the National Aeronautics and Space Administration (NASA), has begun mobile Very Long Baseline Interferometry (VLBI) operations using MV-3, a 5-meter highly mobile VLBI system, and MBS, the Mojave Base Station located at the Goldstone Deep Space Network. Two other mobile VLBI systems, MV-1 and MV-2, continue to be operated by the Jet Propulsion Laboratory until the transfer to NOAA is completed. The NGS is collecting VLBI data in California and the western United States in support of the Crustal Dynamics Project, and processing these data at its facility in Rockville, Maryland. In addition, NGS will soon begin the completion of the National Crustal Motion Network, with 15 new sites distributed across the continental United States. Results of this work and plans for future observations will be discussed.

GD11-09

The Crustal Dynamics Project Mojave VLBI Station

T. A. Clark
(NASA Goddard Space Flight Center, Greenbelt MD 20771)
C. G. Koscielski
(Jet Propulsion Laboratory, Barstow CA 92311)
B. E. Corey
(Haystack Observatory, Westford MA 06111)
N. R. Vandenberg
(Interferometrics Inc., Vienna VA 22180)

In June 1983, the NASA Crustal Dynamics Project (CDP) completed the new Mojave Base Station (MBS) located in the Goldstone Space Station complex near Barstow, CA. This facility was constructed to provide a permanent, dedicated VLBI station to support the CDP's geodetic measurement programs. MBS was built around an existing X-Y mount 12m dish antenna previously used by NASA as an ATS satellite ground station. The antenna and physical facility were well suited for VLBI usage. In order to achieve adequate VLBI performance with the CDP's 4m and 5m mobile VLBI systems, a new receiver system employing cryogenically-cooled GaAsFET low-noise amplifiers and an improved dual S/X-band feed was designed; copies of this receiver are under construction to improve the performance of a number of other VLBI stations. New software was designed for automatic antenna and station operations. The rest of the hardware for the station includes the CDP-designed Mark-3 data acquisition terminal and NR-series hydrogen maser. Initial operations of MBS have been very successful; for example, the first 8 measurements of the 245km MBS-OVRO baseline show 8mm RMS repeatability. Operational responsibility for MBS is in the process of being transferred to the National Geodetic Survey (NGS) in accordance with long-standing NASA/NGS agreements.

GD11-10

Wettzell: a new station for geodynamic VLBI measurements has become operational

R. KILGER (Satellitenbeobachtungsstation Wettzell,D-8493 Kötzting, FRG)

J. CAMPBELL, H. SCHUH (Geodetic Institute, Bonn University,D-5300 Bonn, FRG)

Since the first successful test experiment on the 920km baseline Wettzell-Onsala in July 83 a rapidly increasing number of observations is being routinely performed with the new 20m-antenna of the Satellite Observation Station Wettzell in the Federal Republic of Germany. The compact fast-slewing telescope is operating at the NASA S/X-bands with a dual frequency feed in a cassegrain configuration. The presently installed uncooled paramp (t_{sys} at zenith 180k at S and 190k at X) will be replaced by a cooled system at the end of 84. Maximum geodetic precision is guaranteed using the MkIII data acquisition system in conjunction with a hydrogen maser controlled frequency and timing system.

The performance of the new Swiss-made EFOS-1 maser has proved to be fully satisfactory (better than 1.10^{-14}). The results of some of the first experiments are described, showing e.g. a cm reproduceability on the Wettzell-Onsala baseline.

Since January 84 Wettzell is producing data in the POLARIS/IRIS one-day-in-five schedule of the MERIT Main Campaign. As a major extension of the POLARIS Earth rotation interferometer and as a dedicated partner in the Crustal Dynamics Project Wettzell is now heavily committed to geodynamic work.

GD11-11

VLBI for Geodynamics involving the Hartebeesthoek Radio Astronomy Observatory in South Africa

A. Nothnagel, G.D. Nicolson (HartRAO P O Box 3718 Johannesburg 2000, South Africa)
J. Campbell, H. Schuh (Geodetic Institute Bonn, Nussallee 17, 5300 Bonn 1, FRG)
A. Rius (INTA/NASA Orense 4, Madrid - 20, Spain)
(Sponsor L.S. Walter)

The high geodetic and geophysical interest of baseline determinations between Southern Africa and adjacent continents has prompted efforts at the HartRAO to intensify its geodetic VLBI activities.

In order to explore the exiting geometric potentials of the long N-S baselines connecting Europe and South Africa, two first experiments using the MK II BWS technique have been carried out at S-band (2.3 GHz) between the HartRAO and the NASA DSS 61 and DSS 63 antennas near Madrid. The baseline results which show decimeter accuracy are discussed in relation to the further accuracy improvements needed for crustal motion detection. A Hydrogen Maser frequency standard has been ordered and possible designs for a combined S/X receiver capability are studied. Funding schemes for acquiring a MK III terminal are investigated.

GD11-12

The McDonald Observatory Laser Ranging Station

PETER J. SHELUS (Department of Astronomy and McDonald Observatory, University of Texas at Austin, Austin, Texas 78712)

The McDonald Laser Ranging Station (MLRS) is a dual purpose facility designed to provide artificial satellite ranging capability at the Observatory site near Fort Davis, Texas and to replace the lunar instrumentation which has made use of the 2.7-meter telescope since 1969. Although scheduled to begin routine operations early in calendar year 1982, the first LAGEOS observations from MLRS were not obtained until the late summer of that year. Since that time a continuous series of such observations have been carried out while the attempts to establish lunar capability continued. These latter efforts were finally rewarded in August 1983 with the first confirmed returns from the Apollo 15 retroreflector array. We shall herein highlight the critical construction highlights for MLRS, discuss the main problems encountered with the attempts to establish routine LAGEOS and lunar capability, review the observations so far obtained, and assess the future expectations for this station's operations.

GD11-13

The First U.S.-Japan VLBI Test Observation

Noriyuki Kawaguchi (Radio Research Laboratory (RRL), Kashima, Japan and the RRL/NASA Joint Experiment Group) (Sponsor: L. Walter)

A precision very long baseline interferometer, the K-3 system, has been under development since 1979 in accordance with the five-year plan of the Radio Research Laboratories. It is designed to be compatible with the Mark-III system of NASA for use in a U.S.-Japan joint Pacific Plate motion experiment. The K-3 system, consisting of hardware and software, was almost completed at the end of September, 1983, and various tests have been made as the final phase.

The purpose of the test observation is to detect fringes to check over-all system performance of the K-3 system and compatibility with the Mark-III in preparation for initiation of plate tectonic studies this summer. The observation was made for about two and a half hours from 20 H 00 M to 22 H 34 M UTC on Nov. 4, 1983, by three station: Kashima, Mojave Base Station and Owens Valley Radio Observatory. Signals from three radio sources, 3C273B, 3C345 and 4C39.25, were alternately received six times throughout the time of observation; sampled digital data from 8 video signals for X-Band and those from six video signals for S-Band were recorded on 14 tracks of the tape.

Data processing was made by K-3 correlation processor at the RRL and also by Mark-III correlation processor at Haystack Observatory, independently, and both detected fringes. The result shows that measurement precision or the internal error in the test is better that 20 cm for X, Y and Z components for distance, and better than 1 nano-sec for clock synchronization.

Thus, it is confirmed that the K-3 has expected performance and good compatibility with the Mark-III system. In succession to the first test, we made more precise experiments of 24-hour observation using 13 radio sources in January and February 1984. Analysis for the determination of some parameters is now being made.

Continental Tectonics and Crustal Deformation I

Room 27 Mon PM

Presider, L.S. Walter, NASA

GD12-01

FAULTING HETEROGENEITY IN INTERPLATE SHEAR: THE TRANSVERSE RANGES, CALIFORNIA, AS AN EXAMPLE

Erik R. Ivins
G.A. Lyzenga (both at Jet Propulsion Laboratory, California Institute of Technology, Pasadena, CA 91109)

Faults within the Transverse Ranges of southern California are contradirectional (E-W) with respect to the surrounding northwesterly strike-slip San Andreas system. Quaternary deformation rates and seismicity within the Ranges are significant. Strike-slip and thrusting motions characterize earthquakes within this region. Thrusting by far dominates and north-south compression is apparently enhanced over east-west extension.

A simple analytical model is used to quantify the geometrical influence of the structural contradirectionality upon regional stress in southern California. The theoretical description relies upon idealizing two fault sets as having perfect directionality. Hence, the anisotropy of cracked and/or of laminated plates is applicable. A parameter study reveals that the Transverse Ranges act as a substantial obstruction to northwesterly interplate stress channeling. The model predicts that the recoverable strain energy is increased regionally above the ambient level by factors of as much as 2 to 3. The model is capable of matching the enhanced north-south compression estimated from earthquake focal mechanisms. The Ranges, in effect, act as a stress concentration embedded within the brittle elastic portion of the sheared lithosphere which exists between the North American and Pacific plates. The mechanical influence which the crosscutting structure of the Ranges induces locally may be competitive with, or perhaps dominate over, that of the Big Bend feature along the San Andreas fault.

GD12-02

The Role of Asperities and Barriers in the Propagation of Rupture as Predicted by the Renormalization Group Approach

R. F. SMALLEY, JR. and D. L. TURCOTTE (Dept. Geol. Sci., Cornell Univ., Ithaca, NY 14853)
S. A. SOLLA (Lab. of Atomic and Solid State Phys., Cornell Univ., Ithaca, NY 14853)

It is clear that most faults ruptures occur on preexisting zones of weakness. One approach to faulting is to apply a coefficient of friction. However, friction implies a single scale of roughness or asperities. An actual fault contains a continuum distribution of asperities and barriers (we regard these to be indistinguishable) on all scales. We believe that a statistical distribution of asperities and barriers is an essential feature of fault behavior and leads to the observed frequency - magnitude relation. We model a fault as a linear or two-dimensional array of asperities with a statistical distribution of strengths. We apply the renormalization group approach to this problem including the transfer of stress from a failed asperity to an adjacent asperity. For a single peaked strength distribution we obtain the standard s-curve with a single unstable singular point corresponding to the catastrophic failure of the fault. However, with a double peaked strength distribution a double s-curve is obtained. Three singularities, two unstable and one stable, are found. The stable singularity corresponds to the blocking of rupture progation. The relative magnitudes of the two peaks give the length of rupture (magnitude).

GD12-03

Modeling Deformation on Complex, Transform-Faulted Plate Boundaries

John B. Rundle, (Geophysics Division 1541, Sandia National Laboratories, Albuquerque, New Mexico 87185)

Modeling crustal motions in southern California obtained by VLBI, SERIES, and other space geodetic techniques requires a model in which several important physical processes are included. Since deformation on a time scale of years can be readily observed, both far-field plate motion and asthenospheric stress relaxation must be included. In addition, slip and stress heterogeneity must be allowed on the fault plane, as well as a variable slip history. These elements have been incorporated into a code to calculate horizontal surface deformation due to recurrent faulting on a vertical transform plate boundary. The individual fault segments can have any orientation, and each is given its own slip history.

Using this technique, a number of interesting limiting cases have been examined. Most cases involve a fault whose slip is uniform with depth, ending abruptly against adjacent segments which may be either completely locked, freely slipping, or only partially slipping. The latter case involves a fault segment which is allowed to slip at a depth-averaged rate less than the far-field plate velocity, therefore, not "keeping up" with the far-field plate motion. The central fault has a periodic slip history at discrete

intervals, which when averaged over time, adds up to the far-field plate motion.

Surface deformations for these models will be discussed and compared to various areas in southern California, including Parkfield and Cajon Pass. Both simple and complicated fault geometris will be considered, and applications to data collected by space-geodetic techniques will be discussed.

GD12-04

Viscoelastic Models of Crustal Deformation

Steven C. Cohen (Geodynamics Branch, Labortory for Earth Sciences, Goddard Space Flight Center, Greenbelt, MD 20771

In the past few years various viscoelastic models of the earthquake cycle and the attendant crustal deformations have been published. These models have sometimes differed in their predictions of the temporal and spatial patterns of surface movements. Using finite element modeling I have sought to understand the origin of some of these differences in order to distinguish between physical effects and mathematical artifacts. The models involve strike-slip faulting and include a thin channel asthenosphere model, a model with a varying thickness lithosphere, and a model with a viscoelastic inclusion below the brittle slip plane. The calculations reveal that the surface deformation pattern is most sensitive to the rheology of the material that lies below the slip plane in a volume whose extent is a few times the fault depth. If this material is viscoelastic, the surface deformation pattern resembles that of an elastic layer lying over a viscoelastic half-space. However, when the thickness or breadth of the viscoelastic material is comparable in size to the fault depth then the surface deformation pattern is altered and geodetic measurements are useful for studying subsurface geometry and structure. Although the largest crustal deformations occur in the vicinity of the fault, model differences are most detectable at intermediate distances (10^1 - 10^2 km) away from the fault. These differences are most pronounced shortly after an earthquake when the viscoelastic mechanisms generate signals much larger than those due to elastic mechanisms acting alone.

GD12-05

Postseismic viscoelastic relaxation associated with the 1940 Imperial Valley earthquake

Jeanne Sauber (Dept. of Earth, Atmospheric, and Planetary Sciences, M.I.T., Cambridge, MA 02139)
Robert Reilinger
M. Nafi Toksoz

We examine the contribution of viscoelastic relaxation to postseismic deformation following the 1940 Imperial Valley earthquake. The data used in this study consist of vertical displacements from geodetic leveling and horizontal strains determined from repeated triangulation measurements. The geodetic observations include the 1940 coseismic deformation and span the full interseismic period between the 1940 and 1979 Imperial Valley earthquakes. The time-dependent changes in surface displacements were determined using a 3-dimensional finite element code with a heterogeneous, viscoelastic (Maxwell) earth model. Initial models consider purely horizontal coseismic offsets on the Imperial fault that are consistent with coseismic geodetic observations and observed surface offsets measured shortly after the 1940 earthquake. To isolate the effects of viscoelastic relaxation, strain accumulation due to the relative motion of the lithospheric plates and possible episodic fault creep were not included in the models. Predicted vertical displacements due to purely viscoelastic relaxation during the postseismic period have similar magnitudes (~ 5 cm) and wavelengths (~ 50 km) to those observed, although significant differences exist in the spatial patterns of deformation. Calculated horizontal displacements show values that are in the same sense as coseismic displacements but are smaller in magnitude. Discrepancies between the theoretical and observed deformation are being investigated by considering changes in viscosity structure, coseismic fault slip, and by including contributions from other postseismic mechanisms such as fault creep.

GD12-06

Geodynamics of the Anatolian Plate in Eastern Turkey

M.R. HEMPTON (Geology Department, Carleton College, Northfield, MN 55057)

Evidence from seismicity, structural mapping, LANDSAT images, and regional tectonics shows that the 'Anatolian Plate' (AP) is moving west along the right-lateral North Anatolian Fault (NAF) and the left-lateral East Anatolian Fault (EAF) as a result of continental convergence between the Arabian and Eurasian plates. However, the geometry and kinematics of the westward escape of Anatolia are poorly understood. The AP does not behave as a single rigid plate but deforms internally along numerous active faults. The densest concentrations of faults are near the EAF and NAF zones. The predominant strike of faults is NE-SW parallel to the EAF. North of latitude 39°20' the fault pattern is dominated by long curving faults concave to the south which merge with the NAF to the east. Prominent lineaments outside the AP and complex fault relationships at the junction of the NAF and EAF suggest that the AP was originally larger and is contracting because of continued constriction. Faults in the eastern end of the AP exhibit greater displacements and have accommodated more strain than faults farther west. Strain migrates west. Seismic records suggest that most strain is accommodated episodically by displacemnt along the NAF and then the EAF: from 100 - 600 A.D. the NAF was active and the EAF quiet, from 600 - 1100 the EAF was active, and from 1100 - present the NAF has been active. These time-space features demonstrate that the geodynamics of continental escape as manifested by the AP is more complicated than generally proposed.

GD12-07

Iberian Plate Kinematics: Jumping Plate Boundaries, An Alternative to Ball-Bearing Plate Tectonics

HANS SCHOUTEN (Woods Hole Oceanographic Institution, Woods Hole, Mass. 02543)
S.P. SRIVASTAVA (Atlantic Geoscience Centre, Geological Survey of Canada, Bedford Institute of Oceanography, Dartmouth, Nova Scotia, Canada)
KIM D. KLITGORD (U.S.G.S., Woods Hole, Mass. 02543)

Independent plate tectonic reconstructions relative to North America of the Eurasian, African, and Iberian plates, suggest a promising alternative to the model of an Iberian microplate caught like a ball bearing in the relative motion between Eurasia and Africa. In this alternative model, the Iberian plate was either part of the Eurasian plate or part of the African plate and the boundary between these two plates jumped successively to discrete locations. It is suggested that since Early Cretaceous Iberia may have been part of the African plate until Oligocene or Early Miocene when the plate boundary between Eurasia and Africa jumped to its present Azores-Gibraltar location.

GD12-08

Synoptic Tectonics Along the Altyn Tagh Fault Zone

J.R. Preisig and F.T. Wu (CSNH, SUNY, Binghamton, N.Y., 13901)
A. Gillespie(JPL, Calif. Inst. of Tech, Pasadena, CA, 91103)

The Altyn Tagh fault zone in western China, between the Tibetan Plateau and the Tarim Basin has a total length of 1700 km and is geomorphically prominent and seismically active. LANDSAT images on magnetic tapes for areas around the structure have been collected processed and optimum false color images made. They are used in this work to study the mode of crustal deformation around a major fault.

Major lithologic units are identified on the 1:750,000 images based on the 1:4,000,000 geologic map of China. The fault zone can be seen as a complex structure, often with several parallel or sub-parallel branches at a few to a few tens of kilometers apart. Sections of the main fault zone are curved sharply such that either a high mountain or a basin is formed. Blocks in the area that are surrounded by faults exhibit rotations. East of 80°E strike-slip motion dominates; west of this longitude thrust motion dominates. The compressional stress in the west probably also causes thrust faulting in the middle of the western part of the Tarim Basin; this fault is also clearly seen on LANDSAT images.

We also conclude:

(1) Based on offsets of Paleozoic strata, the horizontal displacement in the eastern part of the fault is estimated to be 200-300 km.

(2) The curved parts of the fault may form major asperities along the fault; they may control the location of major earthquakes. The two M>7 earthquakes near 83°E and 36°20'N in 1924 were probably related to a prominent curvature there.

GD12-09

The Fracture Fabric of the Southeast USA

M. Bevis and L. Gilbert (MEAS, NC State University, Raleigh, NC 27695-8208)

The continental crust of the southeast USA is pervaded by deep-seated fractures and faults organized into a conjugate network whose directional distribution peaks in the intervals NE-NNE and NW-WNW. At several locales within the continental platform it is established that this fabric was emplaced in Precambrian time. Major (NE-trending) and transverse (NW-trending) structures of the S. Appalachians are genetically related to the regional fabric. The fabric was reactivated during the Mesozoic rifting event. It is suggested that the fabric controlled the geometry of the rifted continental margin, hence the orientation of the spreading and transform segments of the embryonic Mid-Atlantic Ridge. Modern fracture zones trend about NW as they intersect the margin of the southeast US continental margin. It is suggested that the regional fabric also controlled late Precambrian and Early Phanerozoic rifting and in this manner influenced the geometry and fabric of the S. Appalachians.

GD12-10

Vertical Tectonics in the South Carolina Coastal Plain

C. M. POLEY
P. TALWANI (both at University of South Carolina, Dept. of Geology, Columbia, S.C. 29208)

A preliminary study in the vicinity of Charleston, S.C. shows evidence of vertical movement in the area of the Ashley River fault (ARF). ARF is a shallow, NW trending fault that has been defined by seismic, potential field, stratigraphic correlations in shallow boreholes and geomorphic data. The sense of motion inferred from fault plane solutions and geomorphic data suggest that the SW side of ARF has been undergoing uplift at least since the last 100,000 years, whereas the stratigraphic data suggest that the SW side was downthrown in Tertiary times.

To independently determine the sense of movement, we examined first order releveling data for the S.C. Coastal Plain. In order to check the accuracy of the leveling data, loop closure analyses were performed for all first order leveling lines. Misclosure along the 1960 survey loop connecting Columbia, Charleston, Yemassee and Fairfax is 3.56 cm over a distance of 670 km for the 1960's data, which is well within the allowable misclosure for first order leveling of 12.93 cm. This suggests that the data are free of systematic errors.

Using the 1960 survey as reference, the misclosure was recalculated using certain segments of the loop releveled in 1974 and 1979 together with 1960 data for the remaining segments. The recalculated misclosures were found to be larger and were isolated in certain segments of the loop, suggesting localized crustal movements since the 1960's. The data for the years 1960 and 1974/79 show relative anomalous uplift of 2-3 mm/yr on the SW side of ARF in the block roughly located between the Edisto and Ashley rivers. This is in agreement with seismic and geomorphic data but in opposition to the stratigraphic data.

GD12-11

Deformation of Orinoco Delta mud diapirs in the South Caribbean strike-slip plate boundary zone.

K. BURKE, J. CASEY and P. ROBERTSON (all at Dept. of Geosciences, Univ. of Houston, University Park, Burke also at LPI, NASA Road One, Houston, TX 77058

Elliptical mud diapirs in Orinoco deltaic sediments off the coast of Trindidad lie within a broad zone of deformation straddling the east-west El-Pilar fault and may provide a measure of the strike-slip displacement taken up in the last 6 Ma by internal strain within a 180 km wide Southern Caribbean Strike-slip Plate Boundary Zone (SCSSPBZ). Assuming that the diapirs were roughly circular in plan at intrusion 6 Ma ago their present elliptical shapes may be used as strain markers. On the scale of the diapirs, the deformation is roughly homogeneous. Modelling of the deformation as a progressive simple shear across a zone whose half width is assumed to be the distance between the El-Pilar fault and the southern limit of the deformed diapirs, we calculated that on average ∿ 100 km of displacement can be attributed to distortions in this zone. If this deformation is symmetrical about the El-Pilar close to 200 km of CARIB wrt SOAM strike-slip motion may have been taken up by internal deformation in the last 6 Ma. Using an average easterly motion of 50 km/Ma for CARIB wrt SOAM (Pindell and Dewey, 1982), the Antillean trench line would have been 300 km west of its present position at 6 Ma. If 200 km of this displacement can be accounted for by internal strain within the SCSSPBZ, only 100 km of displacement has occurred along faults within the zone. Models which do not consider internal strains require larger offsets on faults within the SCSSPBZ.

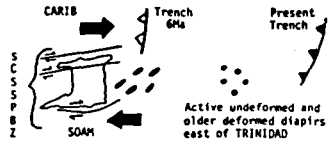

Precise Positioning: Laser Ranging and VLBI
Room 27 Tues AM
Presider, D.E. Smith, GSFC
T. Clark GSFC

GD21-01

Baseline Determination from Simultaneous Lageos Ranging

IVAN I. MUELLER (Geodetic Science and Surveying, Ohio State University, Columbus, Ohio 43210-1247)
MOUSTAFA BARAKA, GEORGE C. DEDES

The advantage of determining baseline lengths from ranging from the terminal stations to mutually visible Lageos passes has been discussed several times in the past. The key gains from such a procedure are the reduction of biases originating in the orbit, the observations and in the reference frame. The paper presents the latest OSU results in these connections, based partially on simulations and also on analyzing real Lageos simultaneous passes.

GD21-02

ANALYSIS OF EIGHT YEARS OF LAGEOS RANGE DATA

B. E. Schutz (Center for Space Research, The University of Texas at Austin, Austin, TX 78712)
B. E. Tapley
R. J. Eanes

Nearly eight years of Lageos laser range data have been analyzed by fitting a single, continuous ephemeris to the data. A recent ephemeris, LLA 8403, has fit the data to an RMS of approximately one meter. The improvement in the quality of the laser range observations is clearly evident from this ephemeris and suggests the existence of data problems early in the Lageos mission. The solve-for parameters in LLA 8403 included the Lageos position and velocity at the May 7, 1976, epoch, a constant "drag" parameter, periodic terms in the along-track direction, selected tide parameters, radiation pressure parameters, and geopotential coefficients. The adopted model is nearly consistent with the MERIT standards; however, some model enhancements have been adopted, including earth radiation pressure. The laser range residuals have been further analyzed through their resolution into orbit element residuals. Geophysical interpretations of the orbit element residuals and tide parameter adjustments are discussed, and the techniques used in the analysis of the range residuals is reviewed.

GD21-03

STATION POSITIONS AND BASELINES FROM LAGEOS LASER RANGING: 1976-1984

B. D. Tapley (Center for Space Research, The University of Texas at Austin, Austin, TX 78712)
B. E. Schutz
R. J. Eanes

Lageos laser range measurements from May 1976 through February 1984 have been used to compute a new global solution for the geocentric positions of 60 sites occupied during this interval. The station position determinations were part of a simultaneous solution for Lageos orbit elements in 15-day arcs and earth rotation parameters in 3-day sub-arcs using residuals from a 7.8-year long arc (LLA 8403). Systematic differences between the terrestrial reference frames implied by the new solution and by previous solutions computed at the University of Texas and at Goddard Space Flight Center are reviewed. The 70-90 cm difference in the z-axis bias between the GSFC solution and the previous UT solution (LSC 8112) is resolved in the new solution, and the factors which contribute to this change are discussed. The geocentricity of the new solution (LSC 8403) and the GSFC solution is now consistent to better than 5 cm in all coordinates, and coordinate differences after removing orientation and scale differences have an RMS of about 8 cm. The RMS difference in baseline length for 20 station pairs used in the recent Crustal Dynamics Project VLBI/SLR intercomparison experiment is 4 cm between the GSFC and UT laser solutions and 6 cm between either laser solution and VLBI. Baseline and station coordinate changes have been investigated by repeated determinations using subsets of the 7.8-year interval and by solution for parameters of a global plate tectonic model. The encouraging preliminary results of these experiments are discussed, and future plans for improvements are described.

GD21-04

Recent Improvements in Data Quality from Mobile Laser Satellite Tracking Stations

D.R. Edge
J.M. Heinick (Bendix Field Engineering Corpoation, Data Services Group, Greenbelt, MD 20771)
R. Kolenkiewicz (Geodynamics Branch, Goddard Space Flight Center, Greenbelt, MD 20771)

Since 1981 NASA's Crustal Dynamics Project has been upgrading thier mobile satellite laser tracking sytsems (MOBLAS) to improve performance. The major hardware modifications include the installation of a short pulse high energy Quantel laser, operating at 5 hertz, with a supporting time interval unit (TIU) and a quad integrator receive energy measurement device. Calibration stability and precision as well as satellite data precision have been improved by these changes based on recent results from MOBLAS stations located in the U.S. and in Australia. The calibration precision has improved by a factor of five and rms values for Lageos passes have dropped from a previous range of 10 to 16 cm to a current range of 2 to 4 cm. These improvements in precision have led to the potential of identifying and correcting systematic effects at the subcentimeter level. Operational calibration and data processing procedures are being modified to support the improved level of laser data quality.

Currently MOBLAS stations 4, 5, 7 and 8 have been modified and are supporting operations. MOBLAS 3, MOBLAS 6, TLRS 1, and HOLLAS are scheduled to be similarly modified during 1984.

Full deployment of these stations will significantly improve the accuracy of the global laser data set which will lead to the more accurate determination of geophysical parameters.

GD21-05

SERIES-X Test Results

R. B. CROW, F. R. DLETZACKER, R. J. NAJARIAN, G. H. PURCELL, JR., J. I. STATMAN, J. B. THOMAS, (Jet Propulsion Laboratory, Pasadena, California 91109)
(Sponsor: D. J. SOVERS)

The purpose of the SERIES-X Project is to demonstrate the feasibility of a navigation scheme conceived at JPL for the TOPEX satellite. Basically this scheme involves a GPS receiver on the satellite, along with a GPS receiver on the satellite, along with a network of receivers at widely separated ground stations. The receiver system uses an omnidirectional antenna and recovers the phases of the L1 and L2 carriers, as well as the P-code and C/A modulation, simultaneously for all visible satellites without using the code. Although the system was designed for satellite navigation, it is equally applicable to geodetic measurements.

We have built two complete, portable receiver systems and completed a series of diagnostic tests on baselines ranging in length from 15 meters to 171 kilometers. In the course of these tests we have developed and refined means of calibrating or otherwise minimizing the principal sources of measurement error, including system noise, receiver characteristics, multipath, ionospheric and tropospheric delays, and satellite ephemerides. The day-to-day repeatability of the measured vector baselines ranges from 2 mm on a 15-meter baseline to about 50 mm on a 171-km baseline, and the results agree well with measurements by other means.

GD21-06

Cost Comparison of Several Techniques for Measuring Crustal Motion

E. ELLER (ORI, Inc., 1400 Spring Street, Silver Spring, MD 20910)
N.G. ROMAN (ORI, Inc.)
A.H. WELLEN (ORI, Inc.)

Comparisons of four technologies have been made based upon scenarios provided by NASA geodynamics experts. These scenarios include global measurements of interplate motion and plate stability and regional deformation measurements in 29 regions. The technologies investigated are Very Long Baseline Interferometry (VLBI), interferometry based on the Global Positioning System transmissions (GPS), Satellite Laser Ranging (SLR), and measurement of ground based corner cubes from a space borne laser

(SLRS). Only VLBI and SLR were compared for the global measurements because the long baseline involved make GPS and SLRS impractical. The primary candidates for regional measurements are GPS ranging and SLRS.

For the global case, individual sites were identified along with the required number of measurements at each. Alternative logistical approaches were considered. The regional case assumes that all sites within a region have similar characteristics, the primary distinction among regions being the travel time between sites and the frequency of measurement.

Key assumptions and results for various circumstances and approaches will be presented along with some preliminary conclusions.

GD21-07

Geodesy by Radio Interferometry: Baseline Length Evolution in North America and between North America and Europe

J. Ryan (NASA/Goddard Space Flight Center, Greenbelt, MD, 20771) for the Goddard/Haystack/CfA/Onsala/U. Bonn VLBI Group

A. Mallama (Science Applications and Research, Riverdale, MD, 20737)

Since 1976 our group together with the National Geodetic Survey and the Jet Propulsion Laboratory has carried out over 200 VLBI observing sessions measuring megameter baselines. The dual-frequency Mark III VLBI system developed by our group was used in all but 14 of these sessions and in each session up to fifteen baselines were measured with precisions of 1 to 4 cm. The baseline from Westford, MA to Owens Valley, CA was measured 46 times and we detected no motion within a three-sigma error of 0.5 cm/year. Tne baseline from Westford to Fort Davis, TX was measured more than 160 times and produced the same null result. The baseline between Westford and Onsala, Sweden was measured 49 times in slightly more than three years. A baseline change of +1.3 cm/year was detected with a three-sigma error of 1.0 cm/year. However, we do not claim to have positively detected tectonic plate motion. The total apparent change is only 4 cm and we cannot exclude the possibility of systematic error at this low level. We continue to monitor this baseline with observing sessions at least once per month.

GD21-08

CONTINENTAL SCALE BASELINES DETERMINED BY VLBI

D. S. ROBERTSON
W. E. CARTER (Both at National Geodetic Survey, Charting and Geodetic Services, National Ocean Service, NOAA, Rockville, Md. 20852)

During the past 4 years more than 30 baselines among permanent Very Long Baseline Interferometry (VLBI) observations in the United States and Europe have been measured repeatedly, from a few to tens of times. The Westford to George R. Agassiz Observatory (GRAS) baseline, which is part of the POLARIS network, has been measured more than 150 times. These data demonstrate that geodetic VLBI, using the MARK III system, routinely achieves a repeatability (RMS) on baselines ranging from 1 to several thousands of kilometers of about 1 part in 10^8, from observing sessions of 24-hour duration. These results have implications for attempts to determine tectonic plate deformations and motions.

GD21-09

Repeatability of Mobile VLBI Baselines

F. P. Wieland (Jet Propulsion Laboratory, California Institute of Technology, Pasadena, CA 91109)

In the past four years, the Mobile VLBI Project has made many measurements of the JPL/Owens Valley/Goldstone/Ft. Davis (JOGF) quadralateral, with these measurements showing consistency at approximately the level of the reported formal errors. For the "remote" baselines (i.e., those outside the well-established JOGF network), the measurements have been relatively sparse, with only eight sites showing multiple occupations in the current Mobile VLBI data base. Most of these sites have been visited only two or three times.

In this paper, we present an assessment of the repeatability of the remote Mobile VLBI baselines. A comparison is made of the scatter in these baselines with the typical scatter in the JOGF baselines, which is taken as the standard. Nonparametric statistical tests are used to assess the significance of differences in variances. Examples of poor remote baseline repeatability are found to be somewhat correlated with poor data quality, characterized by low yields (i.e., less than 50% of all scheduled observations used in the final parameter estimation) and higher than normal post-fit residual scatter.

GD21-10

Geodesy by Radio Interferometry: Effects of Errors in Modeling the Troposphere

J.L. DAVIS (Massachusetts Institute of Technology, Cambridge, MA 02139)
T.A. HERRING, I.I. SHAPIRO (Harvard-Smithsonian Center for Astrophysics, Cambridge, MA 02138)

All models for the electrical path length of the troposphere involve assumptions concerning the temporal and spatial variations of this quantity. Errors in any of these assumptions can induce errors in the estimates of geophysically significant parameters from very-long-baseline interferometric (VLBI) observations. For example, an error in the model of the elevation angle dependence can induce biased estimates of baseline length. A discussion will be given of possible methods of limiting these effects. Also presented will be an analysis of the spectra of short term spatial and temporal variations of tropospheric water vapor and their effect on our ability to model the troposphere.

This work was supported by Air Force Geophysics Laboratory contract F19628-83-K-0031, NASA contract NAS5-27571, and NSF grant NSF-79-20253-EAR.

GD21-11

Empirical Troposphere Modeling From DSN Intercontinental VLBI Data

R. N. Treuhaft
G. E. Lanyi
O. J. Sovers (all at Jet Propulsion Laboratory
California Institute of Technology
4800 Oak Grove Drive
Pasadena, CA 91109)

We derive new dry troposphere mapping functions from a five year span of dual frequency Deep Space Network VLBI data. The results, obtained by adjusting parameters in existing mapping functions, compare favorably with theoretical calculations. The extent to which the troposphere's site and time variability can be determined from the data is examined, and the bounds for the effects of dry troposphere mismodeling on baselines and source positions are delineated. In addition, we determine the effect of a time varying, uncalibrated wet troposphere on VLBI baseline and source position estimates.

GD21-12

On the Accuracy of Doppler Derived Ionospheric Path Delay Corrections for VLBI

F.J. LOHMAR
J. CAMPBELL
(Geodetic Institute University of Bonn, Nussallee 17, 5300 Bonn, F.R.G.)

In order to estimate the accuracy of ionospheric path delay corrections derived from

2-frequency NNSS Doppler satellite observations, several geodetic Mk III VLBI campaigns observed at the S and X-bands have been supplemented with simultaneous Doppler observations. In this way a direct comparison between the S/X ionospheric groupdelay differences and the corresponding values derived with a special interpolation method from Doppler observations could be made. In all cases the Doppler derived X-band corrections agreed within 0.13ns RMS with the S/X values except for a bias which is fully absorbed by the clockterms in the baseline solution. The effect on the VLBI baseline lengths of using Doppler derived corrections instead of S/X differences was in all cases less than 3cm for intercontinental and 0.6cm for a European baseline of 830km length. A typical example is:

Haystack-Effelsberg Mk III Sep.80 X-band			
Solution:	uncorr.	S/X corr.	Dopp.corr
Length :	5591903.610	--903.390	--903.419

This means that in case of loss or even lack of a second VLBI frequency most of the single frequency observations can still be used for high precision baseline determinations.

GD21-13

A WVR Error Model

B. C. Beckman
J. M. Davidson (both at Jet Propulsion Laboratory, California Institute of Technology, Pasadena, CA 91109)

We propose a water vapor radiometer (WVR) error model in which the difference between the "true" line-of-sight wet path length Lt and the measured line-of-sight wet pathlength Lm is set equal to Lm times a scale error c plus an effective additive zenith wet path length Lo. Thus,

$$Lt - Lm = c * Lm + Am * Lo,$$

where Am is the modeled airmass. For a "perfect" WVR, c and Lo will equal zero. Tests of this error model, conducted by comparing data recorded simultaneously with side-by-side WVR's, indicate that for the current total WVR system (including pathlength retrieval algorithm and software) c and Lo have typical absolute values of approximately 0.2 and 1-2 cm, respectively, although they may be larger on occasion. In addition, these data indicate that the proposed model describes WVR error with an accuracy of up to 1.0 cm. The results of a simple covariance analysis will be presented, to indicate whether, given a suitable network geometry and observing schedule, the model parameters can be estimated from the VLBI or GPS data, to produce an effective calibration of 0.5 cm accuracy, using existing WVR's.

GD21-14

Tests of Water Vapor Radiometer Calibration Using VLBI Data

P. M. Kroger
J. E. Patterson (both Jet Propulsion Laboratory, California Institute of Technology, Pasadena, CA 91109)

We have assessed the relative merits of water vapor radiometer (WVR) data and surface meteorology (SM) data for calibration of the wet troposphere in VLBI geodetic experiments. Tests were made using data produced in Mobile VLBI experiments of June 9 and June 29, 1983.

It was found that the RMS scatter of the post-fit residuals of the group delay observables was generally smaller when WVR data were used for calibration. This was reflected in greater precision in the values of estimated geodetic parameters.

We have also investigated the repeatability of estimated baseline parameters when the first and second 12 hour periods, from a 24-hour VLBI experiment, were separately analyzed. Results will be presented showing whether WVR calibration leads to more consistent results than does SM calibration. Special attention will be given to the baseline vertical component, where good quality wet troposphere calibration would be expected to have the greatest beneficial effect.

GD21-15

Nutation Amplitudes from DSN Intercontinental VLBI Data

O. J. Sovers
R. N. Treuhaft (both at Jet Propulsion Laboratory California Institute of Technology 4800 Oak Grove Drive, Pasadena, CA 91109)

Possible effects of precession and nutation mismodeling on the time rates of change of the Deep Space Network intercontinental baselines are investigated. Analysis of 1978-83 dual-frequency VLBI measurements shows statistically significant shifts of the order of a few milliarcseconds/yr in the luni-solar precession constant, and a few mas in the amplitudes of some of the leading terms of the Wahr nutation series. Concomitant changes in the baseline length time derivatives are not significant in the precession case, but of the order of 1 to 2 cm/yr for nutation (approximately twice the formal uncertainties). We conclude that correct modeling of nutation is of importance in extracting baseline drift results from VLBI measurements.

GD21-16

A GSFC Geodetic Reference Solution from Satellite Ranging to LAGEOS: SL5.1AP

D.E. Smith
D.C. Christodoulidis (both at Goddard Space Flight Center, Geodynamics Branch, Greenbelt, MD 20771)
P.J. Dunn
S.M. Klosko
M.H. Torrence (all at EG&G Washington Analytical Services Center, Inc., Riverdale, MD)

A solution for earth orientation and geocentric station positions has been made from LAGEOS laser observations spanning May 1976 to the end of 1982. Annual subsets of this base solution have also been made to assess tectonic motions over this interval. A discussion of the models and products of this solution will be made.

The quality of the results for polar motion, earth rotation and three-dimensional station positioning will be discussed. Products of this solution, like annual inter-and intra-plate baselines and ellipsoidal chords will be examined and compared to indicate probable relative plate motions, their accuracy assessment, and their sensitivity on earth orientation parameters. Work continues on the development of software fully compatible with the MERIT standards. This SL5.1AP solution will serve as a benchmark for asessing the impact of this software conversion on the rigor of SLR reference frame, the global vertical geodetic network, and the laser derived measures of the earth's rotation variability.

Crustal Studies and Deformation

Room 25 Tues PM

Presider, S.C. Cohen, GSFC

G.A. Lyzenga Jet Prop. Lab.

GD22-01

Gravity-Driven Natural Hazards: Their Instrumentation and Public Policy

W.M. ADAMS, R. HENRY, C.-Y. YAN, O.D. ATHENS (Department of Geology and Geophysics, University of Hawaii; Honolulu, Hawaii, 96822)
N. NAKASHIZUKA (GeoMonitor Group Inc., Las Vegas, Nevada, 89121)

Landslides, avalanches, rockfalls, tsunamis, mudflows, and floods are some examples of gravity-driven hazards. Rock avalanches on Oahu in Hawaii are concentrated near the ridges. Economically, the most important slides are those occurring at 70-140 m. elevation on the Lualualei fm. Two slides, one in Palolo Valley and another in Aina Haina, are well documented legally because the City and County of Honolulu purchased the swellings rather than contest law suits for irresponsible issuance of building permits. Field measurements on the surface show average velocity components of thirty meters per century horizontally and almost 10 meters per century vertically. This velocity is strongly dependent upon the rainfall: the drought year of 1983 has resulted in the velocity components decreasing to about one-quarter of their averages.

Gravity microsurveys across these slides find an increase over the slide mass which is interpreted as being due to the intertices being water-filled. Electrical resistivity confirms this conclusion.

Seismic refraction measurements show that layers of varying acoustical impedance exist. Instrumentation development is required to make meaningful studies of the interiors of these slides. Locating a recent subdivision on the Lualualei and ignoring the engineering recommendations will lead to destructive motion in the future when high rainfall occurs over an extended time. The most surprising discovery is the extent of the conspiracy to dupe the buyers and mortgaging institutions. Hawaii has a recourse law with respect to real estate.

GD22-02

Comparing Crustal Deformation Measurement Techniques: A Procedure and An Example

DUNCAN CARR AGNEW (Institute of Geophysics & Planetary Physics; Scripps Institution of Oceanography; University of California, San Diego; La Jolla, CA 92093

In selecting different methods for measuring crustal deformation it is desirable to have a quantitative procedure for comparison. This is difficult if one method makes a continuous relative measurement and the other an occasional absolute one; e.g., a strainmeter and a VLBI system. A comparison of temporal behavior may be made by comparing the power spectrum of the continuous record with the apparent power spectrum of the occasional measurement, computed by assuming that the errors of the latter are independent and that the interval between measurements is constant. At shorter periods than the one at which these spectra cross, the continuous record is quieter; at longer periods, the occasional measurement is quieter. While the crossover period decreases as the sample interval is shortened, the steep drop of the continuous spectrum at short periods means that the geodetic method is quieter over a smaller fraction of the frequency band measured. Realistic error estimates give crossover times from months to years for even new high-precision geodetic measurements. I will give an example using geodetic and strainmeter records from Piñon Flat Observatory.

GD22-03

Earth Crust Deformations due to Heat Sources

P. LANZANO (Naval Research Laboratory, Code 5110, Washington, D.C. 20375)

We have formulated the general analytic problem of thermal expansion of the crust of a spherical Earth due to heat sources located within the mantle and of the determination of the associated stress.

The Navier-Stokes equation and the Heat Conduction equation constitute a system of partial differential equations whose simultaneous solution will provide both temperature and displacements as functions of the radial distance and of time. One also has to specify initial conditions, conditions at the center of the Earth and boundary conditions at the outer surface.

Those two equations are interrelated except in the particular case when the two specific heats C_p and C_v of the material are equal. This is not, however, a plausible physical assumption since the ratio of said quantities is a function of temperature. The system of equations is then bound to be left connected and this ultimately leads to an integro-differential equation.

Our presentation will discuss: (1) a new method of solution which is a variation of certain known results and (2) the role that these limited analytic solutions can play within the overall plan of numerical integration.

GD22-04

Applying Lake Level Gaging Records to the Investigation of Uplift within the Yellowstone Caldera, Yellowstone National Park

W. L. HAMILTON (National Park Service, P.O. Box 168, Yellowstone National Park, Wyo. 82190) (Sponsor: R. B. Smith)

Pelton and Smith (1982) have reported results of first-order releveling in 1976 of benchmarks established in Yellowstone in 1923 showing intra-caldera uplift by as much as 15 mm/yr. Releveling of a portion of the caldera by the U.S.G.S. in 1983 gave comparable or greater rates. A profile based on 1983 measurements is roughly congruent with the earlier profile suggesting a relatively simple geometry.

In this investigation U.S.G.S. gaging records were evaluated to see if Yellowstone Lake basin tipping on the southeast flank of the uplift could be detected and to gain a more detailed picture of deformation over the period of record. Gage records are available for Fishing Bridge (at the lake outlet) from 1923 to present; Lake Hotel from 1921 to 1966; and Bridge Bay from 1966 to present. These gages were releveled to nearby benchmarks approximately every five years. Downcutting at the outlet was assumed to be negligible.

Annual minimum (winter) gage heights for these stations show increasing trends with time, in excess of a minor precipitation increase, that are comparable with uplift rates based on releveling of from 0.7 to 2.9 mm/yr for the respective legs. More importantly, winter gage height differences between stations (independent of precipitation) changed progressively toward higher lake levels southward by 1.2 to 2.4 mm/yr on the respective legs. The gaging record suggests that most recent uplift in Yellowstone commenced in the late 1930's following an irregular interval, accelerated sharply in 1963, and resumed a monotonic rate thereafter.

GD22-05

New Geodetic Measurements of Crustal Deformation in the Rio Grande Rift.

SHAWN LARSEN (Dept. Geological Sciences, Cornell University, Ithaca, NY 14853)
ROBERT REILINGER (Air Force Geophysics Lab, Hanscom AFB, MA 01731)
LARRY BROWN (Dept. Geological Sciences, Cornell University, Ithaca, NY 14853)

Recent leveling conducted by the National Geodetic Survey in central New Mexico and west Texas provides new evidence of ongoing tectonic deformation associated with the Rio Grande Rift. A 1980 resurvey over the mid-crustal magma body near Socorro, New Mexico indicates continued uplift. However, the average rate of uplift between 1951 and 1980, 1.8 mm/yr, is significantly less than the previously reported average rate of 3.4 mm/yr between 1912 and 1951 (e.g. Reilinger et al., Geology, 1980). This decrease in deformation rate is consistent with an apparent reduction in seismicity. The new measurements also confirm a prominent zone of subsidence on the southern border of the main zone of

uplift. If the movements are due to magma inflation in the crust, the process must be more complex than originally considered. A 1981 resurvey of level lines in the Diablo Plateau region of west Texas indicates that the previously reported (Brown et al., JGR, 1978) uparching of that region is continuing roughly at a constant rate. The cause of the west Texas uplift remains less certain than that near Socorro, but similar magmatic activity at depth is suspected. The new levelings also update estimates of subsidence (40 cm between 1956 and 1981) due to water withdrawal near Pecos, Texas, and help identify suspected systematic errors in some of the leveling results. These new measurements further verify that the Rio Grande Rift is an important site for future monitoring of crustal deformation.

GD22-06

Tectonic Implications of Proposed Crustal Dynamics Project Observing Sites in South America

R. J. ALLENBY (Geophysics Branch, Goddard Space Flight Center, Greenbelt, MD 20771)

The locating of possible satellite laser ranging observing sites in South America is essentially complete. Site locations are constrained by operational requirements and seeing conditions. Budget restraints will limit the number of the proposed sites that will actually be occupied.

Working closely with South American scientists, the observing locations were chosen primarily to provide information on the Nazca/South American plate interface; however, the sites are also designed to provide important data on Andean deformation. The primary Nazca plate site is on Easter Island, with possible additional sites in the Galapagos Islands and on San Felix Island off the coast of Chile. On the mainland a baseline from the proposed Quito, Ecuador site to Bayovar on the northern Peruvian coast will monitor motion across the Huancabamba fracture zone that runs east across the Andes from the Carnegie Ridge and the Gulf of Guayaquil. Baselines from Lima, Huancayo, Cuzco and Arequipa in Peru to Oruro, Bolivia and Iquique, Cerro Tololo and Santiago in Chile cross the Abancay fracture zone and the complex Andean elbow area of the Peru, Chile, Bolivia borders. Measurements from the coastal and inter-Andean sites to Santa Cruz, Bolivia on the edge of the Brasilian Shield will provide data on trans-Andean strain.

GD22-07

Statistical tests of intraplate deformation from plate motion inversions

SETH STEIN
RICHARD GORDON (both at Dept. of Geological Sciences, Northwestern University, Evanston, IL 60201)

We have investigated the application of the F-ratio test, a standard statistical technique, to the results of relative plate motion inversions. The method tests whether the improvement in fit of the model to the data resulting from the addition of another plate to the model is greater than that expected purely by chance. This approach appears to be useful in determining whether additional plate boundaries are justified. We confirm previous results favoring separate North American and South American plates with a boundary located between 30°N and the equator. Using Chase's global relative motion data, we show that in addition to separate West African and Somalian plates, separate West Indian and Australian plates, with a best-fitting boundary between 70°E and 90°E, can be resolved. These results are generally consistant with the observation that the Indian plate's internal deformation extends somewhat westward of the Ninetyeast Ridge.

GD22-08

Vertical Tectonics and Temporal Changes in Global Gravity Anomalies

C.B. OFFICER (Earth Sciences Department, Dartmouth College, Hanover, N.H. 03755)
C.L. DRAKE (Earth Sciences Department, Dartmouth College, Hanover, N.H. 03755)

From the variations in the continental shelf break depth off the East Coast, Officer and Drake (1982) have shown that over the past 18,000 years the Scotian shelf has been subsiding at a rate of 0.8 cm yr^{-1} with respect to Miami with the major changes occurring in the region from New York to Cape Hatteras. This observation is confirmed by a variety of features on the continental shelf as well as from recent leveling analyses and the differences between the true sedimentation rates as determined by geochemical tracers and apparent sedimentation rates as determined by historical bathymetric depth changes in the Chesapeake bay region. Similar shelf break depth variations occur along the other passive margins of the Atlantic. From the numerous cyclic sedimentation sequences throughout the Phanerozoic it is surmised that these vertical tectonic movements are cyclic in nature with periods in the range 20,000-300,000 years. The implication is that there have been corresponding temporal changes in global gravity anomalies of the order of 10 mgal. Although the small aspect ratio, Rayleigh-Benard, convection in the upper mantle is not a principal forcing function in the description of horizontal plate tectonics, it is our contention that the inherent instabilities of this convection are the cause of the oscillatory, vertical plate motions observed.

GD22-09

GLOBAL POSITIONING SYSTEM (GPS) MEASUREMENTS AS A CONSTRAINT ON PLATE DRIVING FORCES

T. H. DIXON
M. P. GOLOMBEK
Jet Propulsion Laboratory,
Mail Code 183-701, 4800 Oak Grove Drive, Pasadena, California 91109

Spatially dense and frequent measurements of long baseline lengths are not economically feasible with current geodetic techniques such as mobile VLBI or laser ranging systems. However a dense measurement network is possible using low cost, portable GPS receivers. A properly designed program to monitor both long (> 1000 km) and short (100-500 km) baselines can generate important constraints on possible plate driving mechanisms.

Regular measurement of long and short baselines spanning a fast spreading center should yield accurate plate divergence rates after a 5-10 year period. These velocities can be compared to convergence rates derived from similar measurements across an adjacent subduction zone. Comparison of such rates to instantaneous plate motion rates based on earthquake slip vectors describes the relative proportion of aseismic and seismic slip. In addition, if the velocities derived from baseline length changes differ at the divergent and convergent boundaries of the same plate then a change in the state of stress in that plate can be inferred. This would help constrain the relative importance of ridge push versus slab pull as a plate-driving force, at least on short time scales.

The optimum area to attempt such measurements is in the Pacific, due to fast spreading rates. Such a measurement program would make use of intra-plate islands, and assumes that they are stable platforms for the GPS receivers. This assumption would need careful, long-term evaluation.

GD22-10

Geotectonic Imagery and Aeromagnetics Define the Rio Grande Pseudofault

JOHN L. LaBRECQUE (Lamont-Doherty Geological Observatory, Palisades,N.Y. 10964)
JOHN BROZENA (Naval Research Laboratory, Washington,D.C. 20375)

The Seasat derived Geotectonic Imagery of W.F. Haxby has been used to plan and carry out

an aeromagnetic survey of the Rio Grande Rise area. The GTI provides the necessary detail of the regional tectonic fabric which far exceeds that available from bathymetric compilations. Seafloor spreading magnetic anomalies observed adjacent to the GTI anomalies provide constraints on the interptretation of these anomalies.

The interpretation of the combined data set indicates that the Rio Grande-Walvis Ridge system formed at the tip of a southward propagating rift. The time of propagation is limited to the Late Cretaceous, from Campanian to Latest Maastrichtian. The kinematic interpretation indicates that the large negative gravity anomaly located near 30 West and 35 South is the site of a short lived Late Cretaceous transform fault perhaps associated with some degree of convergent motion. The data recovered during this study should generate some doubt as to the use of the Walvis Ridge lineament as a hot spot trail.

GD22-11

Proper Motions of Pacific-Plate Hotspots

C. G. Chase (Dept. of Geosciences, University of Arizona, Tucson, Ariz. 85721)
D.R. Spraul (Dept. of Geology & Geophysics, University of Minnesota, Minneapolis, Minn. 55455)

The strong correlation of hotspot locations with geoidal highs leads to the suspicion that both are related to the same convective phenomenon. The dominance of long-wavelength geoid anomalies then suggests that relative motions between hotspots may not be random, but that the motions of the hotspots might be coherent at a length scale of thousands of km. The apparent fixity of hotspots might thus be misleading, with spurious rotations introduced by coherent motion of groups of hotspots. If so, differences between paleomagnetic reconstructions and fixed hotspot reconstructions are not necessarily significant of true polar wander.

We have used five well-dated and defined hotspot traces from the Pacific plate in a preliminary test of these hypotheses. Individual poles and rates of motion were fitted to each trace and used to deduce instantaneous Pacific/hotspot motions. Relative to a global mean hotspot reference frame, northern Pacific hotspots move northerly at 10-20 mm/yr, and southern Pacific hotspots move southerly at 15-70 mm/yr. This pattern is consistent with the slope of the long-wavelength geoidal anomaly over the Pacific plate, and constitutes a success of the hypothesis.

GD22-12

Thermoelastic Stress: How Important as a Cause of Earthquakes in Young Oceanic Lithosphere?

ERIC A. BERGMAN, STEVEN R. BRATT, and SEAN C. SOLOMON (Dept. of Earth, Atmospheric, and Planetary Sciences, M.I.T., Cambridge MA 02139)

A synthesis of the source characteristics of over 50 near-ridge earthquakes (intraplate events which occur in oceanic lithosphere 2-30 m.y. in age) indicates that thermoelastic stresses accompanying the early, rapid phase of plate cooling may be an important component of the stress field in young oceanic lithosphere. Features of near-ridge earthquakes that provide qualitative support for this inferrence include the sharp decline in rate of moment release after an age of about 15 m.y., the observation that the deepest events at all ages are characterized by normal faulting, the tendency for the T axis of normal faulting mechanisms (and the P axis of some thrust faulting events) to be oriented subparallel to the ridge axis, and the near-aseismicity of young oceanic crust. The decline in seismic moment release coincides with the age at which cooling rates throughout the lithosphere have dropped to relatively low and slowly changing values. In addition, the maximum centroidal depth of near-ridge earthquakes as a function of lithospheric age parallels, but at a somewhat shallower depth, the age-dependent depth of the maximum rate of cooling calculated from standard plate-cooling models. The discrepancy in depth is readily explained by the rapid decrease in lithospheric strength above a temperature of about 800°C.

We present simple quantitative models for thermoelastic stress in young oceanic lithosphere for comparison with the earthquake data set. The accumulation of thermoelastic stress with time is calculated from an assumed thermal model using thermal displacement potentials; the method of images is used to match boundary conditions at the sea floor. We test both fully elastic models and models in which stresses are not accumulated below a depth defined by a limiting isotherm (e.g., 800°C). In general, these models support the importance of thermoelastic stress in the tectonic evolution of young lithosphere.

Tectonic Movements in California: Measurements and Interpretation

Room 25 Wed PM

Presider, T.H. Dixon, Jet Prop. Lab.

R. Allenby GSFC

GD32-01

REDEAM: Geodetically Derived Strain from San Francisco Bay to the Mendocino Triple Junction, Calif.

M. W. CLINE, R. A. SNAY, E. L. TIMMERMAN (National Geodetic Survey, NOAA, Rockville, Md. 20852)
K. HURST (Lamont-Doherty Geological Observatory of Columbia University, Palisades, N.Y. 10964)

The procedure of Snay et al. (JGR, 1983) is used to obtain REgional Deformation of the EArth Models for the San Francisco, Santa Rosa, and Ukiah regions of California. The total area is best described as covering San Francisco Bay ($\varphi = 37^{\circ}$) north to the Mendocino triple junction ($\varphi = 40^{\circ}$) and from the Great Valley ($\lambda = 121.5^{\circ}$) west to the Pacific Ocean. The data are triangulation, trilateration, and astronomic azimuths observed since late-1906 to 1978.

Each of the three regions is partitioned into a mosaic of microplates or "districts" that are allowed to individually translate, rotate, and deform homogeneously as a linear function of time. By approximating the known geologic faults with district boundaries, the relative motion between districts represents secular fault slip. No earthquakes are modeled in any of the three regions discussed.

The directions and magnitudes of maximum right-lateral shear strains suggest an overall pattern of diffuse but moderate strain ($\sim .3 \pm .1\,\mu$rad/yr) distributed over the San Andreas, Hayward, and Calaveras faults south of San Francisco Bay that build and converge northward onto Point Arena ($\sim 1.4 \pm .2\,\mu$rad/yr). In the Great Valley, insignificant shear strains ($\sim .08 \pm .07\,\mu$rad/yr) parallel the San Andreas strike direction. This pattern implies that north of San Pablo Bay, the as yet unmodeled Tolay-Mount Jackson(?) fault is more important than the Rodgers Creek-Healdsburg fault. The data, however, are contaminated by approximately 30 years of abnormally high shear strain following the 1906 earthquake (Thatcher, JRG, 1975), which drives up the REDEAM linear rate. All data observed prior to 1930 will therefore be discarded and the Tolay fault will be modeled to determine the amount of postseismic relaxation on these results.

GD32-02

Regional Deformation for the Bakersfield Region, Calif.

E. L. TIMMERMAN, R. A. SNAY, M. W. CLINE (National Geodetic Survey, Charting and Geodetic Services, National Ocean Service, NOAA, Rockville, Md. 20852)

A mathematical model is presented for horizontal crustal motion derived from 50+ years of classical geodetic data (triangulation, trilateration, and astronomic

azimuths) in the southern California region bounded N-S by the 35.5° and 34.5° N latitudes and, E-W, by the 118.5° W longitude and the Pacific ocean. The model relates crustal deformation to secular strain rates, secular slip rates on geologic faults, and episodic motion experienced during the 1952 M7.7 Kern County earthquake along the White Wolf fault. For the secular motion, the region was partitioned into a mosaic of microplates or "districts" that were allowed to individually translate, rotate, and deform homogeneously as a linear function of time. The derived shear strain pattern supports the hypothesis that right-lateral shearing between the Pacific and North American plates dominates the regional stress field. Secular shear strain is maximum in the NW direction parallel to the San Andreas fault zone. Secular slip rates were estimated at various points on district boundaries by computing the relative secular velocity between the two districts at those points. The episodic motion experienced during the 1952 earthquake was modeled in accordance with the theory of dislocation in an elastic halfspace. For this application, the White Wolf fault was represented by the finite three planar model of Stein and Thatcher [JGR, 1981], which they derived from the more abundant geodetic leveling data. The horizontal geodetic network in the vicinity of the White Wolf, although relatively sparse, provided an unusually good temporal coverage of the 1952 event, the network being surveyed within 6 months both before and after the earthquake.

GD32-03

Mobile VLBI Measurements of the JPL/Owens Valley/ Goldstone/Ft. Davis Baselines: 1980-1983

S. L. Allen
B. C. Beckman
J. M. Davidson
J. L. Fanselow
J. E. Patterson
D. W. Trask
F. P. Wieland (all at Jet Propulsion Laboratory, California Institute of Technology, Pasadena, CA 91109)

We report results from radio interferometric measurement of the JPL/Owens Valley/Goldstone (JOG) baselines from January 1980 through February 1983, using the mobile VLBI systems. Ten separate measurements were made of the complete JOG triangle. In addition, six separate measurements were made of the JPL/Owens Valley baseline. Thirteen of these measurements involve baselines from the JOG stations to Ft. Davis, Texas; these results are also reported. Average rates of change in baseline length are -0.8 +/- 0.6 cm/yr for the JPL/Owens Valley baseline, +0.4 +/- 0.6 cm/yr for the Goldstone/Owens Valley baseline, and -0.3 +/- 1.0 cm/yr for the Goldstone/JPL baseline, where a positive value denotes increase in baseline length. The Ft. Davis baselines are similarly consistent with no motion. In the analysis of these data, a significant improvement has been made in the treatment of ionosphere for the 1980-1981 data. We examine the sensitivity of these results to this calibration. We also examine the sensitivity of these results to the deletion of individual measurements or the deletion of results from individual bursts. We find that the quoted rates of change are not significantly dependent on the results from any one experiment or burst and that the results from repeated measurements are generally consistent within the quoted formal errors.

GD32-04

Empirical Strain Modeling with VLBI Data

K. S. Wallace
J. L. Fanselow
G. A. Lyzenga (all at Jet Propulsion Laboratory, Pasadena, California 91109)

Past attempts to determine regional-scale strain rates in southern and central California from VLBI data have been susceptible to uncertainties in the input baselines due to errors in earth orientation and rotation data used in the baseline processing. The capability to solve simultaneously for strain rates in particular regions and for small perturbations to the values used for global rotation is being added to empirical strain modeling procedures in order to remove these effects from the estimates of horizontal strain rates. The values obtained for regional strain rates in California with the use of these new procedures and with additional data now available from the Crustal Dynamics Project will be presented and compared with results from other measurements in the region. Results obtained to date indicate that the VLBI network, measuring deformation on the scale of several hundred kilometers, yields considerably smaller rates of deformation than local networks operating on scales of up to tens of kilometers.

GD32-05

Numerical Simulations of Strain Fields in the Vicinity of the San Andreas Fault

G. A. Lyzenga
A. Raefsky (both at Jet Propulsion Laboratory, California Institute of Technology, Pasadena, California 91109

Accumulating evidence from both modern terrestrial geodetic and space-driven geodetic observations suggest spatial and temporal variability in the distribution of crustal strain along the Pacific-North American plate boundary. We present the results of finite element calculations of elastic and viscoelastic responses to motion at this strike-slip boundary.

The results of efforts to physically model recent VLBI geodetic results in three dimensions suggest the possibility that the plate boundary below seismogenic depths differs in configuration from surface faulting. We discuss these and other corroborative measurements relevant to this suggestion.

Moreover, we present the results two-dimensional viscoelastic earthquake cycle calculations, which examine the relationship between distributions of driving stress and strain distribution in the interseismic period.

GD32-06

Plate Motion Along the San Andreas Fault from Satellite Laser Ranging

D.C. Christodoulidis
R. Kolenkiewicz
D.E. Smith (all at: Geodynamics Branch, Goddard Space Flight Center, Greenbelt, MD 20771)
S.M. Klosko
P.J. Dunn
M.H. Torrence (EG&G Washington Analytical Services Center, Inc., Riverdale, MD)

The Crustal Dynamics Project of NASA now supports continuous laser ranging to the LAGEOS satellite. Measurements taken from two sites on opposite sides of the San Andreas Fault have been used to monitor the relative motion between the Pacific and North American Plates in California. LAGEOS results, combined with those obtained from tracking the BE-C satellite, yield measures of this motion extending over the last decade. With new site deployments and, the LAGEOS and BE-C observations treated independently, there are five separate measures of the motion along the San Andreas Fault. If the LAGEOS and BE-C results are assumed to be measures of the same constant tectonic rate, the weighted average rate for the last 11 years is -6.4 ± 2.0 cm/year with all measures agreeing to within their uncertainty. This estimated rate is in good agreement with the -5.6 cm/year value implied by the global plate motion model of Minster and Jordan (1978). These results must be reconciled, however with recent local surveys made near the fault showing considerably lower rates of changes.

GD32-07

Geophysical Interpretation of Length Changes in the Satellite Laser Ranging Baselines in California

Steven C. Cohen (Geodynamics Branch, Laboratory for Earth Sciences, Goddard Space Flight Center, Greenbelt, MD 20771

Since 1972 high precision satellite laser ranging measurements have been made at two sites near Quincy and San Diego, California. The 900 km baseline connecting these sites passes over the boundary between the North American and Pacific Plates, strikes N24°W, and has a measured contraction rate between 5 and 8 cm/yr over the past 10 years. Among the major tectonic features crossing this line are the Elsinor, Cucamonga, San Andreas, Garlock, and Kern Canyon faults. In the vicinity of several of these faults the U.S. Geological Survey has established geodimeter networks for monitoring the rate of strain accumulation. We have compared the contraction rates deduced from the geodimeter measurements over short baselines with the long baseline contractions obtained with satellite laser ranging. Deformation within a few tens-of-kilometers about the San Andreas fault can account for only a fraction (perhaps less than 50%) of the long baseline contraction rate. However, deformation on the other major Southern California faults account for a contraction comparable in size to the San Andreas contribution. The residual difference between the measured long and short baseline contraction rates varies from 0 to about 4 cm/yr depending on measurement accuracy and assumptions made in interpretation. Several mechanisms can explain any residual differences between the measured contraction rates. Among the most promising are elastic strain extending beyond the boundaries of the geodimeter networks, broadscale near-surface aseismic flow, time dependent creep at depth, anelastic flow below the seismogenic zone and local deformation both on mapped and unmapped features. Examination of historical data and measurements made in Northern California provides some insight into the operation of these mechanisms, however, mesurements at intermediate sites along the long baseline are required for an actual understanding of the regional geodynamics.

GD32-08

Polar Deformation Fields and their Application to Western U.S. Tectonics

T. H. JORDAN (Scripps Institution of Oceanography, La Jolla, Ca 92093)
J. B. MINSTER (Science Horizons Inc., Encinitas, CA 92024)

An arbitrary tangent velocity field on the surface of the Earth can be represented as

$$\mathbf{v}(\mathbf{r}) = \Omega(\mathbf{r}) \times \mathbf{r}$$

where $\Omega(\mathbf{r})$ is a pseudovector field of geocentric angular velocities. We model a zone of deformation as a mosaic of domains in each of which the velocity field is *polar*; that is,

$$\Omega(\mathbf{r}) = \omega(\mathbf{r})\hat{\Omega} + \Omega_0$$

$\hat{\Omega}$ is a unit vector defining the pole of deformation, $\omega(\mathbf{r})$ is a scalar function of position, and Ω_0 is a constant vector which specifies the frame of reference. Rigid plates or blocks are domains where ω is constant. We give expressions for the velocity gradient tensor $\nabla_S \mathbf{v}$, the deformation-rate tensor D, and the rotation-rate (vorticity) tensor W in a spherical coordinate system (θ = colatitude, ϕ = longitude) with a pole at $\hat{\Omega}$. Longitudinal variations of the rotation rate ($\partial_\phi \omega \neq 0$) contribute only uniaxial deformation in the $\hat{\phi}$ direction but do not affect W. Latitudinal variations ($\partial_\theta \omega \neq 0$) are a source of both shear deformation and additional vorticity. Over a period of time—in the finite strain regime—this extra vorticity generates local rotations and, therefore, kinematical instabilities of the sort discussed by McKenzie and Jackson (*EPSL, 65,* 182, 1983) in the case of the plane strain with constant velocity gradients. This motivates us to consider a model where $\partial_\phi \omega = 0$ everywhere except possibly at idealized boundaries across which ω is discontinuous. These boundaries separate domains within which ω is a function of ϕ only and which thus undergo distributed (but not necessarily homogeneous) pure longitudinal extension or compression. An attractive feature of the model is that the pole of deformation can be determined in principle by fitting extension or compression axes estimated from focal mechanisms, geological observations, and direct stress measurements. We apply these ideas to deformation in the Basin and Range province of the western United States, where it appears that a single pole can describe the Quaternary deformation in several different domains.

GD32-09

Vector Constraints on Quaternary Deformation of the Western United States East and West of the San Andreas Fault

J. B. MINSTER (Science Horizons, Inc., Encinitas, CA 92024)
T. H. JORDAN (Scripps Institution of Oceanography, La Jolla, CA 92093)

We use boundary conditions imposed by the rigid-plate model to investigate the broad zone of deformation in the western United States separating the Pacific (PCFC) and North America (NOAM) plates. In the tangent plane at a fiducial point *C* on the San Andreas fault in central California, we set up the vector equation

$$\mathbf{v}_{PN} - \mathbf{v}_{SA} = \mathbf{v}_{CN} - \mathbf{v}_{CP}$$

$\mathbf{v}_{PN}$ is the PCFC-NOAM relative velocity vector at *C*, for which we adopt the estimate provided by model RM2 (56 ± 3 mm/yr, N35°W ± 2°). We demonstrate that this estimate is not likely to be biased by complexities within the PCFC-NOAM zone of deformation. $\mathbf{v}_{SA}$ is the rate-of-slip vector across the San Andreas at *C*, estimated from geodetic and Holocene geological data to be 34 ± 3 mm/yr, N41°W ± 2°. The left-hand side of the equation represents a 'discrepancy vector' that must be balanced by velocity vectors representing the deformation east and west of the San Andreas: $\mathbf{v}_{CN}$ and $\mathbf{v}_{CP}$, respectively. We formulate these vectors in terms of frame-independent integrals of the velocity gradient tensor along paths across the zones of deformation. To constrain $\mathbf{v}_{CN}$ we choose a path linking the rigid part of NOAM to the point *C* through the Great Basin, modeled as a zone of pure extension opening in the northwesterly direction at a rate of $\alpha \times$ 10 mm/yr. Conditional on $\alpha = 1$, stress and strain orientation data constrain $\mathbf{v}_{CN}$ to be 10.1 ± 0.7 mm/yr, N63°W ± 5°. Among the various geological and geophysical constraints on the rate parameter α, those established by Holocene paleoseismic mapping ($0.1 \leqslant \alpha \leqslant 1.2$) are the most relevant to the averaging interval of RM2 and, by our assessment, the most reliable. Satellite-geodetic measurements along the Quincy-Otay baseline in California further restrict α to be less than 0.8. Under these constraints, we show that deformation west of the San Andreas must involve 4-13 mm/yr of crustal shortening orthogonal to the fault and 6-25 mm/yr of right-lateral motion parallel to it. These predictions are independent of the rate estimates from geological data west of the San Andreas but consistent with them.

GD32-10

Late Quaternary Displacement Rate on the Owens Valley Fault Zone at Fish Springs Cinder Cone, California

S.J. Martel, (Dept. Applied Earth Sciences, Stanford University, Stanford CA 94305)
T.M. Harrison (Dept. Geological Sciences, State University of New York at Albany, Albany NY 12222)
A.R. Gillespie (Jet Propulsion Lab., Pasadena CA 91109)

The Fish Springs normal fault lies within the northern Owens Valley fault zone. During the late Quaternary Period it appears to have accommodated all the displacement across that zone. The fault vertically offsets a late Pleistocene basaltic cinder cone 74 ± 2m, and an overlying alluvial fan of Tahoe or Sangamon age (50,000-130,000 years B.P.) 36 ± 6m. We have dated the offset cinder cone, using ^{40}Ar-^{39}Ar analysis with stepwise heating, in order to determine the average displacement rate of the Fish Springs fault over the last ~ 200,000 years. We analysed K-feldspar from granitic xenoliths found in the basalt, to take advantage of their high K content. We have previously found that feldspar crystals are largely degassed of their Ar upon immersion in the hot magma. Thus the radiometric clock is reset at the time of eruption. The fraction of Ar that is retained by the feldspar during immersion in the magma is not released during analysis except at temperatures above ~ 900°C. Thus $^{40}Ar/^{39}Ar$ values for low-temperature steps give the age of eruption, although total ages may be excessive. We have previously dated lavas as young as 120,000 years with uncertainties as small as 10,000 years (2σ) using this approach. The Fish Springs cinder cone is of comparable age.

GD32-11

Neotectonics at the Juncture of the Southern San Andreas and Central Mojave Shear Systems

R.E. CRIPPEN (Remote Sensing Research Unit and Department of Geological Sciences, University of California, Santa Barbara, California 93106)

J.C. CROWELL (Department of Geological Sciences, University of California, Santa Barbara, Ca. 93106)
J.E. ESTES (Remote Sensing Research Unit, University of California, Santa Barbara, Ca. 93106)

Recent studies have led to the postulate that the Pacific-American plate boundary at depth may not be everywhere congruent with its primary surficial manifestation, the San Andreas fault. Seismic data and a number of surficial tectonic features may indicate the presence of the plate boundary along a northwest trend beneath the central Mojave Desert. Our study utilizes enhanced satellite imagery and image-formatted seismic, topographic, gravity, and aeromagnetic data to improve recognition of neotectonically significant features near the southern end of the possible incongruity.

Quaternary displacement has been confirmed along a number of fault traces where recent activity had only been inferred before. Offsets of alluvium are clearly seen along the Blue Cut fault, east to the Eagle Mountains, in Landsat Thematic Mapper imagery. Fault traces in the Central Mojave shear system delineate southward bending near its southern terminus.

Detection of subsurface features in Seasat radar imagery has been demonstrated, and the abundance of radar lineaments crossing alluviated areas only within the Central Mojave shear system may indicate a pattern of diffuse neotectonic activity there.

Various geophysical trends bolster the structural significance of some geomorphic patterns. Enhancements of low-resolution topographic and spectral data are suggestive of broad deformation patterns not previously recognized.

GD32-12

Small-Scale Convection Beneath the Transverse Ranges, Southern California

EUGENE HUMPHREYS
BRADFORD H. HAGER (Both at Seismological Laboratory, California Institute of Technology Pasadena, CA 91125)

Inversions of upper mantle P velocity structure beneath southern California show two prominent features: a region up to 3% fast in the 250 km below the Transverse Ranges (TR), and a region up to 4% slow in the 100 km below the Salton Trough (ST), corresponding to temperature differences of ~±300°C and density differences of ~±1%. We interpret these as due to small-scale convection in the mantle. A 3-D flow and stress distribution is calculated assuming seismic velocity and density perturbations to be linearly related. The model shows upwelling under the ST and downwelling beneath the TR. Shear tractions of about 100 bars drive an overall NE-SW motion with convergence in the TR. Normal tractions of a few hundred bars uplift the ST and downwarp the TR, in agreement with the relief found on the Moho (Hearn, 1984). An elastic layer atop the mantle filters this deformation. A 20 km thick layer produces a gravity field that is generally consistent with the observations. This field has no net gravity anomaly along the axis of the TR, and is flanked by a low of about 30 mgal.

We speculate that the downwelling beneath the TR was initiated by the opening of the ST. A 2-D convection model with temperature-dependent viscosity shows that rifting results in downwelling of the lower lithosphere about 200 km away from the rift. This model, which features viscous deformation and sinking of only the base of the lithosphere rather than subduction of the entire sub-crustal lithosphere, can explain: the amplitude of the observed seismic velocity anomaly beneath the TR, the lack of deep seismicity, and the relatively small amount of observed crustal shortening. It suggests that the "big bend" of the San Andreas Fault is the result of active mantle processes, not horizontal "plate forces".

GD32-13

Tectonics of the Gulf and Peninsula of California - Active Fault Traces, Independent Fault Blocks and a Re-evaluation of the Pacific/North American Translation Rate

G.E. NESS, R.W. COUCH, M.C. FEHLER and M. LYLE (CONMAR, College of Oceanography, Oregon State University, Corvallis, OR 97331)
O. SANCHEZ Z. and G. CALDERON R. (Instituto Oceanografico de Manzanillo, Colima)
F SUAREZ V. (CICESE, Ensenada, Baja California)

As part of the NASA Crustal Dynamics Project, we have prepared free-air gravity, bathymetry, and seismo-tectonic maps of the region extending from Point Conception to Punta Mangrove in Michoacan, including the Gulf of California. We are working to complete a magnetic anomaly-crustal isochron map of the same region. From these compilations, we have made a preliminary determination of the loci of both past and active faulting. Many independent fault blocks have been identified in the central and northern Gulf and on the northern peninsula. Like the fault blocks in Alta California, these have a notably narrow aspect. Gravity anomalies in the northern Gulf suggest that little basement extension has occurred there. Our earlier 68 km/m.y. PAC/NAM spreading rate determination, made from data obtained in the mouth of the Gulf, is supported by additional survey results, by satellite-laser-ranging SAFE results in Alta California, and indirectly by evidence that crustal extension is occurring in the Colima Graben - between Lago de Chapala and the Manzanillo Trough.

Detailed, transponder-navigated marine geophysical surveys are to be conducted during March-June of this year, SW of Manzanillo, in the northern Gulf and in the mouth of the Gulf to further examine these critical areas. A local seismic array will also be operated in the central Gulf during the same period.

Gravity Measurements and Analysis II

Room 27 Thurs AM

PRESIDER, C. F. YODER, JET PROPULSION LABORATORY

GD41-01

Constraints on a Standard Linear Solid Rheology from the J_2 observation and the 18.6 yr tidal Love number

ROBERTO SABADINI (Instituto di Geofisica, Univ. di Bologna, 8, Viale Berti Pichat, Bologna, Italy 40127)
David A. Yuen (Dept. of Geology, Arizona State Univ., Tempe, AZ 85287)

The nature of short-term mantle rheology for timescales between the seismic frequency band and a few hundred year remains relatively unknown. For short wavelength phenomena it is difficult to separate the contribution due to mantle relaxation processes from those having intrinsic crustal origins. On the other hand, constraints on the nature of short-term mantle rheology may be more easily derived from geophysical signatures involving long wavelength deformation, as in problems related to the Earth's polar motions. We make use of two pieces of information, which have emerged as a consequence of the recent acquisition of data from the LAGEOS satellite, to place some constraints on the rheological parameters of short-term mantle rheology. The first is the secular variation of the gravitational harmonic J_2 (Yoder et al., 1983, Rubincam, 1984). The second is an estimate of the tidal Love number for the 18.6 yr tide to be k_2^T (t=18.6 yr) = 0.36 on the basis of the LAGEOS observation (Lambeck and Nagiboglu, 1983). The anelastic rheology we have used is a standard linear solid, where the parameters of interests are the short-term viscosity and the modulus defect. We use a three-layer model consisting of an elastic lithosphere, a mantle with a standard-linear solid rheology, and an inviscid core. For large modulus defects and viscosities less than 10^{21} P unacceptably large rates of J_2 would result from large earthquakes. Too high values for k_2^T at 18.6 yrs are also obtained for this range of parameters. The data are more consistent with viscosities between 10^{21} and 10^{22} P and modest values of the modulus defect. We have found that the background long-term viscosity of 10^{22} P associated with a Maxwell rheology can contribute 25% of the tidal Love number dispersion at 18.6 yr.

GD41-02

MAGSAT and Geoidal 'LOWS' of Sarada Depression in Himalaya

J.G. NEGI, P.K. AGRAWAL and N.K. THAKUR
(National Geophysical Research Institute, Hyderabad 500007, India)

Analysis of Satellite gravity data (GEM-6) reveals a significant geoidal low (-70 meters) in the proximity of Sarada depression in the foothills of Himalaya on the Indian subcontinent. Residual vertical intensity MAGSAT data brings out a localised prominent low (-27 nT) over this region. The region exhibits anomalous behaviour in electrical conductivity, seismicity and the surface gravity picture. The Indus suture line also shows a disjointed feature in this zone. The inter-correlation of all these parameters is indicative of deep as well as localised complex tectonic activity.

GD41-03

A Further Estimation of GM from LAGEOS

R. Kolenkiewicz
D.E. Smith
D.C. Christodoulidis (all at: Geodynamics Branch, Goddard Space Flight Center, Greenbelt, MD 20771)

Analysis of nearly 7 years of Lageos laser tracking data has been used to make a re-estimation of GM, the product of the gravitational constant and the earth's mass. The value that has been obtained based on the GEM L2 gravity model, the Wahr earth tides and Schwiderski ocean tides models is 398600.434 ± 0.005 km^3sec^{-2}. This result was obtained in a simultaneous adjustment of the locations of 44 tracking stations, and polar motion and earth rotation at 5-day intervals. Yearly estimates of the value of GM show considerable stability. The model that most significantly affects the recovered value of GM is the geopotential. Adjustment of a large number of geopotential coefficients lowers the value of GM by less than 0.005 km^3sec^{-2}.

GD41-04

A Simplification of the Least Squares Determination of the Gravity Field from Low-Low Satellite Tracking Data Utilizing an Operator Representation of the Range Observable

V. REINHARDT (Bendix Field Engineering Corporation, Columbia, Maryland 21045)

One of the purposes of NASA/Goddard Space Flight Center's proposed Geopotential Research Mission is to map the gravity field of the Earth to 1-2 mgal in 41,253 1 degree x 1 degree blocks using range rate tracking data between two polar low orbiting satellites in the same orbit. Because there are 41,253 blocks in the gravity map, it takes, in general, at least 9.4E13 real floating point operations (flop) to solve the least square fit (LSQF) matrix equation used to determine the gravity potential from the tracking data. In this paper, by studying the symmetry of an operator which generates the range rate acceleration between the satellites from the along track gravity field, it is shown that the LSQF cross correlation matrix (T-matrix) formed from a complex spherical harmonic (Ylm) expansion of the gravity potential is, in the circular orbit infinite trajectory length approximation, diagonal in m. Further, for the actual mission, an iterative method which utilizes the inverse of the m-diagonal portion of the T-matrix, is shown to produce the 32758 coefficients of the Y model of the gravity potential to 64 bit precision in less than 1E12 flop. A second iterative method is shown to produce an approximate covariance matrix for the coefficients in less than another 5E11 flop. This paper also demonstrates a method which eliminates the problem of aliasing when attempting to solve the full problem sequentially, first, by solving for the approximate trajectories of the satellites with a reduced model of the gravity field, and then, by solving for a full model of the gravity field using the approximate trajectories.

GD41-05

Recovery of Gravity Anomalies form a low-low Satellite Mission in a Local Region

C. WICHIENCHAROEN (Dept. of Geodetic Science and Surveying, The Ohio State University, Columbus, OH 43210)

The earth's gravity field has been defined by a spherical harmonic expansion to degree 180 for carrying out simulation studies related to a low-low satellite mission. This spherical harmonic field can be used to calculate line of sight accelerations on a uniform geographic grid over the whole world, if needed, using a very efficient computer program. For test purposes, this data was generated in several areas assuming a satellite height of 160 km and a spatial separation of 200 km. The satellites were assumed to be in a circular polar orbit. This data was then used to recover gravity anomalies in a region using least squares collocation techniques. The true errors of recovery can be determined using the defined gravity field to degree 180. Results of various simulation studies will be described.

GD41-06

Geopotential Mapping Using Satellite to Satellite Tracking Data

E. M. Gaposchkin
M. I. T. Lincoln Laboratory
Lexington, MA 02173

The observable (doppler-velocity) between two satellites is a direct, non-linear, measurement of the potential difference [(T(P)-T(Q)] of the two points (P, Q) in space. T(P)-T(Q) measured along many tracks can be mapped onto a surface (Σ) suitable for a solution of Laplaces equation, which requires regularization of the measured potential. Iterating, is necessary due to the non linarity. This mapping can be done region by region. Σ can be downward continued to the earth's surface if desired. Two surface force compensated polar satellites at 160 km altitude, with 10^{-6} m/sec measurement accuracy are discussed.

GD41-07

GRM Gravity Field Estimation Error Sources

G.E. THOBE, J.T. KOUBA and S.C. BOSE (Applied Science Analytics, Inc., Canoga Park, Calif. 91303)

An error analysis of the Geopotential Research Mission (GRM) is being carried out to identify those error sources which might compromise the scientific value of measurements of the geopotential field. Oscillatory disturbances of low frequency are of special interest in this regard since they directly affect the estimated harmonic coefficients of the anomalous geopotential. The symmetry built into the GRM satellite design leads to a fortuitous separation of error sources by their common - and differential-mode effects. For example, the two-way doppler system of the satellite-to-satellite tracking (SST) system largely cancels the common-mode effects of local oscillator (carrier frequency) variations as well as vehicle pitching motions and odd-symmetry structural bending modes. Also the physical proximity of the two satellites tends to nullify the common-mode effects of solar and lunar gravitational perturbations. A perturbation analysis of the observation equation enables us to form conclusions about the sensitivity of the system to deviations in the trajectory from the nominal condition of identical circular polar orbits separated in time, as well as to doppler beacon and TDRSS tracking errors. Finally we summarize our results in the form of a table of error sources, their characterizations and their impact on the ability of the GRM program to recover the gravity field.

GD41-08

Determination of Short Wavelength Components of the Geopotential Using a Spaceborne Gravity Gradiometer

Werner D. Kahn (Geodynamics Branch, Laboratory for Earth Sciences, Goddard Space Flight Center, Greenbelt, MD 20771

The capabilities of an orbiting gravity gradiometer as a sensor for mapping the fine structure of the earth's gravity field are investigated. Knowledge of the fine structure of the gravity field is essential for studies of the solid earth and the dynamics of the oceans. Although the earth gravity tensor, measured by a gradiometer assembly has nine components, only five components are independent. This latter fact is a consequence of the symmetry and conservative nature of the earth's gravity field. The most dominant component is the radial one. Error analyses which were performed have consequently been based only upon a single axis gradiometer sensing the radial component. The expected global gravity and geoid errors for a 1/2° x 1/2° area (i.e., 55 km horizontal resolution) utilizing a spaceborne gradiometer with a precision of 10^{-3} E in a 160 km circular polar orbit for a mission duration of 180 days are about 3 mgals and 5 cm respectively.

GD41-09

Three-Axis Superconducting Gravity Gradiometer for Spaceborne Gravity Survey

H. J. PAIK, H. A. CHAN, M. V. MOODY, J. W. PARKE (Department of Physics and Astronomy, University of Maryland, College Park, MD 20742)
(Sponsor: L. S. Walter)

A gravity gradiometer with 10^{-4} E $Hz^{-1/2}$ sensitivity orbiting at an altitude of 160 Km could provide a 50 km resolution of the earth gravity field. It appears that an instrument with required sensitivity and stability can be constructed using superconducting technology. The basic principle of common mode rejection and signal coupling by means of persistent currents has been demonstrated with a single-axis system. Experience gained with this prototype instrument is used to design an improved gradiometer system which is sensitive to the inline components of the gravity gradient tensor in three orthogonal directions.

We describe some new concepts that have been introduced to the design of the three-axis gravity gradiometer and report progress in the construction of the instrument and the development of ancillary technologies. We discuss the development schedule and performance goals of the three-axis superconducting gravity gradiometer.

GD41-10

Test of Gravitational Inverse Square Law Using an Orbiting Gravity Gradiometer

H. J. PAIK (Department of Physics and Astronomy, University of Maryland, College Park, MD 20742)
J. MURPHY (NASA Headquarters, Washington, DC 20546)

The inverse square law is a fundamental basis for analyses of all gravity survey data and for geophysical models of the earth and the planets. It has been pointed out, however, that existing gravity data on geological scales cannot exclude a possibility of violation of the inverse square law in kilometer ranges by over 10%. Such a departure from Newton's law would be consistent with some new theories of gravity and elementary particles.

In order to test the law at kilometer ranges, experiments in which a null source (plane slab of water) or a null detector (three-axis gravity gradiometer) is employed have been proposed. An earth orbit experiment could involve a three-axis gravity gradiometer carried in an elliptical orbit.

In this paper, we consider an earth orbit experiment in which the oblateness of the earth is used as a time-varying source of gravity. This configuration will have an advantage of keeping the satellite in a low-altitude circular orbit, as envisioned for a gravity survey mission. If a 160 km altitude polar orbit is chosen, the distance between the gradiometer and the surface of the earth is modulated by 20 km at 3.7 X 10^{-4} Hz due to the equatorial oblateness of the earth. The sum of three orthogonal inline gravity gradients is the Laplacian of the gravitational potential, a null quantity in the inverse square law. Employing an appropriate technique of dropping orthogonality errors, one can obtain a resolution of 6 X 10^{-9} at 100 km, with an instrument sensitivity of 10^{-3} E $Hz^{-1/2}$ and an integration time of 1 year.

GD41-11

Airborne Measurement of the Vertical Gradient of Gravity

Sigmund Hammer (Department of Geology and Geophysics, University of Wisconsin, Madison, WI 53706)
William R. Gumert (Carson Geoscience Company, Perkasie, PA 18944)

A cooperative test of airborne gravity exploration in July 1982, which was planned by several U.S. oil companies, also provides measurements of the vertical gradient of gravity over a range of elevations from 1,500 to 5,500 feet (457 to 1676 m) above sea level. The measurements were made along a selected test line 50 miles (80 km) long in southeastern Pennsylvania, U.S.A. Airborne measurements were made at six flight elevations. Topographic relief in the area is about 1,000 feet (300 m). The free-air gravity anomaly values along the length of the line range from -20 to -65 mgal (referred to the 1930 ellipsoid). The measured vertical gradient varies 1.5% (0.3053-0.3099 mgal/m) but the average for the line (0.3073 mgal/m) departs from the accepted normal value (0.3086 mgal/m) by only -0.3%. A vertical profile of the gradient at a selected point illustrates the data.

GD41-11A

Feasibility of Gravity Gradient Measurements from a Tethered Subsatellite Platform

G. E. GULLAHORN (Harvard-Smithsonian Center for Astrophysics, Cambridge, Mass. 02138)
F. FULIGNI*
M. D. GROSSI

*(Visiting Scientist from IFSI-CNR, Frascati, Italy)

Sponsor: L. Walter

By placing instruments in a tethered subsatellite deployed downwards from the Shuttle, it will be possible to perform gravity gradient measurements from heights as low as 120 to 130 km for expanded periods of time. A gradiometer with 10^{-2} to 10^{-3} EU$\tau^{-1/2}$ sensitivity could achieve, from that height, measurement thresholds of specific interest to NASA geodynamics mission goals. However, the dynamic (acceleration) noise expected in a tethered satellite is far higher than in a free flyer and may negate the advantages of flying at this unusually low "orbital" height.

Investigations underway include both analytical efforts to estimate the dynamic noise experienced by the subsatellite, and experiment design efforts to alleviate the accelerations transmitted to the instrument platform. The first experiment is expected to take place on the demonstration flights of the T.S.S. facility (Tethered Satellite System) and consists of measuring linear and rotational accelerations using three accelerometers (resolution 10^{-6} g/Hz) and three gyros (stability 3 millidegrees/hour). A second experiment is expected to perform measurements of gradiometric noise followed by a third flight devoted to the collection of data of scientific relevance to NASA Geodynamics Research Program. The instruments that will fly these scientific missions are expected to be cryogenic tensorial gradiometers with resolution possibly reaching 10^{-7} EU$\tau^{-1/2}$.

MAGSAT—Theory and Interpretation

Room 21 Wed PM

Presider, C.G.A. Harrison, RSMAS

G.D. Mead NASA/GSFC

GP32-01

Inversions of Satellite Magnetic Field Data to obtain Crustal Magnetizations

C. G. A. HARRISON
K. HAYLING (both at Rosenstiel School of Marine & Atmospheric Science, University of Miami, FL 33149)

Two equivalent source techniques for inverting satellite magnetic field data to obtain crustal magnetizations are described and contrasted. One is appropriate for performing a global inversion and can be used to compare continental and oceanic magnetizations, or to look at latitudinal variations of magnetization. However, since the model is not a reasonable geophysical model it suffers from the inability to cope with real magnetization variations. The second method can satisfactorily produce reasonable geophysical models, provided that care is taken in the source spacing, and provided that an allowance is made for negative magnetizations in the case of situations where the magnetization is believed to be induced. It is shown how the case of susceptibility may be dealt with, by application of the annihilator. This has the effect of driving up the RMS magnetization and hence requiring a larger average susceptibility. The problem of how well the very long wavelength crustal magnetization can be determined will also be discussed in terms of the amount of annihilator used over limited areas of the Earth's surface.

GP32-02

The Character of Equivalent Source Solutions for Magnetization in the Atlantic using MAGSAT data

K. L. HAYLING
C. G. A. HARRISON (Both at Rosenstiel School of Marine & Atmospheric Science, University of Miami, FL 33149)

The equivalent source technique has been applied to 2 X 2 MAGSAT scalar field data taken over the North Central Atlantic Ocean. The modelled magnetization is assumed to be parallel or antiparallel to the Earth's main field. If there is significant anomalous field present in the area under consideration the results tend to show good stability but if the anomalous field is weak then oscillations show up in the dipole sources at spacings which should be resolvable from the MAGSAT altitude. In order to determine the best spacing for the dipole sources it is customary to look at either the goodness of fit between observed and calculated field and to choose a dipole spacing at which this fit ceases to improve significantly with reduction in dipole spacing or to look at the RMS dipole moment, which will show a large increase as soon as the dipole spacing becomes too small for resolution. Neither method can be used unequivocally and recourse must be made to studying the observed pattern of dipole sources to detect unwanted oscillations by eye.

Magnetizations calculated in this way tend to be in the region of 1 to 2 $A.m^{-1}$ if the whole oceanic crust is considered as the source region. This is about what the average magnetization of the oceanic crust would be if NRM measurements of rocks recovered from the oceanic basins are a reliable guide. Induced magnetizations do not contribute significantly to the field. For induced magnetizations, the magnetization has always to be positive, and so an annihilator has to be added to the inversion solution. This has the effect of raising the RMS magnetization, but at the same time the susceptibility of oceanic rocks is so low as to make it impossible to explain the observed fields by induced magnetization. The pattern of magnetization in the Atlantic shows some slight correlation with geological structures.

GP32-03

Global Crustal Scalar Magnetic Anomaly Map Derived from MAGSAT Data

J. ARKANI-HAMED and D.W. STRANGWAY (Department of Geology, University of Toronto, Toronto, Canada)

The MAGSAT vector magnetometer data are separated into two distinct sets, the dawn and the dusk sets. The dawn (dusk) set consists of the data acquired at approximately local dawn (dusk) terminators. The two sets were analysed independently because of the dawn-dusk asymmetry of the external magnetic field components of the data. Two scalar magnetic anomaly maps, the dawn and the dusk maps, are derived on the basis of 0.5 X 0.5 degree averaged samples of the two sets, respectively. The maps are, then, expressed in terms of the spherical harmonics using harmonics up to 120 degree. The degree correlation coefficients between the two expressions indicate significant correlation of the two maps at harmonics with degree between 18 and 44. A global crustal scalar magentic anomaly map is, subsequently, derived by arithmetic averaging of the corresponding harmonics of the dawn and the dusk maps. The map is then downward continued from an average altitude of about 410 km to an altitude of about 10 km. The magnetic anomalies seen in the downward continued map are relatively more localized. They show a close correlation with subduction zones, sedimentary basins and mountain ranges. The anomalies also display differences between continents and oceans. Continents have pronounced magnetic features, whereas oceans, especially the younger parts, are magnetically quiet regions.

GP32-04

Detection of Global Magnetic Anomalies Using Low Altitude Satellites

D.W. STRANGWAY, J. ARKANI-HAMED (Department of Geology, University of Toronto, Toronto, Canada) and P.J. HOOD (Geological Survey of Canada)

Data from the MAGSAT mission have been used to derive a map of the distribution of magnetic anomalies of the world. These anomalies, as resolved from MAGSAT, typically range between ± 10 nT at an orbital height of about 400 km. When downward continued to the surface anomalies are typically limited to a scale of 500 km or greater. It was possible to work with 2 nearly independent sets corresponding to dawn and dusk. These sets each give fairly uniform global coverage so that it was possible to add and to subtract these two maps from each other, thus giving a good sense of the noise level. The addition map suppressed a strong asymmetry-due to different ionospheric currents at dawn and dusk. The dominant remaining feature of the difference map was associated with various orbits, showing that the major noise level problem is directly analogous to the flight-line levelling problem of conventional aeromagnetic surveys. This noise level is $\pm$ 2 nT. Provided a similar level of sampling is possible in a future mission, the noise level associated with field fluctuations will be about $\pm$ 1nT. We therefore conclude that $\pm$ 1 nT is a realistic noise level for satellite mapping. Downward continuation of our MAGSAT anomaly map shows that the anomalies at 160km correspond to a level of $\pm$ 30 nT. Portions of the aeromagnetic anomaly map of Canada have been continued upward confirming that anomalies of 30 nT or more can be expected at 160 km. We can expect an improvement in the signal by a factor of 3 or 4 from flying at lower heights and there could be an improvement in the noise level by a factor of 2.

GP32-05

Mapping Magnetized Geologic Structures from Space: The Effect of Orbital and Body Parameters

PATRICK T. TAYLOR
CHARLES C. SCHNETZLER
ROBERT A. LANGEL (all:Geophysics Branch, Laboratory for Earth Sciences, NASA/GSFC, Greenbelt, MD 20771

When comparing previous satellite-magnetometer missions (such as Magsat) with proposed new programs (for example, Geopotential Research Mission, GRM) it is important to quantify the difference in scientific information obtained. We use the ability to resolve separate magnetic blocks (simulating geological units) as a parameter for evaluating the expected geologic information from each mission. This study evaluates and quantifies the effect of satellite orbital altitude on the ability to resolve two magnetic blocks with varying separations. Other parameters which were changed were: inclination; and intensity of the dipolar field; orientation of the magnetized blocks and orbital pass azimuth.

Our results indicate a systematic, but non-linear, relationship between resolution and distance between magnetic blocks as a function of orbital altitude. The proposed GRM would provide an order-of-magnitude greater anomaly resolution than the earlier Magsat mission for widely separated bodies of any separation (>150 km); difference in resolution increases even more dramatically as body separation approaches the altitude of GRM. The resolution achieved at any particular altitude varies by about a factor of ten depending on the location of the bodies and up to about a factor of two depending on orientation.

GP32-06

Constraints on the Regional Magnetization of the Oceanic Crust

C. A. RAYMOND
J. L. LaBRECQUE (both at: Lamont-Doherty Geological Observatory,Palisades,N.Y. 10964)

We have examined the MAGSAT intermediate wavelength magnetic field over the Shatsky Rise in the North Pacific and over the North Atlantic basin. From these studies we draw the following conclusions about the intermediate wavelength field: 1) a significant anomaly is observed over the Cretaceous oceanic crust which is due to remanent magnetization acquired during the seafloor spreading process; 2) induced magnetization dominates in areas of lateral crustal inhomogeneity; 3) the Moho appears to be the lower boundary of the magnetized layer; 4) the thermal structure of slow spreading centers does not produce an observable anomaly.

The MAGSAT and sea surface intermediate wavelength profiles over the Shatsky Rise can be modeled by a source body whose upper bound is the seafloor topography and whose lower bound is the seismically determined Moho. A magnetization direction along the present field is required, suggesting the induced component dominates.

The North Atlantic basin intermediate wavelength anomaly field is dominated by the remanent magnetization of the seafloor spreading anomalies. The lateral homogeneity of the crustal structure suggests induced magnetization is unimportant, except in the region of the spreading center where the thermal structure must be considered. We have formulated a variety of models which incorporate the thermal structure of the North Atlantic spreading system. We find no evidence for the effects of the thermal structure in the observed field.

GP32-07

Geologic Analysis of Averaged Magnetic Satellite Anomalies

H. K. GOYAL, R. R. B. VON FRESE (Dept. of Geology & Mineralogy, The Ohio State University, Columbus, OH 43210)
J. R. RIDGEWAY, W. J. HINZE (Dept. of Geosciences, Purdue University, W. Lafayette, IN 47907)

To investigate relative advantages and limitations for quantitative geologic analysis of magnetic satellite scalar anomalies derived from arithmetic averaging of orbital profiles within equal-angle or equal-area parallelograms, the anomaly averaging process was simulated by orbital profiles computed from spherical-earth crustal magnetic anomaly modeling experiments using Gauss-Legendre quadrature integration. The results indicate that averaging can provide reasonable values at satellite elevations, where contributing error factors within a given parallelogram include the elevation distribution of the data, and orbital noise and geomagnetic field attributes. Various inversion schemes including the use of equivalent point dipoles are also investigated as an alternative to arithmetic averaging. Although inversion can provide improved spherical grid anomaly estimates, these procedures are problematic in practice where computer scaling difficulties frequently arise due to a combination of factors including large source-to-observation distances (> 400 km), high geographic latitudes, and low geomagnetic field inclinations. Finally, a comparison of averaged scalar anomalies over South America taken from the global <2°> MAGSAT anomaly map with anomalies derived from a detailed analysis of orbital profiles by equivalent point source inversion indicates that external field and variable elevation effects contribute significantly to distortion in the <2°> anomalies.

GP32-08

The South-Central United States Magnetic Anomaly

P.J. STARICH, W.J. HINZE, L.W. BRAILE (Dept. of Geosciences, Purdue University, West Lafayette, IN 47907)

A positive magnetic anomaly, which dominates the MAGSAT scalar field over the south-central United States, results from the superposition of magnetic effects from several geologic sources and tectonic structures in the crust. The highly magnetic basement rocks of this region show good correlation with increased crustal thickness, above average crustal velocity and predominantly negative free-air gravity anomalies, all of which are useful constraints for modeling the magnetic sources.

The positive anomaly is composed of two primary elements. The westernmost segment is related to middle Proterozoic granite intrusions, rhyolite flows and interspersed metamorphic basement rocks in the Texas panhandle and eastern New Mexico. The anomaly and the magnetic crust are bounded to the west by the north-south striking Rio Grande Rift, a zone of lithospheric thinning and elevated heat flow, in central New Mexico. The anomaly extends eastward over the Grenville age basement rocks of central Texas, and is terminated to the south and east by the buried extension of the Ouachita System.

The northern segment of the anomaly extends eastward across Oklahoma and Arkansas to the Mississippi Embayment. It corresponds to a general positive magnetic region associated with the Wichita Mountains igneous complex in south-central Oklahoma and 1.2 to 1.5 Ga. felsic terrane to the north. The magnetic terrane terminates along a roughly east-west line in southern Kansas.

A subdued northeasterly extension of the anomaly, from southwest Missouri into the Great Lakes region, appears to be related to the felsic terrane which extends northeast across the Midcontinent.

GP32-09

MAGSAT Scalar Anomaly Map of South America

J.R. RIDGWAY, W.J. HINZE and L.W. BRAILE (Dept. of Geosciences, Purdue University, West Lafayette, IN 47907)

A scalar magnetic anomaly map has been prepared for South America and adjacent marine areas directly from original MAGSAT orbits. The preparation of the map poses special problems, notably in the separation of external field and crustal anomalies, and in the reduction of data to a common altitude. External fields are manifested in a long-wavelength ring current effect, a medium-wavelength equatorial electrojet, and short-wavelength noise. The noise is reduced by selecting profiles from "quiet" periods ($K_p \leq 3$), and since the electrojet is confined primarily to dusk profiles, its effect is minimized by drawing the data set from dawn profiles only. The ring current is corrected through the use of the standard ring current equation, augmented by further filtering with a Butterworth bandpass filter. Under the assumption that the time-variant ring current is best removed when a replication of redundant profiles is achieved, a test set of 25 groups of 3 nearly coincident orbits per group is set up for filtering with a range of long-wavelength cutoffs, spanning 22 degrees to infinite wavelength, to determine which cutoff best replicates the residual profiles. Replication is determined by linear regression, which results in a correlation coefficient, a slope, and an intercept. By using these parameters in a triple test, the long-wavelength cutoff which best removes the ring current is found to be 50 degrees. Profiles thus filtered differ primarily in amplitude due solely to satellite altitude differences. These differences are then normalized by an inversion of the profile data onto a grid of equivalent point dipoles, and recalculated at an altitude of 350 km. The resulting map, when compared to the 2° averaged map, shows more coherent anomalies, with notable differences in the region affected by the electrojet, and promises much in regard to improved geologic interpretation.

GP32-10

Satellite-Elevation Magnetic Anomalies Over Submarine Plateaus: The Ontong-Java Anomaly

H. FREY (Geophysics Branch, Goddard Space Flight Center, Greenbelt, MD 20771)

Satellite crustal anomaly data shows a prominent negative anomaly overlying the Ontong Java Plateau. When reduced-to-pole (RTP), POGO data show that the anomaly is really positive with a total contrast of +14nT between the plateau and deep ocean to the north, over which lies a -4nT negative anomaly. Profiles across the region show good agreement between topography and RTP anomaly contrast. The available seismic refraction data indicate the Ontong Java Plateau is at least 35km thick, which together with a V_p=6.1km/sec layer in the crustal section has led to some debate about the nature of the plateau. Three-dimensional models of the plateau and its surroundings were calculated, assuming a simple induction model for the anomaly over the plateau. The anomaly contrast is well matched by a model in which the plateau is simply thickened oceanic crust, with magnetizations in each crustal layer identical to that in the corresponding layer of the surrounding oceanic crust. Both the positive over the plateau and the negative over the deeper ocean basin at 165°W, +8° are explained this way. The POGO RTP data cannot be matched by an extreme continental model. The great thickness of the plateau does not overcome the lower continental susceptibilities, and the resulting anomaly over such a plateau would be negative. Likewise a "Lord Howe Rise" type model in which an otherwise continental plateau has an altered high susceptibility lowest crustal layer, does not satisfy the POGO RTP data.

GP32-11

Satellite-Elevation Magnetic Anomalies Over Subduction Zones: The Middle American Trench

J. VASICEK (Astronomy Program, University of Maryland, College Park, MD 20742 and Geophysics Branch, Goddard Space Flight Center, Greenbelt, MD 20771), H. FREY and H. THOMAS

Both POGO and MAGSAT data show several prominent signatures over subduction zones. Previous work has demonstrated that such anomalies could result from the magnetization contrast between the cold subducting slab and the surrounding nonmagnetic mantle. The Middle American Trench is associated with a positive anomaly in the satellite elevation data. This paper presents a three-dimensional model of this subduction zone. The model is divided into two bodies by the Tehuantepec Ridge. North of the Techuantepec Ridge a 7 km thick slab dips at about 30° to 150 km depth; south of the Ridge a 4 km thick slab dips at about 45° to 200 km depth. With this geometry a magnetization contrast of about 5 A/m produces a 10 nT anomaly in agreement with a radially polarized MAGSAT map by Hinze et al. (GRL 9, 314, 1982). The model contours highly correlate with existing data except north of the intersection of the Tehuantepec Ridge and the Middle American Trench. In this area, no high quality data exists to constrain the geometry of the slab. This and other detailed problems observed in the model will be discussed.

GP32-12

Satellite Elevation Magnetic Anomaly Contrasts Over Continent/Ocean Boundaries

C.C. SCHNETZLER, H.V. FREY and H.H. THOMAS (Geophysics Branch, Goddard Space Flight Center, Greenbelt, MD 20771)

One surprising feature of the MAGSAT crustal anomaly map is the apparent paucity of obvious anomaly contrasts at the continental/oceanic crustal boundary. Such contrasts might be expected if the magnetic properties of continental rocks (susceptibility x thickness of the source layer) were significantly different from oceanic rocks. Continent/ocean crustal anomaly contrasts do occur, and are most easily recognized in reduced-to-pole (RTP) data where the effects of magnetic inclination do not confuse the sign and location of anomalies. We have identified a number of cases. Particularly good examples are southern Australia, western Antarctica, northeast Labrador, the U.S. east coast anomaly, northwest Canada and northeast South America. In all these cases, the anomaly changes from a positive (RTP) over the continent to a negative over the ocean. All these cases have the continental/oceanic crustal boundary oriented at high angles to the local geomagnetic longtitude (which enhances the ability to detect an edge effect) and to the satellite orbital track (which avoids the along-track filtering effects which subdue N-S anomaly structure). These anomalies may be due to an edge effect between oceanic and continental crust of different (susceptibility x thickness). Magsat measured anomaly field variations above boundaries are compared with the field produced by models of boundaries with various magnetic field and orbit orientations.

GP32-13

Magsat Crustal Signatures over the Eastern U.S.

M. E. RUDER and S. S. ALEXANDER (Pennsylvania State University, Dept. of Geosciences, University Park, PA 16802)

A high-quality (K_p less than 2) subset of ascending and descending Magsat passes has been analyzed for the region 270°-300°W, 20°-50°N. Spectral content of the crustal anomaly field is examined for wavenumber energy maxima, prominent trends in the transformed data and contaminating noise. A filtered data set is constructed, using block averages, at various altitudes. Attempts to model the largest anomaly in the subset,

the Kentucky anomaly, using the results of Thomas et al. (1981) show that the satellite data cannot resolve the three distinct long wavelength aeromagnetic anomalies. However, in order to reproduce the anomaly signature observed at 400 km altitude, all three sources must be used in the calculation. Modeling of the Kentucky anomaly using different block configurations indicates that the total volume of the anomalous body together with its susceptibility contrast, not body geometry, are the dominant factors controlling anomaly amplitude and spatial location. The upper (granitic) crust that contributes relatively little to the total crustal magnetic field, is thinned in this region of Precambrian rifting in Kentucky, based on seismic information. Its effect can be stripped from the total observed anomaly. The remaining signature can then be inverted to obtain a value for the magnetic susceptibility of the three anomalous bodies that protrude into the granitic crust, if the thickness of the magnetic crust is known or assumed. If these values are representative of typical lower crustal rocks, they can be used to model thickness of the magnetic crust in regions of poor seismic control. Spatial variations in the inferred thickness of the magnetic crust can then be used together with other geophysical and geologic data to interpret the regional tectonic fabric in the eastern United States.

GP32-14

Analysis and Use of Magsat satellite magnetic data for Interpretation of Crustal Structure and Character in the U.S. Midcontinent

ROBERT S. CARMICHAEL (Department of Geology, University of Iowa, Iowa City Iowa 52242)
ROSS A. BLACK (as above, and Iowa Geological Survey, Iowa City Iowa 52240)

Magnetic anomaly data acquired by NASA's Magsat satellite have been processed, analysed, and interpreted in terms of causative crustal sources (major structures, tectonic development, geologic provinces, crustal composition and magnetic properties) in the central U.S. midcontinent. An optimum data set was developed by cleaning, correcting, and correlation of the data, reducing to a 1°x1° latitude/longitude grid at a common altitude of 400 km, two-dimensional filtering, reducing to-the-magnetic-pole, and plotting as an anomaly map. The observed satellite anomalies have a magnitude range up to ±15 nT in the region.

The relationship between these long-wavelength anomalies and crustal sources is investigated for magnetic highs over Kentucky/Tennessee and NW Texas/Okla. with a zone trending northeast through Missouri towards Lake Michigan; for magnetic lows over the Mississippi Embayment/aulacogen, South Dakota, and west-central Georgia; for a magnetic anomaly pattern which generally follows and reflects the southern (late-Precambrian) rifted continental margin of the North American craton; and for a lack of apparent magnetic expression of the Central North American Rift system/ Midcontinent Geophysical Anomaly (MCA).

Work supported by the NASA Goddard Space Flight Center.

GP32-15

MAGSAT ANOMALIES OVER INDIA AND THEIR CORRELATIVE STUDIES - D.C.Mishra,NGRI, Hyderabad-7 India.

(Sponsor: L.S.Walter)

MAGSAT anomaly maps over India and adjoining areas are prepared using all the satellite observations over this region. The observed magnetic anomalies are discussed and analysed using available geological and geophysical information such as Regional Bouguer anomaly, crustal thickness, large-scale intrusions, heat-flow studies etc. . First order features are a magnetic 'high' of the order of 18-20 γ over central Indian shield extending from 12°N upto Indo-Gangetic plains and deflecting towards east upto Shillong plateau and a 'low' of the order of 25 γ over the Himalayas.

The magnetic 'high' over the Indian shield covers entire stable portion of the shield and extends almost upto continental margins dissected by the Gondwana trends of Godavari and Mahanadi rift valleys which are comparatively unstable regions with high heat flow. The magnetic 'low' over the Himalayas coincide with the Punjab Lesser Himalayas and follow the general trends of major tectonic elements in this region. This area is further characterized by several hot springs suggesting a shallow Curie point geotherm. The magnetic 'high' over the Indian shield is separated from an elongated 'high' over Saurashtra shelf by a comparative 'low' coinciding with Aravali Ranges and extending below Deccan Trap upto 16°N. This might be another region of shallow Curie point geotherm as also suggested by high heat flow measurements at a specific point. A magnetic 'low' in vertical intensity is observed in the Indian ocean east of Comorin Ridge which might be indicative of a thick crust. An equivalent source magnetization map and a depth contour map of Curie point geotherm will be presented.

Author Index

Eubanks T M (G42-04)
Evans A G (G12-05)

Fanselow J L (GD32-03)
Fanselow J L (GD32-04)
Fehler M C (GD32-13)
Fischetti T L (GD11-01)
Fisher P C (G32-10)
Frey H (GD11-04)
Frey H (GP32-10)
Frey H (GP32-11)
Frey H V (GP32-12)
Fuligni F (GD41-11A)

Gaposchkin E M (GD41-06)
Gilbert L (GD12-09)
Gillespie A (GD12-08)
Gillespie A R (GD32-10)
Goad C C (G12-09)
Golombek M P (GD22-09)
Gordon R (GD22-07)
Goyal H K (GP32-07)
Gross R S (G41-10)
Grossi M D (GD41-11A)
Gullahorn G E (GD41-11A)
Gumert W R (GD41-11)

Hager B H (G32-03)
Hager B H (GD32-12)
Hajela D P (G12-07)
Hamilton W L (GD22-04)
Hammer S (GD41-11)
Hardy R L (G12-11)
Harrison C G A (GP32-01)
Harrison C G A (GP32-02)
Harrison T M (GD32-10)
Haxby W F (G32-09)
Haxby W F (G32-12)
Hayling K (GP32-01)
Hayling K L (GP32-02)
Heinick J M (GD21-04)
Hempton M R (GD12-06)
Henry R (GD22-01)
Hernquist D C (G42-03)
Herring T A (GD21-10)
Hide R (G41-02)
Hinojosa J (G32-11)
Hinze W J (G12-12)
Hinze W J (GP32-07)
Hinze W J (GP32-08)
Hinze W J (GP32-09)
Hood P J (GP32-04)
Hothem L D (G12-06)
Humphreys E (GD32-12)
Hurst K (GD32-01)

Ivins E R (GD12-01)

Jordan T H (GD32-08)
Jordan T H (GD32-09)

Kahn W D (GD41-08)
Kawaguchi N (GD11-13)
Kilger R (GD11-10)
King R W (G42-02)
Klitgord K D (GD12-07)
Klosko S M (GD21-16)
Klosko S M (GD32-06)
Kolaczek R A (G42-02)
Kolenkiewicz R (GD21-04)
Kolenkiewicz R (GD32-06)
Kolenkiewicz R (GD41-03)
Koscielski C G (GD11-09)
Kouba J T (GD41-07)
Kovacs L C (G32-13)
Kramer L (G41-09)
Kroger P M (GD21-14)
Kuo J T (G12-04)

LaBrecque J L (GD22-10)
LaBrecque J L (GP32-06)
Langel R A (GP32-05)
Lanyi G E (GD21-11)
Lanzano P (G32-13)
Lanzano P (GD22-03)
Larsen S (GD22-05)
Lefebvre M (G32-05)
Lohmar F J (GD21-12)
Lyle M (GD32-13)
Lyzenga G A (G41-11)
Lyzenga G A (GD12-01)
Lyzenga G A (GD32-04)
Lyzenga G A (GD32-05)

Mader G L (GD11-08)
Mallama A (GD21-07)
Marsh B D (G32-11)
Marsh J G (G32-11)
Martel S J (GD32-10)
Martin C F (G32-04)
Mayr H G (G41-09)
McAdoo D C (G32-04)
McCarthy D D (G41-04)
Melvin P J (G12-10)
Minster J B (GD32-08)
Minster J B (GD32-09)
Mishra D C (GP32-15)
Moody M V (GD41-09)
Moose R E (G12-01)
Mueller I I (GD21-01)
Murphy J (GD41-10)

Najarian R J (GD21-05)
Nakashizuka N (GD22-01)
Negi J G (GD41-02)
Ness G E (GD32-13)
Nicolson G D (GD11-11)
Nothnagel A (GD11-11)

Officer C B (GD22-08)

Paik H J (GD41-09)
Paik H J (GD41-10)
Parke J W (GD41-09)
Parr J T (G32-10)
Parrott M H (G12-12)
Patriat P (G32-06)
Patterson J E (GD21-14)
Patterson J E (GD32-03)
Poley C M (GD12-10)
Potash R (G41-08)
Poulose S (G32-04)
Preisig J R (GD12-08)
Purcell, Jr. G H (GD21-05)

Raefsky A (G41-11)
Raefsky A (GD32-05)
Rapp R H (G12-03)
Raymond C A (GP32-06)
Reilinger R (GD12-05)
Reilinger R (GD22-05)
Reinhardt V (GD41-04)
Ren L K (G12-04)
Richards M A (G32-03)
Ridgeway J R (GP32-07)
Ridgway J R (GP32-09)
Rius A (GD11-11)
Robertson D S (G42-05)
Robertson D S (GD21-08)
Robertson P (GD12-11)
Rochester M G (G41-03)
Roman N G (GD21-06)
Rosen R D (G41-05)
Ruder M E (GP32-13)
Ruff L (G32-08)
Rundle J B (GD12-03)
Ryan J (GD21-07)

Sabadini R (GD41-01)
Sailor R V (G32-10)
Salstein D A (G41-05)
Sanchez Z. O (GD32-13)
Sandwell D T (G32-14)
Sauber J (GD12-05)
Schnetzler C C (GP32-05)
Schnetzler C C (GP32-12)
Schouten H (GD12-07)
Schuh H (GD11-10)
Schuh H (GD11-11)
Schutz B E (G42-06)
Schutz B E (GD21-02)
Schutz B E (GD21-03)
Schwiderski E W (G42-09)
Shapiro I I (G42-02)
Shapiro I I (GD21-10)
Shelus P J (GD11-12)
Slade M A (G41-11)
Smalley, Jr. R F (GD12-02)
Smith D E (GD21-16)
Smith D E (GD32-06)
Smith D E (GD41-03)
Snay R A (GD32-01)
Snay R A (GD32-02)
Solla S A (GD12-02)
Solomon S C (GD22-12)
Sovers O J (GD21-11)
Sovers O J (GD21-15)
Spieth M A (G42-04)
Spraul D R (GD22-11)
Srivastava S P (GD12-07)
Starich P J (GP32-08)
Statman J I (GD21-05)
Stein S (GD22-07)
Stein W L (G42-07)
Steppe J A (G41-06)
Steppe J A (G42-03)
Steppe J A (G42-04)
Strangway D W (GP32-03)
Strangway D W (GP32-04)
Suarez V. F (GD32-13)

Talwani P (GD12-10)
Tapley B D (G42-06)
Tapley B D (GD21-03)
Tapley B E (GD21-02)
Taylor P T (GP32-05)
Taylor, Jr. H A (G41-09)
Thakur N K (GD41-02)
Thobe G E (GD41-07)
Thomas H (GP32-11)
Thomas H H (GP32-12)
Thomas J B (GD21-05)
Thornton C L (GD11-06)
Thornton C L (GD11-07)
Timmerman E L (GD32-01)
Timmerman E L (GD32-02)
Toksoz M N (GD12-05)
Torrence M H (GD21-16)
Torrence M H (GD32-06)
Trask D W (GD32-03)
Treuhaft R N (GD21-11)
Treuhaft R N (GD21-15)
Tscherning C C (G12-03)
Turcotte D L (G32-01)
Turcotte D L (GD12-02)

Vandenberg N R (GD11-09)
Vasicek J (GP32-11)
Von Frese R R B (G12-12)
Von Frese R R B (GP32-07)

Wahr J M (G41-01)
Wallace K S (GD32-04)
Walter L S (GD11-02)
Watts A B (G32-02)
Watts A B (G32-06)
Weissel J K (G32-12)
Wellen A H (GD21-06)
Wichiencharoen C (GD41-05)
Wieland F P (GD21-09)
Wieland F P (GD32-03)
Wu F T (GD12-08)

Xu G G (G12-04)

Yan C Y (GD22-01)
Yuen D A (GD41-01)

Appendix 3

Current Publications on Research Associated with

NASA Geodynamics Program

The following were provided by investigators associated with the Program in response to a request for references to their recent papers (or those of their collaborators) in this field.

Aardoom, L., On Strain in Geodetic Baseline Networks. Dept. of Geodesy Report, No. 19, Delft Univ. of Tech., 1983.

Aardoom, L. and P. Wilson, A Modular Transportable Laser Ranging System-MTLRS. CSTG Bulletin, No. 5, Delft Univ. of Tech., 1983.

Aardoom, L., B. van Gelder, and E. Vermaat, Design of SLR Networks for Studies of Crustal Dynamics. Reports of the Dept. of Geodesy, Mathematical and Physical Geodesym., No. 83.3, Delft Univ. of Tech., 1984.

Afonse, G. et al, Status on the Neutral and Charge Drag Effects of LAGEOS. Congres Erminoni, September, in press, 1982.

Afonse, G. et al, Reassessment of the Charge and Neutral Drag of LAGEOS and its Geophysical Implications. Centre d'Etudes et de Recherches, 1983.

Allen, S., Global Coordinate Orientation Effects on ARIES Baseline. EOS, Transactions, American Geophys. Union, Vol. 64, No. 18, 1983.

Anderson, D. L., The Earth as a Planet: Paradigms and Paradoxes. Science, Vol. 223, CA Inst. of Tech., 1983.

Anderson, D. L., Surface Wave Tomography. CA Inst. of Tech., 1984.

Anderson, D. L. and J. Regan, Uppermantle Anisotropy and the Oceanic Lithosphere. Geophys. Res. Ltrs., Vol. 10, No. 9, CA Inst. of Tech., 1983.

Anderson, J. and R. Rosen, The Latitude-Height Structure of 40-50 Day Variations in Atmospheric Angular Momentum. Science, Atmos. and Env. Res., 1983.

Aruv, M., P. Bains, and J. Lal, Survey of India in 1983: Anomaly Map of Z Component of Indian Subcontinent from Magnetic Satellite Data. Survey of India, 1983.

Baldi, P. and S. Zerbini, Crustal Movements in the Mediterranean Basin: Simulation of a Satellite-Laser Ranging Network. Bollettino di Geodesia e Scienze Affini, Anno XLII, No. 3, Univ. of Bologna, 1983.

Beckman, B. and C. Hildebrand, Requirements for GPS Geodesy at One Centimeter Precision in the Caribbean. EOS, Transactions, Am. Geophys. Union, Vol. 64, No. 18, Jet Prop. Lab., 1983.

Beckman, B., On Geodesy with the Global Positioning System: Caribbean and Pacific Scenarios. EOS, Transactions, Am. Geophys. Union, Vol. 64, No. 45, Jet Prop. Lab., 1983.

Beetz, H., B. Richter, and P. Wolf, Messungen Im Lokalen Hoehen - Und Schwereueberwachungsnetz Im Bereich der Station Wettzell. Institut fuer Angewandte Geodaesie, 1983.

Bergman, E. A. and S. Solomon, Do Oceanic as Well as Continental Plates Have "Stress Provinces?" Abstracts, Fifth Annual NASA Geodynamics Program Conference, MA Inst. of Tech., 1983.

Bergman, E. A. and S. Solomon, Source Mechanisms of Earthquakes Near Mid-Ocean Ridges from Body Waveform Inversion: Implications for the Early Evolution of Oceanic Lithosphere. J. Geophys. Res., MA Inst. of Tech., 1984.

Bergman, E. A. and S. Solomon, Source Studies of Near-Ridge Earthquakes: Implications for the Early Evolution of Oceanic Lithosphere. EOS, Trans., Amer. Geophys. Union, Vol. 64, MA Inst. of Tech., 1983.

Bergman, E. A. and S. Solomon, Intraplate Stress. Encyclopedia of Structural Geology and Plate Tectonics, MA Inst. of Tech., 1984.

Bergman, E. A., J. Nabelek, and S. Solomon, An Extensive Region of Off-Ridge Normal-Faulting Earthquakes in the Southern Indian Ocean. J. Geophys. Res., MA Inst. of Tech., 1984.

Bergman, E. A., S. Bratt, and S. Solomon, Thermoelastic Stress: How Important as a Cause of Earthquakes in Young Oceanic Lithosphere?. EOS, Trans., Amer. Geophys. Un., Vol. 65, MA Inst. of Tech., 1984.

Bernard, J. et al, First SEASAT Altimeter Data Analysis on the Western Mediterranean Sea. J. Geophys. Res., Vol. 88, Am. Geophys. Un., 1983.

Bilham, R. and D. Simpson, Indo-Asian Convergence and the 1913 Survey Line Connecting the Indian and Russian Triangulation Surveys. Int'l. Karakoram Project, Vol. 1, Columbia Univ., 1984.

Bills, B. G., Thermoelastic Bending of the Lithosphere: Implications for Basin Subsidence. Geophys. J. R. Astr. Soc., Vol. 75, Jet Propulsion Lab., 1983.

Bock, Y., On the Time Delay Weight Matrix in VLBI Geodetic Parameter Estimation. Dept. of Geodetic Sci. and Surveying Report 348, Ohio State Univ., 1983.

Boschi, E. et al, Selection of Geodynamic Sites for Mobile Laser Systems in Italy. Bollettino di Geodesia e Scienze Affini, Univ. of Bologna, 1984.

Bowin, C. and C. Monster, Geology of the Dominican Republic: ARC Polarity Reversal and Effects of Cessation of Subduction. Woods Hole Ocean. Inst., 1984.

Brown, L. and R. Reilinger, Crustal Movement. Rev. Geophys. and Space Phys., Vol. 21, 1983.

Brown, L. and R. Reilinger, Epirogenic and Intraplate Movement. EOS, Trans. Am. Geophys. Union, Vol. 64, Am. Geophys. Un., 1983.

Brown, R. et al, Roughness of the Marine Geoid from SEASAT Altimetry. J. Geophys. Res., Vol. 88, No. C3, 1983.

Brunner, F., ed., Geodetic Aspects of Electromagnetic Wave Propagation Through the Atmosphere. Springer Verlag (Berlin), Jet Prop. Lab., 1984.

Buennagel, L., D. Spitzmesser, and L. Young, One Nano-Second Time Synchronization Using SERIES and GPS. Proceedings of the Fourteenth Ann. Precise Time and Time Interval Application and Planning Meeting, December, Jet Prop. Lab., 1982.

Cain, J. et al, The Use of Magsat Data to Determine Secular Variation. Journ. of Geophys. Res., Vol. 88, No. B7, U.S. Geological Survey, 1983.

Cain, J., J. Frayser, L. Muth, and D. Schmitz, The Use of MAGSAT Data to Determine Secular Variation. Journ. of Geophys. Res., Vol. 88, No. B7, U. S. Geological Survey, 1983.

Cain, J., Schmitz, D., and L. Muth, Small-Scale Features in the Earth's Magnetic Field Observed by MAGSAT. Journal of Geophys. Res., Vol. 89, No. B2, U. S. Geological Survey, 1984.

Carter, W. E., Polar Motion and Earth Rotation, Multidisciplinar use of the Very Long Baseline Array, Proceedings of a Workshop. National Academy Press, Nat. Geod. Survey, 1983.

Carter, W., D. Robertson, and J. Mackay, POLARIS Earth Rotation Time Series. Proceedings of the IUGG General Assembly, Nat. Geod. Survey, 1983.

Carter, W., et al, Variations in the Rotation of the Earth. Science, Nat. Geod. Survey, 1984.

Cazenave, A. and K. Do Minh, Thermal Parameters of the Oceanic Lithosphere Estimated from Geoid Height Data. J. Geophys. Res., Vol. 88, Am. Geophys. Un., 1983.

Cazenave, A. and K. Do Minh, Geoid Anomalies Above the Louisville Ridge: Possible Inferences on its Origin. J. Geophys. Res., Am. Geophys. Un., 1984.

Chan, H., M. Moody, H. Paik, and J. Parke, Development of Three-Axis Superconducting Gravity Gradiometer. Proceedings of the Seventeenth International Low Temperature Physics Conference, Univ. of MD, 1984.

Chao, B. F., Autoregressive Harmonic Analysis of the Earth's Polar Motion Using Homogeneous ILS Data. J. Geophys. Res., Vol. 88, NASA/GSFC, 1983.

Chao, B. F., On Excitation of Earth's Free Wobble and Reference Frames. NASA Tech. Memorandum 85028, NASA/GSFC, 1983.

Chao, B. F., Normal Mode Study of the Earth's Rigid Body Motions. J. Geophys. Res., Vol. 88, NASA/GSFC, 1983.

Chao, B. F., On the Maximum Entropy/Autoregressive Modeling of Time Series. NASA Tech. Memorandum 86057, NASA/GSFC, 1984.

Chi, S. and R. Reilinger, Geodetic Evidence for Subsidence due to Groundwater Withdrawl in Many Parts of the U.S. J. of Hydrology, Vol. 67, 1984.

Coates, R. J., Highly Mobile Laser Ranging Facilities of the Crustal Dynamics Project. Given at the WEGENER Meeting in Zurich, Switzerland, May 9-11, 1983.

Coates, R. J., Constraints on Future Observing Plans. Given at the WEGENER Meeting in Zurich, Switzerland, May 9-11, 1983.

Cohen, S. and M. Kramer, Crustal Deformation Associated with Viscoelastic Relaxation of a Thin Asthenosphere. EOS Transactions Am. Geophys. Un., Vol. 64, No. 858, 1983.

Cohen, S. C., Postseismic Deformation due to Viscoelastic Relaxation Following Dip-Slip Earthquakes. J. Geophys. Res., Vol. 89, 1984.

Cohen, S. C., Finite Element Viscoelastic Models. Workshop on Geodynamic Modeling, MA Inst. of Tech., 1983.

Cohen, S. C. and M. Kramer, Crustal Deformation, the Earthquake Cycle, and Models of Viscoelastic Flow in the Asthenosphere. Geophys. Journ., Vol. 75, 1984.

Cox, B. and R. Richardson, Elastic and Viscous Modeling of Plate Driving Forces for the Nazca Plate. EOS, Trans., Amer. Geophys. Union, Vol. 64, Univ. of AZ, 1983.

Dahlen, F., J. Suppe, and D. Davis, Mechanics of Fold-and-Thrust Belts and Accretionary Wedges (continued): Cohesive Coulomb Theory. J. Geophys. Res., MA Inst. of Tech., 1984.

Davidson, J. et al, Mobile VLBI Results for 1980 to 1982. EOS, Transaction, Am. Geophys. Union, Vol. 64, No. 18, Jet Prop. Lab., 1983.

Davidson, J. et al, Radio Interferometric Measurement of the JPL/Owens Valley/Goldstone Baselines Using the Mobile VLBI Systems: 1980-1982. EOS, Transactions, Am. Geophys. Union, Vol. 64, No. 45, Jet Prop. Lab., 1983.

Davis, D. and S. Solomon, True Polar Wander and Plate Driving Forces. EOS, Trans., Amer. Geophys. Un., Vol. 64, No. 843, MA Inst. of Tech., 1983.

Davis, D. M., Thin-Skinned Deformation and Plate Driving Forces Associated with Convergent Margins. Ph.D. thesis, MA Inst. of Tech., 1983.

Degnan, J., W. Kahn, and T. Englar, Centimeter Precision Airborne Laser Ranging Systems. Journ. of Surveying Engineering, Vol. 109, NASA/GSFC, 1983.

Dickey, J., Activities and Goals of the International Union of Geodesy and Geophysics/International Association of Geodesy (IUGG/IAG Special Study Group 5.98). EOS, Transactions, Am. Geophys. Un., Jet Prop. Lab., 1984.

Dickey, J. and J. Williams, Earth Rotation from Lunar Laser Ranging. Astron. and Astrophys. Supplement Series., No. 54, Jet Prop. Lab., 1983.

Dickey, J. and J. Williams, Earth Rotation: Results from Lunar Laser Ranging (LLR) and an Analysis of Lageos Polar Motion Results. EOS, Transactions, Am. Geophys. Un., Vol. 64, No. 45, Jet Prop. Lab., 1984.

Dickey, J. et al, Geophysical Application of Lunar Laser Ranging. Proceedings of the Int'l Assoc. of Geodesy Symposia, August 15-27, Jet Prop. Lab., 1984.

Dickey, J. et al, Modulation of the Lunar Tidal Acceleration. EOS, Transactions, Am. Geophys. Un., Vol. 64, No. 18, Jet Prop. Lab., 1983.

Dickey, J., J. Williams, and T. Eubanks, Earth Rotation: Results from Lunar Laser Ranging and an Intercomparison Study. Proceedings of the Int'l Assoc. of Geodesy Symposia, August 15-27, Jet Prop. Lab., 1984.

Dickey, J., J. Williams, and T. Eubanks, Earth Rotation and Polar Motion: Results from Lunar Laser Ranging Analysis and an Intercomparison Study. Proceedings of the Int'l Assoc. of Geodesy Symposia, Vol. 2, Jet Prop. Lab., 1983.

Dickey, J., X. Newhall, and J. Williams, Earth Orientation from Lunar Laser Ranging. Proceedings of the International Assoc. of Geodesy Symposia, Vol. 2, Jet Prop. Lab., 1983.

Dickey, J., X. Newhall, and J. Williams, Earth Orientation from Lunar Laser Ranging and an Error Analysis of Polar Motion Services. Proceedings of the International Assoc. of Geodesy Symposia, Vol. 2, Jet Prop. Lab., 1983.

Dickman, S. R., The Rotation of the Ocean-Solid Earth System. Journ. of Geophys. Res., Vol. 88, No. B8, American Geophys. Union, 1983.

Dickman, S. R., The Self-Consistent Dynamic Pole Tide. J. Geophys. Res., May, Am. Geophys. Union, 1984.

Douglas, B., R. Cheney, and R. Agreen, Eddy Energy of the Northwest Atlantic and Gulf of Mexico Determined from GEOS 3 Altimetry. Journ. Geophys. Res., Vol. 88, No. C14, NOAA, 1983.

Elgered, G., Water Vapor Radiometry with Applications to Radio Interferometry and Meteorology. Technical Report, No. 137, Chalmers Univ. of Tech., 1983.

Elgered, G. and P. Lundh, A Dual Channel Water Vapor Radiometer System. Research Report, No. 145, Chalmers Univ. of Tech., 1983.

Ellsworth, K., G. Schubert, and C. Sammis, Models of Viscosity Variation in the Mantle: A Case for Non-Newtonian Rheology. Geophys. J. Roy. Astron. Soc., Univ. of CA, 1984.

England, P. and G. Houseman, On the Geodynamic Setting of Kimberlite Genesis. Earth Planet. Sci. Lett., Vol. 67, Harvard Univ., 1984.

England, P. and M. Bickle, Constraints on Archaean Thermal and Tectonic Regimes. J. Geol., in press, 1984.

Eubanks, T. et al, Length of Day and the Atmospheric Angular Momentum: the Cross Validation of Earth Rotation and Meteorological Data. IEEE Digest, Catalog No. 83CH1837-4, 1983.

Eubanks, T. et al, The 1982-83 El Nino and the Earth Rotation. EOS, Transactions, Am. Geophys. Union, Jet Prop. Lab., 1984.

Eubanks, T. et al, The Earth's Polar Motion and the Atmospheric Angular Momentum. EOS, Transactions, Am. Geophys. Un., Vol. 64, No. 45, Jet Prop. Lab., 1984.

Eubanks, T., J. Dickey, and J. Steppe, The Southern Oscillation and Changes in the Length of Day. EOS, Transactions, Am. Geophys. Un., Jet Prop. Lab., 1984.

Eubanks, T., J. Dickey, and J. Steppe, The Geophysical Significance of Systematic Errors in the Earth's Angular Momentum Budget. Proceedings of the Int'l Assoc. of Geodesy Symposia, August 15-27, Jet Prop. Lab., 1984.

Eubanks, T., J. Dickey, and J. Steppe, A Spectral Analysis of the Earth's Angular Momentum Budget: Geophysical Implications. EOS, Transactions, Am. Geophys. Un., Vol. 64, No. 18, Jet Prop. Lab., 1983.

Eubanks, T., J. Steppe, and M. Spieth, VLBI Earth Orientation Results from TEMPO Work at JPL. Jet Prop. Lab., 1984.

Farrell, W., and J. Wang, State Space Design of a Digitally Controlled Gravity Meter. Final Technical Report, S-Cubed, November, 1983.

Final Report of Magsat Project: Analysis of Magsat and Surface data of the Indian Region. Survey of India, 1982.

Fleitout, L. and C. Froidevaux, Tectonics and Topography for a Lithosphere Containing Density Heterogeneities. Univ. of Paris, 1983.

Fleitout, L. and C. Froidevaux, Tectonic Stresses in the Lithosphere. Laboratoire de Geophysique et Geodynamique Interne, 1984.

Fuligni, F. and M. Grosso, Research Relative to the Development of a Cryogenic Microwave Cavity Gradiometer for Orbital Use. Semiannual Report on NASA Grant NAG5-338, December, SAO, Harvard - Smithsonian Cntr. for Astrophys., 1983.

Gambis, D., Possibility of Detecting the Diurnal Forced Nutation by the Study of Artificial Satellites Orbits. Centre d'Etudes et de Recherches, 1983.

Gambis, D., Compression of LAGEOS Laser Data. Centre d'Etudes et de Recherches, 1983.

Gaposchkin, E. and S. Zerbini, Determination of Interstation Baselines by Satellite Laser Ranging Scalar Translocation. Annales Geophysicae, Vol. 1, Univ. of Bologna, 1983.

Grange, F. et al, The Configuration of the Seismic Zone and the Downgoing Slab in Southern Peru. Geophys. Res. Lett., Vol. 11, Am. Geophys. Un., 1984.

Grange, F. et al, Microearthquake Seismicity and Fault Plane Solutions in Southern Peru and their Tectonic Implications. In preparation, MA Inst. of Tech., 1984.

Gullahorn, G. E., Investigation of Dynamic Noise Affecting Geodynamics Information in a Tethered Subsatellite. Semiannual Report on NASA Grant NAG5-325, January, SAO, Harvard - Smithsonian Cntr. for Astrophys., 1984.

Gullahorn, G. E., F. Fuligni, and M. Grossi, Feasibility of Gravity Gradient Measurements from a Tethered Subsatellite Platform. NASA Geodynamics Conference, AGU Spring Meeting, Harvard - Smithsonian Cntr. for Astrophys., 1984.

Hager, B., Subducted Slabs and the Geoid: Constraints on Mantle Rheology and Flow. J. Geophys. Res., CA Inst. of Tech., 1984.

Hager, B., Global Isostatic Geoid Anomalies for Plate and Boundary Layer Models of the Lithosphere. Earth Planet. Sci. Lett., Vol. 63, CA Inst. of Tech., 1983.

Hager, B., Slab Dip and Length and the Dynamics of Back-Arc Opening and Closing. EOS, Trans., Amer. Geophys. Union, Vol. 64, CA Inst. of Tech., 1984.

Hager, B., R. O'Connell, and A. Raefsky, Subduction, Back-Arc Spreading and Global Mantle Flow. Tectonophysics, Vol. 99, CA Inst. of Tech., 1983.

Harrison, C., Magnetic Anomalies. Am. Geophys. Un., Vol. 21, No. 3, University of Miami, 1983.

Harvey, B. et al, Results of the Australian Geodetic VLBI Experiment. Telecomm. and Data Acquisitions Rep., Vols. 42-75, Jet Prop. Lab., 1983.

Harvey, B. et al, Results of the Australian Geodetic VLBI Experiment. Australian Journ. of Geodesy, Vol. 38, 1983.

Hastings, D. A., An Updated Bouguer Anomaly Map of South-Central West Africa. Technicolor Govt. Services, Inc., 1982.

Hauck, H., The Program ORBDOP (Extended GEODOP). Institut fuer Angewandte Geodaesie, 1983.

Hauck, H. and K. Herzberger, Ein Bahnvorhersageprogramm fuer Wettzell. Institut fuer Angewandte Geodaesie, 1983.

Haxby, W. et al, Digital Images of Combined Oceanic and Continental Data Sets and their use in Tectonic Studies. EOS, Vol. 64, No. 52, Columbia Univ., 1983.

Hermance, J., Electromagnetic Induction by Finite Wave-Number Source Fields in 2-D Lateral Heterogeneities; The Traverse Electric Mode. Geophys. J. R. Astr. Soc., in press, 1984.

Hermance, J., Electomagnetic Induction Studies. Geophys. and Space Phys., Vol. 21, Brown Univ., 1983.

Hermance, J., Internal/External and Ionospheric/Magnetospheric Current Systems. IUGG General Assembly, 1983.

Hermance, J., Global and Regional Electromagnetic Induction Effects in MAGSAT Satellite Data. Brown Univ., 1984.

Hermance, J., Regionalization of Global Electromagnetic Induction Data: A Theoretical Model. Phys. of the Earth and Planet. Int., Vol. 27, Brown Univ., 1982.

Hermance, J., The Internal Contribution to Sq Current Systems. IUGG General Assembly, 1983.

Hermance, J., Are There Electromagnetic Induction Effects in MAGSAT Data? Some Model Simulations. Geophys. Res. Letts., Vol. 9, Am. Geophys. Un., 1982.

Hermance, J. and M. Rossen, Global Induction Studies Using MAGSAT Data. IUGG General Assembly, 1983.

Hermance, J. and M. Rossen, Global and Regional Electromagnetic Induction Effects in MAGSAT Satellite Data. Journ. Geophys. Res., Brown Univ., 1984.

Hermance, J. F., Electromagnetic Induction Studies, IUGG Quadrennial Report. Rev. Geophys. and Space Phys., Vol. 21, Brown Univ., 1983.

Herring, T. et al, Determination of Tidal Parameters from VLBI Observations. E. Schweizerbart'sche Verlagsbuchhandlung, 1983.

Hinze, W, R. Oliver, and R. von Frese, Euro-African MAGSAT Anomaly-Tectonic Observations. IUGG XVIII General Assembly, Programme and Abstracts, Vol. 2, 1983.

Hoepfl, R. and N. Brandl, Ein Neues Empfaengerkonzept fuer das Laserentfernungsmessystem. Institut fuer Angewandte Geodaesie, 1983.

Humphreys, E., R. Clayton, and B. Hager, A Tomographic Image of Mantle Structure Beneath Southern California. Geophys. Res. Lett., CA Inst. of Tech., 1984.

Ihnen, S., and J. Whitcomb, The Indian Ocean Gravity Low: Evidence for an Isostatically Uncompensated Depression in the Upper Mantle. Geophys. Res. Ltrs., Vol. 10, No. 6, Univ. of CO/NOAA, 1983.

Ivins, E., G. Lyzenga, and S. Saunders, Stress Patterns in an Interplate Shear Zone: An Effective Anistropic Model and Implications for the Transverse Ranges, California. JPL Geodesy and Geophys. Preprint, No. 110, Jet Prop. Lab., 1984.

Kahn, W., J. Degnan, and T. Englar, The Airborne Laser Ranging System: Its Capabilities and Applications. Bull. Geod., Vol. 57, NASA/GSFC, 1983.

Kanamori, H., J. Given, and T. Lay, Analysis of Seismic Body Waves Excited by the Mount St. Helens Eruption of May 18, 1980. Am. Geophys. Union, CA Inst. of Tech., 1984.

Kaula, W., Minimum Upper Mantle Temperature Variations Consistent with Observed Heat Flow and Plate Velocities. J. Geophys. Res., Vol. 88, No. 10, Univ. of CA, 1983.

Kaula, W., Inference of Variations in the Gravity Field from Satellite-to-Satellite Range-Data. J. Geophys. Res., Vol. 88, Univ. of CA, 1983.

Kaula, W. and D. Williams, Transformation of Velocity Fields on a Spherical Suface. Geodesy in Transition, Univ. of CA, 1983.

Khan, W., J. Degan, and T. Englar, The Airborne Laser Ranging System, Its Capabilities and Applications. Bulletin Geodesique, Vol. 57, NASA/GSFC, 1983.

LaBrecque, J. and C. Raymond, Seafloor Spreading Anomalies in the MAGSAT Field of the North Atlantic. Submitted to JGR, Columbia Univ., 1984.

LaBrecque, J. and S. Cande, Intermediate Wavelength Magnetic Anomalies Over the Central Pacific. submitted to JGR, Columbia Univ., 1984.

LaBrecque, J., S. Cande, and R. Jarrard, The Intermediate Wavelength Magnetic Anomaly Field of the North Pacific and Possible Source Distributions. submitted to JGR, Columbia Univ., 1984.

Lagios, V. and M. Wyss, Vertical Tectonic Stability Over the Last 15 Years, Estimated from Annual Mean Sea Levels in Greece. Pure and Appl. Geophys., Univ. of CO, 1984.

Lambeck, K., Satellite Geophysics. Terra Cognita, 3, Australian Nat. Univ., 1983.

Lambeck, K., Hula Dancers, Walter Munk and the Rotation of the Earth. Australian Nat. Univ., 1983.

Lambeck, K., and R. Coleman, The Earth's Shape and Gravity Field: A Report of Progress from 1958 to 1982. Geophys. J. R. Astr. Soc., Vol. 74, Australian Nat. Obs., 1983.

Lambeck, K., and S. Nakiboglu, Long Period Love Numbers and their Frequency Dependence due to Dispersion Effects. Geophys. Res. Lett., Vol. 10, Australian Nat. Obs., 1983.

Lambeck, K., C. Penney, S. Nakiboglu, and R. Coleman, Subsidence and Flexure along the Pratt-Welder Seamount Chain. J. Geodynamics, Vol. 1, Australian Nat. Obs., 1983.

Langel, R. and R. Estes, The Near-Earth Magnetic Field at 198 Determined from MAGSAT Data. Business and Technological Systems, Inc., 1984.

Langel, R. and R. Estes, Large-Scale, Near-Earth Magnetic Fields from External Sources and the Corresponding Induced Internal Field. Business and Technological Systems, Inc., 1984.

Larsen, S. and R. Reilinger, Recent Measurements of Crustal Deformation Related to the Socorro Magma Body. New Mexico Geological Society Guidebook, No. 34, 1983.

Lelgemann, D., Application of Laser Ranging to Geodynamics. Institut fuer Angewandte Geodaesie, 1983.

Loo, H. Y., Three-Dimensional Numerical Analysis of Continental Margin Basin Deformation Related to Large Earthquake Development. To appear in Proceedings of the 27th International Geological Congress, MA Inst. of Tech., 1984.

Loper, D., Structure of the Inner Core Boundary. Geophys. Astrophy. Fluid Dyn., Vol. 25, 1983.

Loper, D. and F. Stacey, The Dynamical and Thermal Structure of Deep Mantle Plumes. Phys. of the Earth and Planet. Interiors, 1983.

Lyzenga, G. and K. Wallace, Southern California Strain Rates Derived form VLBI Observations. EOS, Transactions, Am. Geophys. Union, Vol. 64, No. 18, Jet Prop. Lab., 1983.

Lyzenga, G., K. Wallace, and J. Fanselow, Modeling of the Surface Static Displacements and Fault Plane Slip for the 1979 Imperial Valley Earthquake. JPL Geodesy and Geophys. Preprint, No. 107, Jet Prop. Lab., 1984.

Lyzenga, G., K. Wallace, and J. Fanselow, Strain Changes from 1980 through 1982 on the Southern California Mobile VLBI Net: Results and Implications. EOS, Transactions, Am. Geophys. Union, Vol. 64, No. 45, Jet Prop. Lab., 1983.

Marsh, B. D., J. Marsh, and R. Williamson, On Gravity from SST, Geoid from SEASAT, and Plate Age and Fracture Zones in the Pacific. Journ. Geophys. Res., Johns Hopkins Univ., 1984.

Marsh, J., F. Lerch, R. Williamson, Geodynamic and Geodetic Parameter Estimation from Starlette Laser Tracking Data. J. Geophys. Res., NASA/GSFC, 1984.

Martinec, Z., and K. Pec, Spherical Harmonic Coefficients of the External Equipotential Surface Inferred from Stokes' Constants. Proc. Int. Symp., Charles Univ., 1983.

Masters, E., A. Stolz, and B. Hirsch, A Method of Filtering and Compressing LAGEOS Range Data. Bulletin Geodesique, Vol. 57, 1983.

Mazzega, P., The M2 Ocean Tide Recovered from SEASAT Altimetry in the Indian Ocean. Nature, Vol. 302, 1983.

McAdoo, D. and C. Martin, SEASAT Observations of Lithospheric Flexure Seaward of Trenches. J. Geophys. Res., in press, 1984.

McLeod, M. G., Crustal Geomagnetic Field: Two-Dimensional Intermediate-Wavelength Spatial Power Spectra. Phys. Earth Planet. Interiors, Vol. 31, Univ. of CA - Los Angeles, 1983.

McLeod, M. G., Optimal Processing of Satellite Derived Magnetic Anomaly Data. Phys. Earth Planet. Interiors, Vol. 31, Univ. of CA - Los Angeles, 1983.

Mead, G., Significant Accomplishments and Work, in Progress as Reported by Crustal Dynamics Investigators. Vol. 3, NASA/GSFC, October 1983 - February 1984.

Mead, G. D, et al, Significant Accomplishments and Work in Progress as Reported by Crustal Dynamics Investigators. July - February, NASA/GSFC, 1982-1983.

Mead, G. D., et al, Significant Accomplishments and Work in Progress as Reported by Crustal Dynamics Investigators. March - September, NASA/GSFC, 1983.

Ming, Z., G. Zheng-nian, S. Guo-xuan, On the Influence of Turbulence in the Core of the Earth Upon the Annual Term in Polar Motion. Shanghai Obs., 1983.

Minster, J., and T. Jordan, Vector Constraints on Quaternary Deformation of the Western United States East and West of the San Andreas Fault. Science Horizons, Inc./Scripps Inst. of Oceanography, 1984.

Moody, M., H. Chan, H. Paik, and C. Stephens, A Superconducting Penetration Depth Thermometer. Proceedings of the Seventeenth International Low Temperature Physics Conference, Univ. of MD, 1984.

Moon, W. and R. Tang, On Hydrodynamic Correction of SEASAT-ALT Data. Marine Geodesy, Univ. of Manitoba, 1984.

Mori, A, B. Hager, and A. Raefsky, The Evolution of Large-Scale Temperature Variation in a Convecting System: Application to the Evolution of Long-Wavelength Temperature and Geoid Anomalies in the Earth. EOS, Trans., Amer. Geophys. Union, Vol. 64, CA Inst. of Tech., 1984.

Mueller, I., Report of the IAG/IAU Joint Working Group on the Establishment and Maintenance of a Conventional Terrestrial Reference System (COTES). Proc. of IAG Symposia, XVIII Gen. Assembly, Vol. 2, Ohio State Univ., 1983.

Nakanishi, I., and D. Anderson, Measurements of Mantle Wave Velocities and Inversion for Lateral Heterogeneity and Anisotropy; Part I: Analysis of Great Circle Phase Velocities. Journal of Geophys. Res., Vol. 88, CA Inst. of Tech., 1983.

Nakanishi, I., and D. Anderson, Measurements of Mantle Wave Velocities and Inversion for Lateral Heterogeneity and Anisotropy; Part II: Analysis by the Single-Station Method. Geophys. Journal of the Royal Astron. Soc., CA Inst. of Tech., 1983.

Nakanishi, I., and D. Anderson, Aspherical Heterogeneity of the Mantle From Phase Velocities of Mantle Waves. Nature, CA Inst. of Tech., 1984.

Nataf, H., B. Hager, and R. Scott, Convection Experiments in a Centrifuge and the Generation of Plumes in a Very Viscous Fluid. CA Inst. of Tech., 1983.

Nataf, H., B. Hager, and R. Scott, Hotspots in a Very Viscous Fluid: Convection Experiments in a Centrifuge. Annales Geophysicae, CA Inst. of Tech., 1983.

Nataf, H., I. Nakanishi, and D. Anderson, Anisotropy and Shear-Velocity Heterogeneities in the Upper Mantle. Geophys. Res. Lett., Vol. 11, No. 2, Am. Geophys. Un., 1984.

Negi, J., P. Agarwal, and N. Thakur, Vertical Component Magsat Anomalies and Indian Tectonic Boundaries. Survey of India, 1983.

Noomen, R., Aerodynamic Drag and Geomagnetic Perturbations: Their Modeling and Effect on Spacecraft Dynamics. Technical Thesis, Dept. of Aerospace Eng., Delft Univ. of Tech., 1983.

O'Connell, R. and B. Hager, Estimates of Driving Forces and Stresses for Lithospheric Plates. EOS, Trans. Amer. Geophys. Union, Vol. 64, CA Inst. of Tech., 1984.

Oliver, R., Satellite Magnetic Anomalies of Africa and Europe. Geophys., Vol. 48, 1983.

Oliver, R., W. Hinze, and R. von Frese, Reduced to Pole Long-Wavelength Magnetic Anomalies of Africa and Europe. Am. Geophys. Un. Trans., Vol. 64, Am. Geophys. Un., 1983.

Pavlis, E. and I. Mueller, The Effect of Earth Orientation Errors in Baseline Determination. Bulletin Geodesique, Vol. 57, No. 3, Ohio State Univ., 1983.

Pec, K. and Z. Martinec, Expansion of Geoid Heights Over a Triaxial Earth's Ellipsoid into a Spherical Harmonic Series. Studia Geoph. et Geod., Vol. 27, Charles Univ., 1983.

Pec, K., and Z. Martinec, Expansion of Geoid Heights into a Spherical Harmonic Series. Studia Geoph. et Geod., Vol. 26, Charles Univ., 1982.

Piersma, H., K. Wakker, and B. Ambrosius, Numerical Experiments on the Estimation of Relative Station Station Positions Using Single Passes of LAEGOS and STARLETTE Laser Range Observations. Memorandum M-456, Delft Univ. of Tech., 1983.

Piuzzi, A., A. Souriau and M. Souriau, Absolute Movements in the Djibouti Area in Relation with Seismic Activity. EOS, Trans., Vol. 64, 1983.

Puell, H. and P. Wilson, Aufbau und Funktionsweise des Nd: Yap-Lasers im Modularen Transportablen Laserentfernungsmessystem. Institut fuer Angewandte Geodaesie, 1983.

Rabinowicz, M., B. Lago, and M. Souriau, Large Scale Gravity Profiles Across Subduction Zones. Geophys. J. R. Astron. Soc., Vol. 73, 1983.

Rabinowicz, M., B. Lago, and M. Souriau, Landward Flow in the Upper Mantle: Effcts of the Heat Sink and Vscous Coupling of the Sinking Slab. Earth Planet. Sc. Lett., Vol. 63, 1983.

Rajbanshi, K. et al, Isolating the Components of Crustal Origin in Satellite Magnetic Measurements. Indian Inst. of Geomagnetism, 1983.

Rajbanshi, K. et al, Comparison of MAGSAT Anomalies over Indian Region with POGO and Ground Data. Indian Inst. of Geomagnetism, 1983.

Rapp, R., Problems in the Development of Improved High Degree Spherical Harmonic Expansions of the Gravity Field. OH State Univ., 1984.

Rapp, R., The Development of the January 1983 1^{o}x 1^{o} Mean Free-Air Anomaly Data Tape. Internal Report of the Department of Geodetic Science and Surveying, OH State Univ., 1983.

Rapp, R., and C. Wichiencharoen, A Comparison of Satellite Doppler and Gravimetric Geoid Undulations Considering Terrain-Corrected Gravity Data. Journ. of Geophys. Res., Vol. 89, No. B2, Ohio State Univ., 1984.

Rastogi, R., Sixth Progress Report on MAGSAT for Geomagnetic Studies over Indian region. Indian Inst. of Geomagnetism, 1984.

Rastogi, R., Fifth Progress Report on MAGSAT for Geomagnetic Studies over Indian region. Indian Inst. of Geomagnetism, 1983.

Reding L. and R. Richardson, Ridge Push Forces: How Important as a Driving Force?. EOS, Trans., Amer. Geophys. Un., Vol. 64, Univ. of AZ, 1983.

Reigber, C., An Improved GRIM3 Earth Gravity Model (GRIM3B). Proceedings of the IAG Symposium C, XVIIIth IUGG General Assembly, 1983.

Reigber, C., G. Balmino, and B. Moynot, The GRIM 3 Earth Gravity Field Model. Manusc. Geodaet., Vol. 4, 1983.

Reilinger, R., Coseismic and Postseismic Vertical Movements Associated with the 1940, M7.1 Imperial Valley, California Earthquake. J. of Geophys. Res., in press, 1984.

Reilinger, R., Geodetic Evidence for Aseismic Slip on the Brawley Fault, Southern California. EOS, Trans., Am. Geophys. Union, Vol. 64, Am. Geophys. Un., 1983.

Reilinger, R., M. Bevis, and G. Jurkowski, Tilt from Releveling: An Overview of the U.S. Data Base. Tectonophysics, in press, 1984.

Reinhardt, V., Determining the Gravity Potential from Low-Low Satellite Tracking Data Utilizing a Complex Spherical Harmonic Expansion of the Potential. Bendix Field Engineering Corp., 1984.

Reinhart, E., Global Positioning Systems - Present Status of Technology and Future Trends. Institut fuer Angewandte Geodaesie, 1983.

Resch, G. M., Water Vapor Radiometry in Geodetic Applications. TDA Tech. Development, 1983.

Resch, G. M., Inversion Algorithms for Water Vapor Radiometers Operating at 20.7 and 31.4 GHz. TDA Prog. Rep. 42-76, TDA Tech. Development, 1983.

Resch, G. M., Another Look at the Optimum Frequencies for a Water Vapor Radiometer. TDA Prog. Rep. 42-76, TDA Tech. Development, 1983.

Resch, G., D. Hogg, and P. Napier, Radiometric Correction of Atmospheric Path Length Fluctuations in Interferometric Experiments. Radio Science, Vol. 19, No. 1, TDA Tech. Development, 1984.

Ricard, Y., C. Froidevaux, and J. Hermance, Model Heat Flow and Magnetotellurics for the San Andreas and Oceanic Transform Faults. Annales Geophysicae, Vol. 1, Gauthier-Villars, 1983.

Richards, M. A., and B. Hager, Geoid Anomalies in a Dynamic Earth. Journal of Geophys. Res., CA Inst. of Tech., 1983.

Richards, M. and B. Hager, Geoid Anomalies in a Dynamic Earth. J. Geophys. Res., CA Inst. of Tech., 1984.

Richardson, R., Inversion for the Driving Forces of Plate Tectonics. IEEE Int'l Geosci. and Remote Sensing Symp., II, Univ. of AZ, 1983.

Richardson, R. and B. Cox, Evolution of Oceanic Lithosphere: A Driving Force Study of Nazca Plate. J. Geophys. Res., Univ. of AZ, 1984.

Rizos, C. and P. Wilson, Simulations on the Application of Satellite Laser Tracking for Geodynamical Studies in the Eastern Mediterranean. Institut fuer Angewandte Geodaesie, 1983.

Robertson, D. S., The Astrometric Possibilities of VLBI. Proceedings of the IAU Symposium 109, D. Reidel Co., 1984.

Robertson, D. S. et al, Comparison of Earth Rotation as Inferred from Radio Interferometric, Laser Ranging and Astrometric Observations. Nature, Vol. 302, No. 5908, Macmillan Journals, Ltd., 1983.

Rogers, A. E., Very-Long Baseline Radio Interferometry: The Mark II System for Geodesy, Astrometry, and Aperture Synthesis. Science, Vol. 219, Am. Assoc. for the Advancement of Sci., 1983.

Rogers, A. E. et al, Very-Long Baseline Radio Interferometry: The Mark III System for Geodesy, Astrometry, and Aperture Synthesis. Science, Vol. 219, Am. Assoc. for the Advancement of Sci., 1983.

Rosen, R. and D. Salstein, The 1982-83 El Nino, the Southern Oscillation, and Changes in the Length of Day. Science, Jet Prop. Lab., 1983.

Rosen, R. and D. Salstein, Variations in Atmospheric Angular Momentum on Global and Regional Scales and the Length of Day. J. Geophys. Res., Vol. 88, Atmos. and Env. Res., 1983.

Rosen, R. et al, An El Nino Signal in Atmospheric Angular Momentum and Earth Rotation. Science, Atmos. and Env. Res., 1983.

Rossen, M. and J. Hermance, Identifying Origin of Instabilities of Induction Parameter Estimations from Sq Data. EOS, Vol. 64, 1983.

Royden, H., R. Miller, and R. Buennagel, Comparison of NAVSTAR Satellite L-Band Ionospheric Calibrations with Faraday-Rotation Measurements. Radio Science, May-June issue, Jet Prop. Lab., 1984.

Rubincam, D., Postglacial Rebound Observed by LAGEOS and the Effective Viscosity of the Lower Mantle. Journ. of Geophys. Res., Vol. 89, No. B2, Am. Geophys. Un., 1984.

Ruff, L. and A. Cazenave, Geoid Anomalies over the Macquarie Ridge Complex Indicate an Unexpected Subducted Slab. EOS, Trans., Vol. 64, 1983.

Saburi, Y. et al, Development of K-3 VLBI System in RRL for US-Japan Joint Experiment. Fifth Ann. NASA Geod. Prog. Conf. and Crustal Dyn. Proj. Review, NASA Headquarters, 1982.

Saburi, Y. et al, The First US-Japan VLBI Test Observation by use of K-3 System at the Radio Research Laboratories. Journ. of the Radio Research Lab., Vol. 31, No. 132, 1984.

Sauber, J., R. Reilinger, and M. Toksoz, Postseismic Viscoelastic Relaxation Associated with the 1940 Imperial Valley Earthquake. EOS, Trans., Amer. Geophys. Un., Vol. 65, MA Inst. of Tech., 1984.

Schaffrin, B., Model Choice and Adjustment Techniques in the Presence of Prior Information. Dept. of Geodetic Sci. and Surveying Rep. 351, Ohio State Univ., 1983.

Schneider, M. et al, VLBI in Wettzell. CSTG Buletin, No. 5, Institut fuer Angewandte Geodaesie, 1983.

Schubert, G., and Z. Garfunkel, Mantle Upwelling in the Dead Sea and Salton Trough-Gulf of California Leaky Transforms. Ann. Geophys., Univ. of CA, 1984.

Scott, D., D. Stevenson, and B. Hager, Melt Migration Using Darcy's Law Generalized to Include Matrix Deformation. EOS, Trans., Amer. Geophys. Union, Vol. 64, CA Inst. of Tech., 1984.

Shapiro, I., Use of Space Techniques for Geodesy. MA Inst. of Tech., 1983.

Sheng-Yuan, Z. and I. Mueller, Effects of Adopting New Precession Nutation and Equinox Correction on the Terrestrial Reference Frame. Bulletin Geodesique, Vol. 57, No. 1, Ohio State Univ., 1983.

Shoberg, L. E., The Fennoscandian Land Uplift Spectrum and its Correlation with Gravity. Univ. of Uppsala, 1983.

Singh, B. et al, Comparison of MAGSAT-POGO-Ground Magnetic Anomalies Over Indian Region. Journ. of Geophys. Res., Indian Inst. of Geomagnetism, 1983.

Singh, B. et al, On Utility of Space-Borne Vector Measurements in Crustal Studies. Phys. of Earth and Planet. Interiors, Indian Inst. of Geomagnetism, 1983.

Singh, B., A. Agarwal, and R. Rastogi, A Study on Isolation of Components of Crustal and External Field Origin in MAGSAT Scaler and Vector Data. Journ. of Geophys. Research, Indian Inst. of Geomagnetism, 1983.

Slade, M. et al, Stress Field and Seismic Release Release in the Parkfield-Coalinga, California Region. EOS, Trans., Amer. Geophys. Union, Vol. 64, CA Inst. of Tech., 1984.

Smalley, R., J. Liu, and S. Solla, A Renormalization Group Model for the Stick-Slip Behavior of Faults. J. Geophys. Res., Cornell Univ., 1984.

Soltau, G., Terrestrial Supplementary Geodetic Survey at the Stations of a Global Geodetic Network. Institut fuer Angewandte Geodaesie, 1983.

Soltau, G., GPS-Macrometer Test at the Geodetic Observatory at Wettzell, FR Germany. Institut fuer Angewandte Geodaesie, 1983.

Soltau, G. and L. Amberg, Testmessungen mit dem Macrometer im Kontrollnetz Wettzell. Institut fuer Angewandte Geodaesie, 1983.

Souriau, A., Geoid Anomalies Over Gorringe Ridge North Atlantic Ocean. Earth Plan. Sc. Letts., 1984.

Souriau, A. and M. Souriau, A Filtering Procedure of Great Circle Data. Ann. Geophys., Vol. 1, 1983.

Souriau, A. and M. Souriau, Test of Tectonic Models by Great Circle Data. Geophys. J. R. Astr. Soc., Vol. 73, 1983.

Souriau, M., Loading of a Partly Viscous Continental Crust: Implications for Isostasy. EOS, Trans., Vol. 64, 1983.

Spohn, T., and G. Schubert, Convective Thinning of the Lithosphere: A Mechanism for Rifting and Mid-Plate Volcanism on Earth, Venus, and Mars. Tectonophysics, 94, Univ. of CA, 1983.

Srinivasan, S. et al, Analysis of Data from Overlapping Passes over Indian Region. Indian Inst. of Geomagnetism, 1983.

Steinberg, D. and S. Dickman, Comments on the Equilibrium Pole Tide. Geophys. Res. Letts., 1984.

Stolz, A. and E. Masters, Satellite Laser Range Measurements of the 3200 km Orroral-Yarragadee Baseline. The Australian Surveyor, Vol. 31, 1983.

Stolz, A. and K. Lambeck, Geodetic Monitoring of Tectonic Deformation in the Australian Region. Journ. of the Geological Society, Vol. 30, 1983.

Stolz, A. et al, Australian Baselines Measured by Radiointerferometry. The Australian Surveyor, Vol. 31, 1983.

Stolz, A. et al, Geodesy in Australia: National Report for 1979-83. Australian Academy of Sci. Report, July, 1983.

Stolz, A., E. Masters, and B. Harvey, Use of Space Techniques to Measure Crustal Motions in the Australian Region. Bulletin of the Royal Soc. of New Zealand, in press.

Stolz, A., et al, Geodetic Surveying with Quasar Radio Interferometry. The Australian Surveyor, Vol. 31, No. 5, University of New South Wales, 1983.

Suarez, G. et al, Tectonic Deformation of the Andes and the Configuration of the Subducted Slab in Central Peru: Results from a Microseismic Experiment. Geophys. J. Roy. Astron. Soc., 1983.

Suarez, G., P. Molnar, and B. Burchfiel, Seismicity, Fault Plane Solutions, Depth of Faulting, and Active Tectonics of the Andes of Peru, Ecuador, and Southern Colombia. J. Geophys. Res., Vol. 88, Am. Geophys. Un., 1983.

Tanimoto, T., A Simple Derivation of the Formula to Calculate Synthetic Long-Period Seismograms in a Heterogeneous Earth by Normal Mode Summation. CA Inst. of Tech., 1984.

Tanimoto, T., Waveform Inverson of Mantle Love Waves: the Born Seismogram Approach. Geophys. J. R. Astr. Soc., in press, 1984.

Tanimoto, T. and D. Anderson, Mapping Convection in the Mantle. Matrix Typography, CA Inst. of Tech., 1983.

Thomas, H., Petrologic Model of the Northern Mississippi Embayment Based on Satellite Magnetic and Ground Based Geophysical Data. Earth and Planet. Sci. Letters, NASA/GSFC, 1983.

Turcotte, D. L., Mechanisms of Crustal Deformation. J. Geol. Soc., 140, Cornell Univ., 1983.

Turcotte, D., J. Liu, F. Kulhawy, The Role of an Intracrustal Asthenosphere on the Behavior of Major Strike-Slip Faults. J. Geophys. Res., Cornell Univ., 1984.

van Gelder, B. and L. Aardoom, SLR Network Designs in View of Reliable Detection of Plate Kinematics in the East Mediterranean. Dept. of Geodesy Report, No. 82.2, Delft Univ. of Tech., 1982.

Vassiliou, M. and B. Hager, The State of Stress in Subconducting Slabs as Revealed by Earthquakes Analysed by Moment Tensor Inversion. Planet. Sci. Lett., CA Inst. of Tech., 1984.

Vassiliou, M., B. Hager, and A. Raifsky, The Distribution of Earthquakes with Depth and Stress in Subducting Slabs. J. Geodyn., Vol. 1, CA Inst. of Tech., 1984.

Vermaat, E., Site Selection for MTLRS. Dept. of Geodesy Report, No. 83.2, Delft Univ. of Tech., 1983.

Vermaat, E. and B. van Gelder, On the Eccentricity of MTLRS. Reports on the Dept. of Geodesy, Mathematical and Physical Geodesy, No. 83.4, Delft Univ. of Tech., 1984.

von Frese, R., Long-Wavelength Magnetic and Gravity Anomaly Correlations of Africa and Europe. IAGA Bulletin, Vol. 47, 1983.

von Frese, R., Regional Geophysical Analysis of Mississippi Embayment Crustal Structure,. 112th Ann. Mtng. of the Soc. of Mining Engineers, Technical Prog. and Abstracts, 1983.

von Frese, R., Regional Anomalies of the Mississippi River Aulacogen. Geophysics, Vol. 48, 1983.

Wakker, K. and B. Ambrosius, ERS-1 Orbit Determination from Laser TRANET and PRARE Tracking Data. Memorandum M-464, Delft Univ. of Tech., 1983.

Wakker, K., and B. Ambrosius, Orbit Determination of LAGEOS and STARLETTE and the Position Estimation of the European Laser Tracking Stations at Kootwijk, Wettzell, Grasse and Metsahovi. Memorandum M-455, Delft Univ. of Tech., 1983.

Wakker, K., B. Ambrosius and L. Aardoom, Precise Orbit Determination for ERS-1. ESA Contract Report, Contract 5227/82/D/IM(SC), Delft Univ. of Tech., 1983.

Wakker, K., B. Ambrosius and T. van der Ploeg, SEASAT Orbit Determination from Laser Range Observations. Satellite Microwave Remote Sensing, Delft Univ. of Tech., 1983.

Wakker, K., B. Ambrosius, and H. Piersma, Analysis of POPSAT Gravity Model Errors. Final Report, ESTEC Contract 5512/83/NL/MS, Delft Univ. of Tech., 1983.

Wasch, J., Choix D'un Modele de Rayonnement K'albedo Terrestre. Calcul Pratique de son Effet sur la Trajectoire D'un Satellite. Congres Ermioni, September, in press, 1982.

Wells, W. C., ed., Spaceborne Gravity Gradiomenters. NASA Conference Publication 2305, NASA, 1983.

Wichiencharoen, C., A Comparison of Gravimetric Unidulations Computed by the Modified Molodensky Truncation Method and the Method of Least Squares Spectral Combination by Optimal Integral Kernels. Bulletin Geodesique, OH State Univ., 1984.

Williams, J. et al, Unification of Celestial and Terrestrial Coordinate Systems. Proceedings of the Int'l Assoc. of Geodesy Symposia, August 15-27, Jet Prop. Lab., 1984.

Williams, J., J. Dickey, W. Melbourne, and E. Standish, Unification of Celestial and Terrestrial Coordinate Systems. Proceedings of the Int'l Assoc. of Geodesy Symposia, Vol. 2, Jet Prop. Lab., 1983.

Williamson, R., D. Christodoulidis, and J. Marsh, Ocean Tidal Parameter Recovery From Starlette Laser Data. J. Geophys. Res., NASA/GSFC, 1984.

Wilson, P., Das Mobile Laserentfernungsmessystem und sein geplanter Einsatz im Rahmen der Internationalen Arbeiten zur Geodynamik. Institut fuer Angewandte Geodaesie, 1983.

Wilson, P., Regional Activities: Western, Central and Eastern Mediterranean Areas. Institut fuer Angewandte Geodaesie, 1983.

Wilson, P., Crustal Dynamics of the Eastern Mediterranean. CSTG Bulletin, No. 5, Institut fuer Angewandte Geodaesie, 1983.

Wilson, P., A Modular Transportable Laser Ranging System. CSTG Buletin, No. 5, Institut fuer Angewandte Geodaesie, 1983.

Wilson, P., Ueber die Nachfuehrungseigenschaften der Montierung des Mobilen Laserentfernungsmessystems. Institut fuer Angewandte Geodaesie, 1983.

Wilson, P. and L. Aardoom, SEASAT Tracking Over Europe. Ellis Horwook Ltd. Publ., 1983.

Wong, K. and M. Wyss, Cluster of Foreshocks and Preshocks in the Circum-Aegean Region. Earthq. Prediction Res., Univ. of CO, 1983.

Yanick, R., F. Luce, and C. Froidevaux, Geoid Heights and Lithospheric Stresses for a Dynamic Earth. Univ. of Paris, 1983.

Yoder, C. et al, Secular Variation of Earth's Gravitational Harmonic J_2 from LAEGOS and the Nontidal Acceleration of Earth's Rotation. Nature, Vol. 303, No. 5920, Jet Prop. Lab., 1983.

Young, L., D. Spitzmesser, L. Buennagel, SERIES, A Novel Use of GPS Satellites for Positioning. Proceedings of IAG/IUGG Symposium on Point Positioning in Marine Geodesy, Jet Prop. Lab., 1983.

Zhang, J. and B. Hager, A Critical Assessment of Viscous Models of Trench Topography and Subduction Zone Flow. EOS, Trans. Amer. Geophys. Union, Vol. 64, CA Inst. of Tech., 1984.

1. Report No.	2. Government Accession No.	3. Recipient's Catalog No.
NASA TM-87359		

4. Title and Subtitle	5. Report Date
NASA Geodynamics Program: Fifth Annual Report	October 1984
	6. Performing Organization Code: EEG

7. Author(s)	8. Performing Organization Report No.
Geodynamics Program Office	

9. Performing Organization Name and Address	10. Work Unit No.
Geodynamics Branch Earth Science and Applications Division Office of Space Science and Applications	11. Contract or Grant No.

12. Sponsoring Agency Name and Address	13. Type of Report and Period Covered
National Aeronautics and Space Administration Washington, DC 20546	Technical Memorandum
	14. Sponsoring Agency Code

15. Supplementary Notes

16. Abstract

This, the fifth annual report, summarizes program activities and achievements for the period of May 1983 to May 1984. This year the annual NASA Geodynamics Program Conference was held in Cincinnati, Ohio during May 14-17, 1984, in conjunction with the Spring Meeting of the American Geophysical Union (AGU). Abstracts of papers presented at the Conference are included in this Report (Appendix 2). Current publications associated with the NASA Geodynamics Program are listed in Appendix 3.

17. Key Words (Suggested by Author(s))	18. Distribution Statement
Geodynamics, Geodetic, Crustal Dynamics, Tectonics, Laser Ranging, VLBI, Earthquake, Gravity Field, Magnetic Field	Unclassified - Unlimited Subject Category 42

19. Security Classif. (of this report)	20. Security Classif. (of this page)	21. No. of Pages	22. Price
Unclassified	Unclassified	98	A05

For sale by the National Technical Information Service, Springfield, Virginia 22161

NASA-Langley, 1984

End of Document